CLEARANCE REQUEST FOR PUBLIC RELEASE OF DEPARTMENT OF DEFENSE INFORMATION

(See Instructions on back.)

(This form is to be used in requesting review and clearance of DoD information proposed for public release in accordance with DoDD 5230.09.)

TO: *(See Note)* **Chief, Office of Security Review, 1155 Defense Pentagon, Washington, DC 20301-1155**

Note: Regular mail address shown above. For drop-off/next day delivery, use:
Room 12047, 1777 North Kent Street, Rosslyn, VA 22209-2133

1. DOCUMENT DESCRIPTION

a. TYPE Report	b. TITLE National Security Science and Engineering Faculty Fellowship Research Summaries
c. PAGE COUNT 86	d. SUBJECT AREA Basic research projects funded by DoD

2. AUTHOR/SPEAKER

a. NAME *(Last, First, Middle Initial)* Gimm, J. Aura	b. RANK ctr	c. TITLE AAAS Science & Technology Policy Fellow
d. OFFICE Basic Research Office, OSAD (R&E), AT&L		e. AGENCY OSD

3. PRESENTATION/PUBLICATION DATA *(Date, Place, Event)*

13 June 2013
Capital Conference Center, Arlington, VA
National Security Science and Engineering Faculty Fellowship Program Review & Working Meeting

4. POINT OF CONTACT

a. NAME *(Last, First, Middle Initial)* Gimm, J. Aura	b. TELEPHONE NO. *(Include Area Code)* 571.372.6475

5. PRIOR COORDINATION

a. NAME *(Last, First, Middle Initial)*	b. OFFICE/AGENCY	c. TELEPHONE NO. *(Include Area Code)*

CLEARED
For Open Publication
JUN 05 2013 14
Office of Security Review
Department of Defense

6. REMARKS

Compilation of research summaries submitted by university basic researchers supported by DoD through NSSEFF Program

7. RECOMMENDATION OF SUBMITTING OFFICE/AGENCY

a. THE ATTACHED MATERIAL HAS DEPARTMENT/OFFICE/AGENCY APPROVAL FOR PUBLIC RELEASE *(qualifications, if any, are indicated in Remarks section)* AND CLEARANCE FOR OPEN PUBLICATION IS RECOMMENDED UNDER PROVISIONS OF DODD 5230.09. I AM AUTHORIZED TO MAKE THIS RECOMMENDATION FOR RELEASE ON BEHALF OF:

Assistant Secretary of Defense for Research and Engineering

b. CLEARANCE IS REQUESTED BY 20130529 *(YYYYMMDD).*

c. NAME *(Last, First, Middle Initial)* Staffin, Robin	d. TITLE Director
e. OFFICE Basic Research Office, ASD (R&E), AT&L	f. AGENCY OSD
g. SIGNATURE	h. DATE SIGNED *(YYYYMMDD)* 20130521

DD FORM 1910, JAN 2006 PREVIOUS EDITION MAY BE USED. Adobe Professional 8.0

13-S-2062

CLEARED
For Open Publication

JUN 05 2013 14

Office of Security Review
Department of Defense

National Security Science and Engineering Faculty Fellowship

Research Summaries

Basic Research Office
Office of Assistant Secretary of Defense for Research and Engineering
June 2013

13-S-2062

National Security Science and Engineering Faculty Fellowship

Research Summaries

Basic Research Office
Office of Assistant Secretary of Defense for Research and Engineering
June 2013

The NSSEFF Program provides large single-investigator grants to distinguished university scientists and engineers with the goal of deepening their engagement with DoD in research areas of interest to the Department.

Purpose:

- Support scientific research that advances emerging fields that may lead to breakthroughs for DoD.
- Educate and train outstanding student and post-doctoral researchers in support of DoD and national security research areas.
- Foster long term relationships between leading university researchers and DoD.
- Increase the number of exceptionally talented technical experts who contribute to DoD's mission and upon whom DoD may draw to serve on advisory boards, panels, and groups.

NSSEFF Program started in 2008 with 8 single principle investigators; there are currently 29 active Fellows.

Name	Affiliation	Project	Page
Class of 2008			
Connie Chang-Hasnain	University of California, Berkeley	Nanostructured Materials for Low Power, Low Weight, High Performance Electronic and Optoelectronic Devices	4
Diana Huffaker	University of California, Los Angeles	Exploring Dissimilar and NanoMaterials Integration as a Platform for New MWIR Device Functionality	7
Stephen Mayo	California Institute of Technology	Engineering Proteins for Viral Applications	10
Chad Mirkin	Northwestern University	Functional 1-D Structures Based Upon On-Wire Lithography (OWL)	12
Margaret Murnane	University of Colorado at Boulder	Development of High Power Ultrafast Lasers and Applications in Hyperspectral Imaging and Nanotechnology	15
Carey Priebe	Johns Hopkins University	Fusion and Inference from Multiple and Massive Disparate Data Sources	18
Barbara Shinn-Cunningham	Boston University	Managing Acoustic Communications in High-Stress Settings	21
Susan Trolier-McKinstry	Penn State University	High Strain Actuators for Miniaturized Actuators and Self-Powered Sensors	24
Class of 2009			
Graham Candler	University of Minnesota	Multi-Physics Simulations of Hypersonic Flows	27
Steve Elgar	Woods Hole Oceanographic Institution	Manipulating Nearshore Morphology to Determine the Coupling and Feedback Between Waves, Currents, and Bathymetric Change	30
Sharon Glotzer	University of Michigan	Smart, Autonomous, Adaptive Phenomena in Self-Organizing Reconfigurable Materials	33
Naomi Halas	Rice University	3D Nanophotonics: Bending Light in New Directions	36
Mark Kasevich	Stanford University	Atomic de Broglie Wave Navigation Sensors	39
Charles Lieber	Harvard University	One-Dimensional Nanostructures as Building Blocks for Functional Electronic and Bioelectronic Materials	42
Christine Ortiz	MIT	Natural Armor: An Untapped Encyclopedia of Engineering Designs for Protective Defense Applications	45
John Rogers	University of Illinois at Urbana-Champaign	Materials and Mechanics for Stretchable Electronics / Optoelectronics	48
Scott Strobel	Yale University	Exploitation of Diesel Producing Fungi as a Renewable Source of Fuel	51
Andy Weiner	Purdue University	Novel Ultrabroadband Photonic and Radio-Frequency Systems	54

Name	Affiliation	Project	Page
Class of 2010			
Meigan Aronson	Stony Brook University	Designing New Higher Temperature Superconductors	57
Alper Atamturk	University of California, Berkeley	Optimal Design of Resilient Capacitated Networks	60
Andrew Ellington	University of Texas at Austin	Developing Biological Software via Genetically Augmented Proteins	63
Leslie Greengard	New York University	Novel Methods for Electromagnetic Simulation and Design	66
Lene Hau	Harvard University	Quantum Control of Light and Matter: From the Microscopic to the Nanoscale	67
Jeff Kimble	California Institute of Technology	Quantum Networks with Single Atoms, Photons, and Phonons	70
Stephen Leone	University of California, Berkeley	Attosecond Electron Processes in Materials: Science of Excitons, Plasmons, and Charge Dynamics	73
Todd Martinez	Stanford University	Computational and Theoretical Design of Photo- and Mechano-Responsive	76
Monica Olvera de la Cruz	Northwestern University	Paradigms for Emergence of Shape and Function in Biomolecular Electrolytes for the Design of Biomimetic Materials	79
Lenya Ryzhik	Stanford University	Mathematical Modeling in Random Media: From Homogenization to Stochasticity	82
Guillermo Sapiro	Duke University	Information Acquisition, Analysis, and Integration	85

Nanostructured Materials for Low Power, Low Weight, High Performance Electronic and Optoelectronic Devices

Constance Chang-Hasnain
University of California, Berkeley, *cch@berkeley.edu*
NSSEFF Award Year: 2008

Project Description:

The capabilities to detect, image, process and communicate high bandwidth data with security are critical for soldiers in the field or autonomous platforms. The vision of this proposed program is to investigate novel nano-material synthesis and nano-optoelectronic devices to achieve energy-efficient, light-weight, and compact integrated microsystems for ultra-wideband communication, imaging and sensing. The project includes two thrusts focusing on tailoring material properties using nanostructures to achieve that could not be obtained otherwise.

Monolithic integration is of grave importance to achieve functionalities greater than the sum of those of the parts and alleviate power, speed and bandwidth bottlenecks in data transport as microprocessor performance continues to scale. In particular, it is critical to integrate active optical components based on III-V compound, e.g. lasers and semiconductor optical amplifiers, with CMOS electronic circuits, MEMS and silicon-based photonics. We discovered a completely new growth mode for monolithic integration of III-V compound on lattice-mismatched substrates at CMOS-compatible temperatures. We show that (In,Al)GaAs and In(Ga)P nanopillars are directly grown on silicon with extraordinary capability to accommodate mismatches of lattice constants and thermal expansion coefficients. The nanopillars are fully scalable from nanometer to microns in size and maintain single crystalline phase. We demonstrated devices on such III-V nanopillars grown on silicon, including light emitting diodes, avalanche photodiodes, photovoltaic device and lasers with ground-breaking performance. This growth mode will completely change the design rules for heterostructures and make possible integration of various III-V materials device structures on CMOS-silicon and Si-photonics.

We discovered a new class of flat, ultra-thin optics using near-wavelength gratings with a large refractive index contrast, referred as high-contrast gratings (HCG) or high contrast metastructures (HCM). This seemingly simple structure lends itself to extraordinary properties, which can be designed top-down based for integrated optics on a silicon substrate. The extraordinary features include an ultra broadband high reflectivity reflector and a high quality-factor resonance (Q>1E7) with surface-normal emission. We incorporated HCG in vertical cavity surface emitting lasers (VCSELs) making the fastest tunable laser. By varying HCG dimensions, a curved wave front can be obtained by locally changing each grating dimension. This leads to planar, ultra-thin lens and focusing reflectors with high focusing power, or arbitrary transmitted wavefront generator which can be used to split or route light. The extraordinary properties show that HCM is a promising new platform for redefining flat, chip-scale optics.

Accomplishments:

(1) Nano- laser and optoelectronics on silicon substrates

Silicon has been the basis for large-scale electronic integrated circuits (IC), which has transformed our societies with hand-held mobile devices changing the way the world works. However, silicon does not emit light and is a terrible sun light absorber, which making them unattractive for applications involving light. The III-V compound semiconductors, on the other hand, have 1,000-10,000 times better light absorptivity and emission, which are ideal for

photonic devices. Monolithic integration of the two families of devices can enable revolutionary functionalities with applications limited only by our imagination. However, mismatches of crystal lattice constants made such integration a longstanding research problem.

My group discovered a new method to grow III-V nanostructures directly on silicon that overcomes this bottleneck. This can be a new platform that empowers materials mixing to create multifunctionality that a single material system might not achieve alone. We specifically developed a method to grow GaAs-based nanopillars on silicon as nano-optoelectronic building blocks to shore up silicon's optical deficiencies. To validate this concept, we demonstrate a litany of critical optoelectronic functions on silicon including avalanche photodetection, amplified spontaneouse emission, and photovoltaics. One most important aspect of the core-shell nanopillars is high-quality radial p-n junctions within a nanopillar geometry.

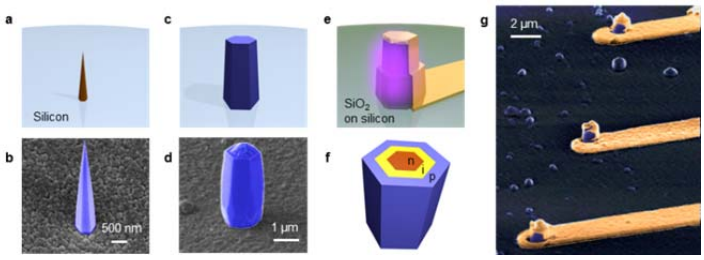

Figure 1 Bottom-up integration of III-V nano-optoelectronics on silicon. a, A schematic and b, an SEM image of a GaAs-based nanoneedle grown directly on silicon. Through core-shell growth, nanoneedles can transform into nanopillars that form the basis of our nano-optoelectronic devices. A schematic and SEM image of a nanopillar are shown in c and d, respectively. e, A schematic of a nanopillar-based device integrated on silicon, made possible by radial p-i-n heterojunctions that form within nanopillars as schematized in f. g, An SEM image shows a fabricated array of nanopillar-based devices, demonstrating bottom-up optoelectronic integration on silicon.

Furthermore, our growth process is CMOS-compatible (low temperature of 400 °C), meaning nanopillar optoelectronics can be tightly integrated on electronics chips after fabrication in CMOS foundries. No other method has shown this type of flexibility accommodating the stringent constraints of CMOS infrastructure. We created devices from individual nanostructures that remain monolithically integrated on silicon after a CMOS-compatible process (Fig. 1). To the best of our knowledge, this is the first time that bottom-up-integrated nano-devices have shown >1 Gbps performance as photodetectors and amplified spontaneous emission as electrically-injected emitters. Such progress reflects a major breakthrough towards making semiconductor nanophotonics ubiquitous and mass-deployable technologies. We demonstrated for the first time optically pumped nanolaser and light emitting diode (LED) directly grown on silicon (Fig. 2).

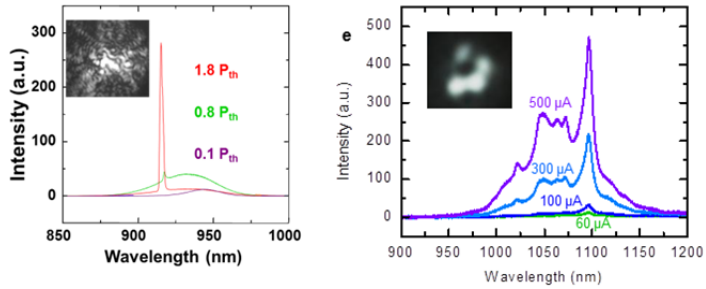

Figure 2 (Left) NanoLaser – optically pumped laser is achieved with the spectra showing below and above threshold. Inset shows speckle exhibiting coherent interference due to lasing. (right) Amplified spontaneous emission from resonant light-emitting diodes exhibiting ASE peaks in their spectra under CW injection at 4 K. The inset shows an image of ASE, revealing an apparent mode pattern. This particular device featured silver encapsulation and a nominal 30% indium active layer.

This work has been chosen as cover stories of Nature Photonics (Fig. 3) and Applied Physics Letters, and won Best Student Paper awards at two major international conferences. The concept and methodology can be extended beyond optoelectronics on silicon to any situation where materials mixing is critical for driving technological progress. The future of semiconductors relies on the emergence of bottom-up fabrication and materials integration processes, and our work reflects discontinuous, step-function-like progress in that direction. We envision diverse

applications for the pillars including broadband optical communications, labs-on-a-chip, 3D camera and display, advanced microscopy, high efficiency solar cells, sensors, and displays.

(2) Flat integrated optics

We recently discovered a new way to make ultra-thin mirrors, lenses, transparent windows, and resonators, all dramatically different from *Newtonian* optics. We discovered extraordinary properties from a simple, planar, subwavelength, one-dimensional (1D) and two-dimensional (2D) structures fully surround by a large contrast of refractive index, henceforth named high contrast grating (HCG) or high contrast metastructures (HCM) (Fig. 4).

We show that light can be manipulated in ways that were totally unexpected by an ultra-thin layer of HCG/HCM, in some cases less than 15% of one wavelength:

- super broadband reflection
- super broadband transparency
- super high quality factor with arbitrarily chosen output angle in 2π Steradian
- planar focusing and defocusing
- bend or deflect light
- arbitrary polarization
- slow down the speed of light.

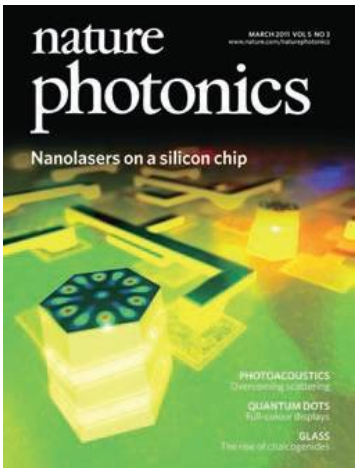

Figure 3 Nature Photonics (Cover) nanolasers on silicon

The HCG has made it possible to realize high-speed wavelength-tunable lasers with manufacturability and reliability. Most noticeable results are 1550-nm wavelength HCG vertical cavity surface emitting laser (VCSEL) and wavelength-tunable VCSELs for low-cost high-speed datacenter communication and fiber-to-the-home applications (Fig. 3). I co-founded a company, Bandwidth10 Inc., with my former PhD students to commercialize this technology. In addition, we demonstrated HCM microlens, hollow core waveguide and HCG array for beam steering. We believe HCM will be a new platform to revolutionize chip-scale integrated optics. The potential impact is tremendous, including compact or even hand-held microscope, telescope, beam steering, transponders, recorders and sensors all on a chip.

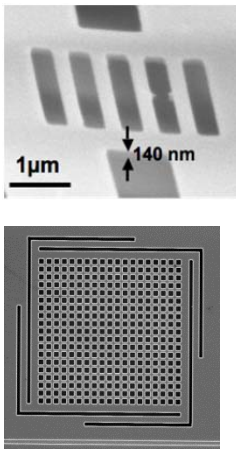

Fig. 4 (top) Scanning electron micrograph (SEM) of a high contrast grating (bottom) of 2D high contrast metastructure.

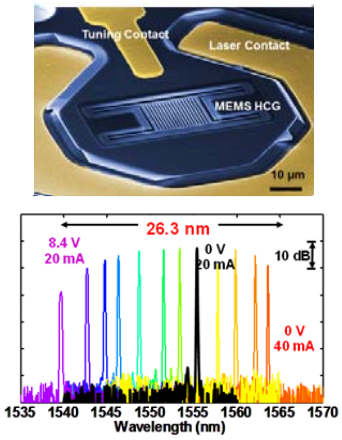

Fig. 5. (top) Scanning electron micrograph (SEM) image of a 1550 nm tunable VCSEL (bottom) Tuning range of an MEMS tunable HCG-VCSEL under room temperature, CW operation. The laser lases over a range of 26.3 nm.

Representative Publications:

Chen, R.; Tran, T.T.D.; Ng, K.W.; Ko, W.S.; Chuang, L.C.; Sedgwick, F.G.; Chang-Hasnain, C.J.; *Nat Photon* **2011**, 5, 170–175

Ren, F; Ng, K.W.; Li, K; Sun H.; Chang-Hasnain, C.J.; *Appl. Phys. Lett.* 2013, 102, 012115

Chuang, L.C.; Sedgwick, F.G.; Chen, R.; Ko, W. S.; Moewe, M.; Ng, K. W.; Tran, T. D.; Chang-Hasnain, C. J.; *Nano Letters*, DOI: 10.1021/nl102988w (2010)

Chuang, L. C.; Moewe, M.; Ng, K. W.; Tran, T.-T. D.; Crankshaw, S.; Chen, R.; Ko, W. S; Chang-Hasnain, C. J.; *Appl. Phys. Lett.* 2011, 98, p. 123101

Chang-Hasnain, C. J.; Yang, W.; *Adv. Opt. Photon.* 2012, 4, 379-440.

Exploring Dissimilar and NanoMaterials Integration as a Platform for New MWIR Device Functionality

Diana L. Huffaker
University of California Los Angeles, *huffaker.diana@gmail.com*
NSSEFF Award Year: 2009

Project Description:

This project aims to explore novel approach for dissimilar and nanomaterials integration leading to new functionality for optoelectronic device applications using III-V semiconductor nanopillars (NPs). Unique dissimilar materials combinations, unachievable by conventional planar approach, are investigated via both axial and core-shell NP heterogeneous integration. This approach has led to low-threshold, continuous-wave ***photonic crystal lasers***, low-noise, high-speed plasmonically enhanced ***avalanche photodetectors (APDs)***, and low-cost, high-efficiency ***solar cells***.

Accomplishments:

Growth and transport characterization:

There have been many difficult challenges to overcome to successfully realize high-quality NPs and NP heterostructures with different III-V semiconductors that can cover a wide range of the IR spectrum. Vertical NPs are grown on patterned {111} substrates by *catalyst-free, selective-area epitaxy* using a metal-organic chemical vapor deposition (MOCVD) reactor. Without the metal catalysts, NP and heterostructure formations solely depend on adatom diffusion dynamics based on the surface energetics in the growth environment, making them extremely sensitive to local environments and very difficult to control. Much effort has been devoted to understand and better control NP axial and lateral heterostructure formations. Through first-principle calculations using density function theory (DFT) and carefully designed experiments, we have been able to achieve lattice-matched and dissimilar NPs and NP heterostructures, including a wide variety of materials combinations with the group-III (Ga, In) and group-V (As, P, Sb) elements. These high-quality, heterogeneous materials systems are normally unachievable using conventional planar approach because of defect formations. However, due to the small footprint in our NP approach, strain can be more readily relieved at the interface to achieve high-quality materials even in extreme dissimilar systems. Furthermore, we have precise control over the position, geometry, and dimension of the NPs to form *highly uniform NP arrays*. Manipulating these degrees of freedom has allowed us to probe new functionalities in optoelectronic devices, such as light trapping, self-aligned plasmonic grating, and creating photonic crystals, using purely bottom-up approach.

Another major obstacle has been the *susceptibility to surface state effects* because of the large surface-to-volume ratio in these III-V NPs. The surface states can cause carrier depletion or accumulation at the surface, depending on the alignment of the bands. To mitigate these undesirable phenomena, we have invested a lot of effort to investigate and optimize *an in-situ passivation technique* by forming a thin shell using materials with a higher band-gap. We have demonstrated that both optical and electrical properties can be greatly enhanced with surface passivation. Doping control in these NPs has also been difficult because of the different atom incorporation rates and amphoteric behavior of the dopants. We have been able to obtain doping control through extensive transport studies by single-NP transport measurements and from the I-V and C-V profiles of difference device arrays. Ultimately, overcoming these difficult growth

challenges has made the exploration of new device functionalities based on dissimilar nanomaterials integration possible.

Patterned GaAs NP solar cells:

In our lab, we have demonstrated three-dimensional GaAs solar cell arrays using a core-shell p-n junction to increase the junction area for light collection. The geometry of the NP array and pitch between each NP have been experimentally and theoretically optimized to enhance absorption due to light-trapping effects. Surface passivation using in-situ InGaP shell growth of these NP solar cells have proven to be an essential component to improve performance. Proof-of-concept devices have shown efficiency improvements of >700%, shown in Fig. 1. Another important aspect is a maximized coupling of solar radiation within the device. We use finite-difference time-domain simulations that directly implement Maxwell's equations to solve for the optical field in proximity of the nanopillars to optimize the particular dome-shaped morphology and peridicity of the top transparent contact. Such indium tin oxide contact constitutes a two-dimensional periodic array of subwavelength lenses that focus the local density of optical states within the photo-active p-n junctions embedded in the nanopillars for enhanced absorsption.

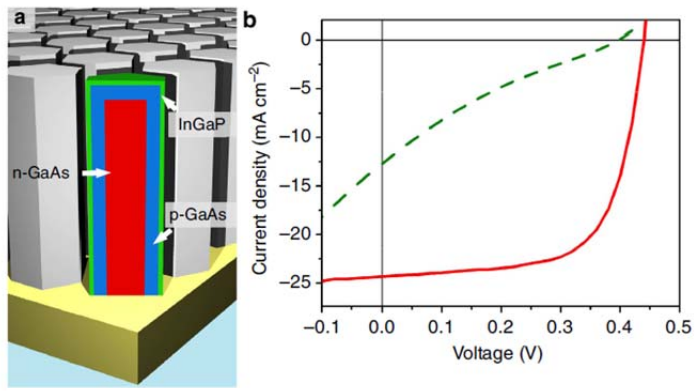

Figure 1: (a) Schematic drawing of the GaAs radial p-n junctions with InGaP passivation shell (not to scale). (b) Current density-voltage characteristics under air mass 1.5 global illumination conditions with (solid red line) and without (dashed green line) InGaP passivation.

Bottom-up photonic crystal lasers:

Using our patterned NP approach, we have been able to manipulate and engineer the position and geometry of the NP array for form bottom-up photonic crystal arrays to achieve lasing (Fig. 2a). We can simultaneously form both the photonic band gap and active gain region by selective-area epitaxy. These NPs consist of a GaAs/InGaAs/GaAs axial double heterostructure for accurate, arbitrary placement of gain within the photonic crystal cavity and lateral InGaP shells to reduce surface recombination, shown by the scanning transmission electron microscope image in Fig 2b. The continuous-wave lasers operate at single-mode at room temperature with low threshold peak power density of

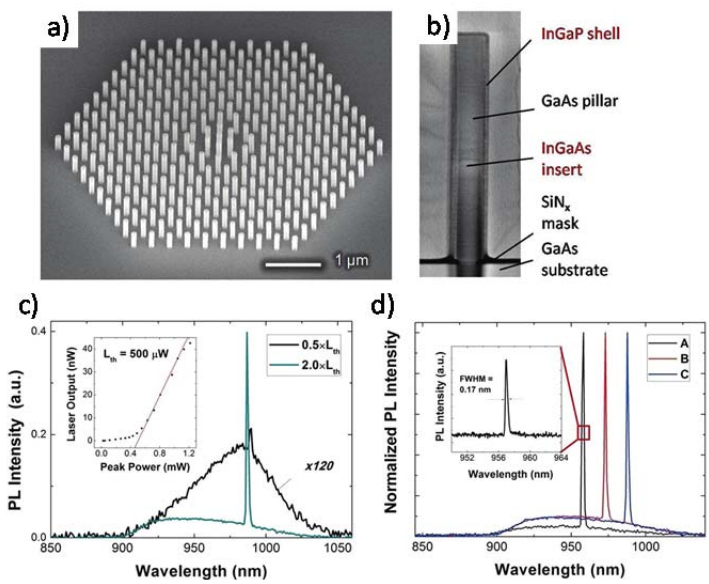

Figure 2: (a) A tilted SEM of an NP photonic crystal array as grown on the substrate. (b) Cross-section STEM of an NP showing the InGaAs insert located at the center of the pillar and InGaP shell. (c) Emission spectra of an NP photonic crystal laser emitting at 989 nm. (d) Lasing spectra of devices with different design to demonstrate tunable lasing.

625 W/cm^2. We can also tune the cavity resonance by lithographically controlling the pitch and diameter of NP array from 960 to 989 nm (Fig 2d). The bottom-up approach to photonic crystal lasers introduces many new design possibilities, which cannot be realized with the top-down method, such as in-situ passivation and atomically smooth surface, without the need for etching. We are currently working on a similar approach but with different NP materials to extend the lasing wavelength further to the IR spectrum, as well as a electrical injection scheme.

Plasmonically enhanced NP avalanche photodetectors:

We have demonstrated a NP device structure for implementing plasmonically enhanced APDs with very thin avalanche volumes. The plasmonic grating is achieved by utilizing our ordered NP array as a self-aligned mask to form these sub-wavelength metal holes in a periodic fashion (Fig. 3a). These nanohole lattice create surface plasmon polariton Bloch wave modes and the metal-NP interface creates localized surface plasmon modes to significantly enhance the photon absorption at the "hot spots" within the NPs. The photo-generated carriers are then multiplied in a localized 3D electric field due to the core-shell p-n junction configuration. Avalanche gain of ~ 216 at 730 nm at -12 V has been demonstrated. Theoretical calculations using dead space multiplication theory show that the multiplication process is dominated by dead space effects because of the thin avalanche regions in NP-APDs. Future work involves utilizing such separate absorption multiplication approach to take advantage of combinations provided by dissimilar materials capability to use smaller band gap NP for detection further out in the IR spectrum and materials with better multiplication characteristics, such as InAsSb/InAs absorption/multiplication.

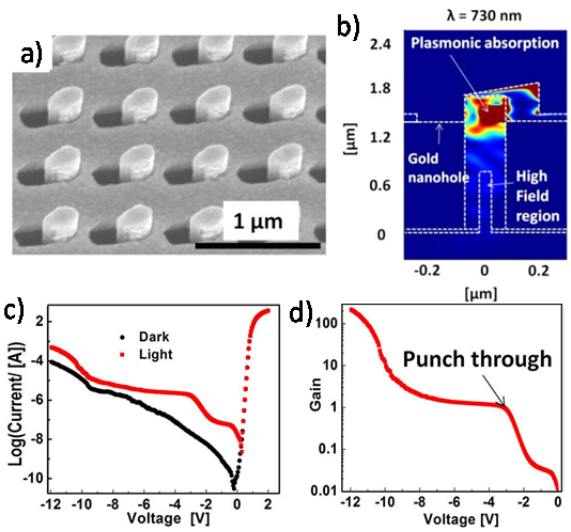

Figure 3: (a) Self-aligned metal nanohole lattice for plasmonically enhanced absorption. (b) Plasmonically enhanced photogeneration within the NP. (c) Light and dark I-V characteristic and (d) the multiplication of the core-shell APD.

Representative Publications:

1. Shapiro, J.N.; Lin, A.; Wong, P.S.; Scofield, A.C.; Tu, C.; Senanayake, P.N.; Mariani, G.; Liang, B.L., Huffaker, D.L., *Appl. Phys. Lett.* **2010**, 97, 243102.

2. Lin, A.; Shapiro, J.N.; Scofield, A.C.; Liang, B.L.; Huffaker, D.L., *Appl. Phys. Lett.* **2013**, 102, 053115.

3. Mariani, G.; Scofield, A.C.; Hung, C.-H.; Huffaker, D.L., *Nat. Comm.* **2013**, *4*, 1497.

4. Scofield, A.C.; Kim, S.H.; Shapiro, J.N.; Lin, A.; Liang, B.L.; Scherer, A.; Huffaker, D.L., *Nano Lett.* **2011**, 11, 5387.

5. Senanayake, P.N.; Hung, C.-H.; Shapiro, J.N.; Lin, A.; Liang, B.L.; Williams, B.S.; Huffaker, D.L., *Nano Lett.* **2011**, 11, 5279.

Engineering Proteins for Anti-Viral Applications

Stephen L. Mayo
California Institute of Technology, *steve@mayo.caltech.edu*
NSSEFF Award Year: 2008

Project Description:

My main NSSEFF project revolved around the development and use of structure and computation-based protein design to engineer proteins with broad-spectrum anti-viral activity. Traditional avenues for the prevention (e.g., vaccination) and treatment of viral infection (e.g., anti-viral medications) are routinely overcome by the natural evolution of viral antigens. We proposed the development of two classes of engineered proteins that, by design, are less susceptible to changes in viral antigens. First, computationally designed, multi-specific antibodies provide a route to antibody-based therapies that can accommodate the known and potential future evolution of targeted viral antigens. And second, enhanced lectins (i.e., proteins that bind carbohydrates) provide a route to target the carbohydrate chains on the glycoproteins of enveloped viruses, which are difficult to manipulate by viral sequence evolution. In addition, we proposed the development of a new class of therapeutic protein that we call a "lectibody" that combines the carbohydrate binding ability of a lectin with the immune system activating ability of the Fc region of an antibody in order to achieve a completely novel mode of therapeutic action for viral neutralization.

Accomplishments:

Cyanovirin-N (CV-N) is a small naturally occurring lectin that has been shown to neutralize many enveloped viruses including HIV. We designed an obligate dimer of CV-N through an engineered tandem repeat (CVN_2). CVN_2 shows improved HIV neutralization activity by up to 18-fold compared to wild-type CV-N and shows broad cross-strain HIV neutralization, both likely due to CVN_2's enhanced binding to gp120, an HIV envelope glycoprotein (Keeffe et al., 2011). The X-ray crystal structure of CVN_2 reveled a domain-swapped dimer structure similar to wild-type CV-N that positions carbohydrate binding sites at distances similar to those on 2G12, a previously described anti-HIV antibody.

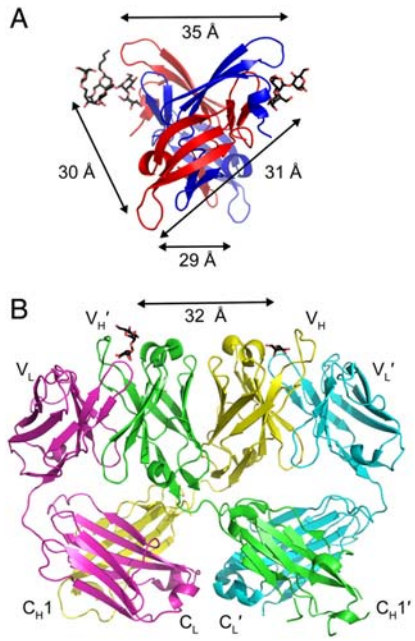

Similarity of carbohydrate binding site spacing in domain-swapped dimer of CVN-N (A) and 2G12 (B).

In addition to our work on cyanovirin-based anti-viral proteins, we leveraged NSSEFF funding to make advances in several areas of protein design: we demonstrated the utility of using large structural ensembles for computational protein design (Allen, et al., 2010); we developed a new computational method called GRID for

high-resolution protein structure refinement (Chitsaz and Mayo, 2013); we created an enzyme for the Kemp elimination using computational enzyme design (Privett et al., 2011) and have evolved it to perform with kinetic parameters similar to naturally occurring enzymes (Blomberg et al., in preparation); we solved the structure of *Hypocrea jecorina* Cel5A, an important cellulase for the conversion of cellulosic material to biofuels (Lee et al., 2011) and are using computational protein design to generate Cel5A variants with enhanced thermal properties (work in progress); and, we are utilizing computational protein design to enhance the neutralization potency of antibodies against influenza (work in progress).

Representative Publications:

Allen, B. D.; Nisthal, A.; Mayo, S. L. *Proc. Natl. Acad. Sci. USA* **2010**, *107*, 19838-19843

Keeffe, J. R.; Gnanapragasam, P. N. P.; Gillespie, S. K.; Yong, J.; Bjorkman, P. J.; Mayo, S. L. *Proc. Natl. Acad. Sci. USA* **2011**, *108*, 14079-1408

Privett, H. K.; Kiss, G.; Lee, T. M.; Blomberg, R.; Chica, R. A.; Thomas, L. M.; Hilvert, D.; Houk, K. N.; Mayo, S. L. *Proc. Natl. Acad. Sci. USA* **2011**, *109*, 3790-3795

Lee, T. M.; Farrow, M. F.; Arnold, F. H.; Mayo, S. L. *Protein Sci.* **2011**, *20*, 1935-1940

Chisaz, M.; Mayo, S. L. *J. Comp. Chem.* **2013**, *34*, 445-450

Functional One-Dimensional Structures Based Upon On-Wire Lithography

Chad A. Mirkin
Northwestern University, *chadnano@northwestern.edu*
NSSEFF Award Year: 2008

Project Description:

One-dimensional nanosystems represent an area of intense research interest. In contrast to their zero-dimensional counterparts (e.g. nanoparticles and quantum dots), the design space available to these nanowire-like structures is significantly increased. By controlling the diameter, length, and composition of such structures, one can envision ways of introducing positive and negative architectural features along the wire to realize structures with even greater functionality. To this end, methods for nanowire fabrication and manipulation, analogous to the many powerful types of nanolithographies, would be extremely useful. The Mirkin group has developed On-Wire Lithography (OWL), an extraordinarily powerful method for synthesizing nanowires with controllable positive and negative architectural features along the long axis of the wire. This method, allows one to control feature composition and size from the sub-5 nm to many micrometer length scales (Scheme 1).

This approach allows one to prepare nanometer scale gaps, rod segments, and segment arrays with precise control over not only the size of the gap, but also the thickness, composition, and periodicity of the segments. OWL offers many advantages over other nanofabrication techniques while avoiding important weaknesses. Few techniques, namely scanning tunneling microscopy and electron-beam lithography, can match the resolution of OWL, but while these techniques are serial, OWL can be used to produce billions of structures in parallel. Other more parallel techniques, such as photolithography, are limited in resolution and cannot reach the sub-5 nm capabilities of OWL. Finally, structures produced via OWL are dispersible, allowing for a range of applications not possible with substrate-immobilized nanostructures.

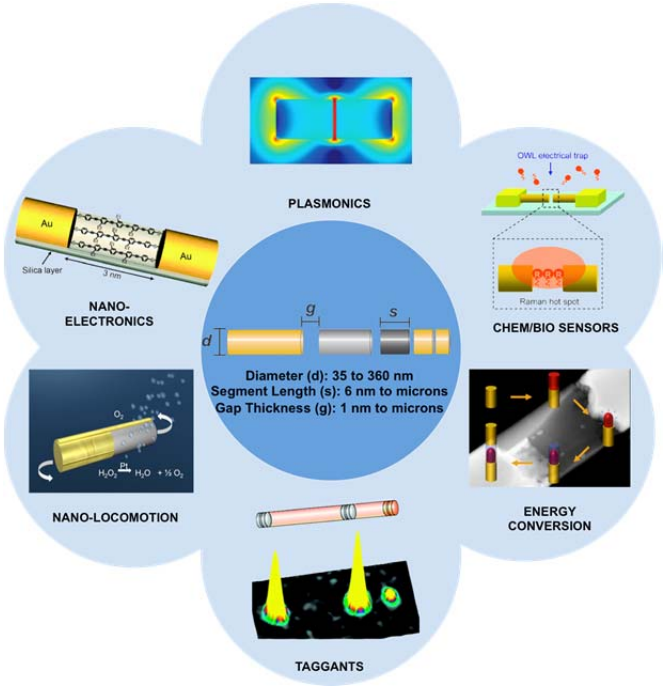

Scheme 1. OWL capabilities and applications.

Accomplishments:

During the NSSEFF program, we have worked to fully define the design space possible via OWL and to use the novel capabilities of OWL to synthesize and fabricate functional architectures. Our efforts have impacted the fields of plasmonics, chemical and biological sensors, energy conversion, taggants, nanolocomotion, and nanoelectronics.

Plasmonics: One area of focus for our work was to determine the resolution limits of OWL. We are now able to prepare OWL nanostructures with diameters as small as 35 nm, disk thicknesses down to 6 nm, and gap sizes down to 1 nm. Taking advantage of these advances, we have applied the principles of OWL for fundamental and applied plasmonic studies. As a proof-of-concept, we studied the effect of gap size on the plasmonic coupling of gold nanorods. We prepared a set of 35 ± 5 nm diameter nanorod dimers comprised of 68 ± 10 nm long Au rod segments (aspect ratio of approximately 2:1) spaced by gap thicknesses between 16 and 0 nm (Figure 1). The transverse plasmon mode (around 550 nm) of these

structures is relatively unaffected by coupling in the axial dimension, but there is a significant redshift in the longitudinal mode (peaks at 800-1200 nm) with decreasing gap thicknesses of 16 ± 3, 10.3 ± 1.7, 3.3 ± 1.2, and 0 nm. The 0 nm gap used in these studies corresponds to a nanorod with no gap region and a length that is twice as long as the nanorods comprising the dimer structures (144 ± 16 nm). This is a significant demonstration of how one can use this method to rationally and precisely probe the solution-averaged optical properties of coupled plasmonic nanostructures over a large range of gap sizes. Unlike other methods to probe plasmon coupling, this method has the advantage of allowing one to measure their extinction spectra in solution to determine the orientationally-averaged optical properties of the entire population.

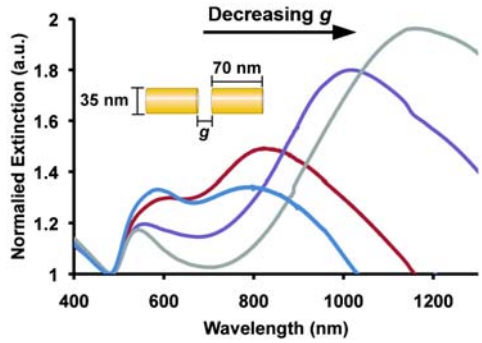

Figure 1. Normalized solution-averaged extinction spectra collected in water of ~35 nm diameter dimers comprised of ~70 nm long Au nanorods with decreasing gap sizes from approximately 16 to 0 nm (left to right). The transverse plasmon mode (around 550 nm) is mostly unchanged, whereas the longitudinal mode (between 800 and 1200 nm) redshifts with decreasing gap sizes of ~16 nm (blue), ~10 nm (red), ~3 nm (purple), and 0 nm (grey).

We then performed a study of the SERS properties of these smaller diameter structures. Here, we focused on optimizing the geometry of the small structures for maximum SERS enhancement. It is well established that this maximum will occur when the plasmon resonance coincides with the laser excitation for structures with gap sizes below 5 nm. To achieve these conditions, we prepared a series of Au nanorod dimers with gaps around 3 nm in size. By systematically changing the length of the rod segments, we were able to find the geometry that had a resonance wavelength of 785 nm (the desired SERS laser wavelength). As expected, the resonance redshifts as the length of the nanorods comprising the dimer increase, with segments ~60 nm in length falling closest to 785 nm. With this important optimization complete, we began to study the SERS properties of the optimized dimers. With the aid of a SEM map, single dimers of interest were located, and SERS spectra were obtained at 785 nm. The spectra demonstrate two important properties of these structures as SERS sensors: large SERS signal enhancement and high degree of signal reproducibility between different rod dimers in the same batch. We then calculated the enhancement factor (EF) of the structures to be $7.4 \times 10^9 \pm 8.1\%$, which is among the largest values reported for gold structures.

Chemical and Biological Sensors: By leveraging the gap structures synthesized by OWL, we have demonstrated that we can localize biomolecules with an electric field and provide a powerful means to spectroscopically identify them based upon surface-enhanced Raman spectroscopy (SERS). This addresses one of the greatest challenges in nanoscience, i.e. the development of efficient methods for physically probing or trapping a nanomaterial or small collection of molecules with the capability to spectroscopically identify these entities. The small size of nanomaterials often prohibits the use of conventional spectroscopic tools to locate and identify them. These nanotraps can be used to detect DNA in a moderately sensitive manner. In our proof-of-concept experiments, the lowest measurable DNA concentration is 230 fM, which is over 20 times more sensitive than previous nanogap Raman detection results without an applied field, and at least twice the sensitivity of reported methods based upon tip-enhanced-Raman spectroscopy (TERS). This approach may open up a host of new opportunities for integrating SERS nanostructures and lab-on-chip electrical nanodevices for many applications.

Energy Conversion: We have further developed the OWL methodology to utilize organic and semiconductor materials organized in a core-shell geometry. Many of the challenges that face the field of nanowire photovoltaics relate to the difficulties associated with electrically contacting the nanowires, the fabrication of high quality semiconductor heterojunctions with built-in metallic leads could dramatically accelerate progress. Fabrication of a photodetector based on a single P3HT@CdSe nanowire with an impressive on/off ratio was achieved (comparable to the best reported thin film photodetectors using P3HT@CdSe), demonstrating the functionality of the nanowires produced. Finally, the precision with which electrochemically-generated plasmonically-active nanostructures may be placed proximally to

these heterojunctions points towards a new test-bed for rapidly studying light-matter interactions and energy conversion in a facile and straightforward manner.

Taggants: Covert encoding and tracking are becoming increasingly important for a variety of applications and industries, including authentication in anti-counterfeiting strategies, materials and personnel tracking, and in chemical and biological detection. Using OWL, we developed the synthesis and characterization of novel Ag-based nanodisk codes. The Ag nanodisks exhibit larger SERS enhancements than their Au counterparts over a broader range of excitation wavelengths, and when heterostructures consisting of both Au and Ag disk pairs are made, trinary encoding becomes possible. Further, because readout is both wavelength and material dependent a significant increase in the density of stored information is possible. This advance increases the number of possible codes to 98 from the 13 that were proposed in the original 5 disk pair Au system.

Nanolocomotion: We have employed OWL as a method for tailoring the architecture of nanorod materials to synthesize a set of structures with compositional asymmetry and there by realize a new class of catalytically powered nanorotors (NR). These rotors are composed of Pt-Au segmented nanowires, with one side of the wire completely masked by a gold backing. By utilizing the catalytic decomposition of H_2O_2 and formation of O_2 on the surface of the exposed Pt segment, we were able to observe the rotation of the nanowires. The described method opens a new avenue for generating nanomotors with more complex movement patterns. They also have the potential to facilitate the development of nanomechanical devices that could find utility in microfluidics and drug delivery.

***Nanoelectronics*:** We have developed a platform for the *in situ* synthesis of molecular wires inside the nanoscale gaps using a click chemistry approach (Figure 2). This approach circumvents some of the steric limitations of assembling a full-length molecular wire inside the nanogap. In this experiment, the yield of functional devices increased from 10% to 40% just by following the *in situ* synthetic approach. We have also worked to develop heterometallic electrode designs (Au-Pt) to create molecular diodes for next-generation electronics and described the synthesis of one such system with OWL-generated heterogap nanowires where a thin gap (sub-5 nm) is placed between gold and platinum nanowire segments. We then studied the conductance properties of a symmetric conjugated molecule bridging the gap. We observed that nanogap devices loaded with OPE show a significant I−V response with rectifying behavior suggesting the assembly of the molecules across the gap with chemical connectivity to each of the metal electrodes on opposite sides of the gap. We then determined that the rectifying behavior is likely a result of the different modes of contact between the ends of the molecules and the different electrode materials that span the heterometallic nanogap.

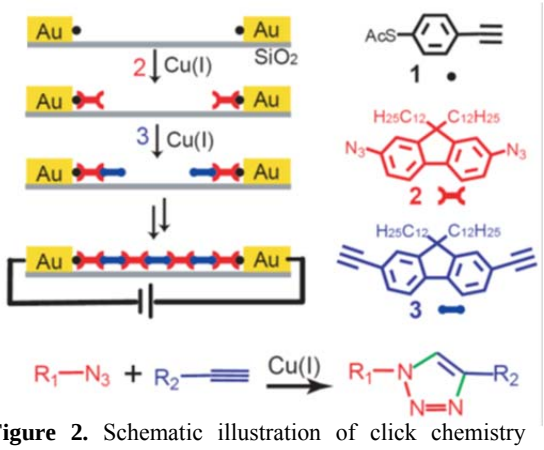

Figure 2. Schematic illustration of click chemistry within nano-gaps, the chemical structures of molecules used in this study, and the alkyne–azide click reaction.

Representative Publications:

(1) Chen, X. D.; Braunschweig, A. B.; Wiester, M. J.; Yeganeh, S.; Ratner, M. A.; Mirkin, C. A. *Angew. Chem., Int. Ed.* **2009**, *48*, 5178.

(2) Wei, W.; Li, S. Z.; Millstone, J. E.; Banholzer, M. J.; Chen, X. D.; Xu, X. Y.; Schatz, G. C.; Mirkin, C. A. *Angew. Chem., Int. Ed.* **2009**, *48*, 4210.

(3) Banholzer, M. J.; Osberg, K. D.; Li, S.; Mangelson, B. F.; Schatz, G. C.; Mirkin, C. A. *ACS Nano* **2010**, *4*, 5446.

(4) Osberg, K. D.; Schmucker, A. L.; Senesi, A. J.; Mirkin, C. A. *Nano Lett.* **2011**, *11*, 820.

(5) Osberg, K. D.; Rycenga, M.; Harris, N.; Schmucker, A. L.; Langille, M. R.; Schatz, G. C.; Mirkin, C. A. *Nano Lett.* **2012**, *12*, 3828.

Development of High Power Ultrafast Lasers and Applications in Hyperspectral Imaging and Nanotechnology

Margaret M. Murnane
University of Colorado, Boulder, *Margaret.Murnane@colorado.edu*
NSSEFF Award Year: 2008

Project Description:

The goals of this NSSEFF project were threefold –

1. To develop new approaches for generating ultrashort pulses in the mid-infrared region of the spectrum (at wavelengths around 1.5 - 4μm), with sufficient intensity to ionize matter and explore new strong-field quantum physics. This work required the development of new frequency conversion techniques and investigating new laser materials suitable for ultrashort-pulse amplification in the mid-infrared.

2. To explore coherent X-ray generation from atoms driven by ultrafast mid-infrared lasers. Our theoretical models had predicted that it would be possible to efficiently convert mid-infrared laser light into the soft X-ray regions of the spectrum, with sufficient flux useful for a variety of applications in nanoimaging, materials science, nanoscience and nanotechnology (Fig. 1). However, the fundamental quantum physics underlying these predictions had not been verified experimentally prior to the NSSEFF project.

3. To harness a new type of microscopy called coherent diffraction imaging (CDI) (also known as lensless imaging) to implement powerful new tabletop nanoscale imaging capabilities. In CDI, rather than using a conventional imaging lens system to form an image, the light scattered from the object is captured on a CCD. Only the intensity of the scattered light is recorded by a CCD, missing the phase information.necessary to reconstruct an image. However, provided that constraints can be placed on the object or the illuminating beam, a computer algorithm can be used to iteratively extract the optical phase, and therefore an image of the object. A great attraction of CDI is that it obviates the need for the most-difficult part of a soft X-ray microscope—the imaging lens.

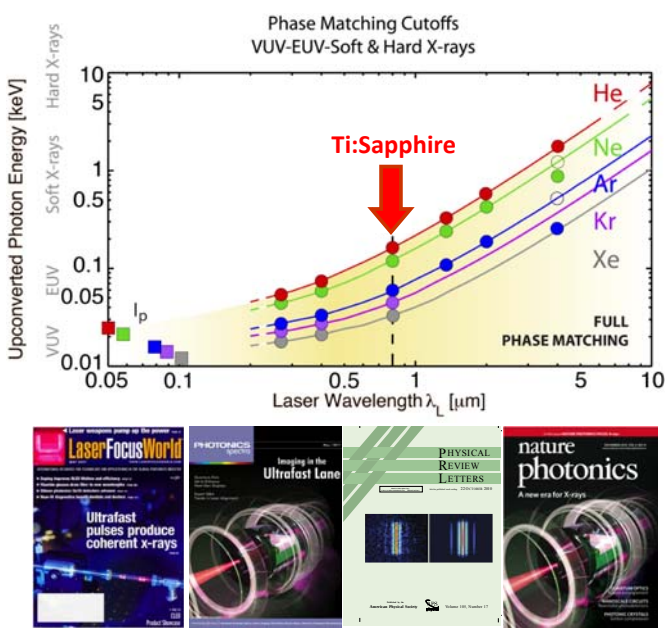

Fig. 1. (Top) Phase matching of HHG using mid-infrared lasers (lines - theory, dots – experiment). Using mid-IR driving lasers, bright HHG emission is possible over broad regions of the x-ray spectrum. (Bottom) Example covers.

Accomplishments:

Nonlinear optics revolutionized laser science by making it possible to efficiently convert laser light from one wavelength into another. The most dramatic advance enabled by the NSSEFF grant was to show that the beautiful quantum physics of how atoms ionize in strong laser fields can be combined with extreme nonlinear optics to produce coherent, tabletop, light sources in the

X-ray region of the spectrum for the first time. This solved the long-standing challenge of how to efficiently convert laser light into the soft X-ray region - to regimes not even imagined prior to this work.[1-3]

To achieve this, we used the extreme nonlinear-optical process of high harmonic generation (HHG), where light from an ultrafast laser can be coherently upshifted to produce useful, tabletop, coherent (laser-like) light source in the extreme ultraviolet region of the spectrum. In HHG, short wavelength light is emitted as a result of the highly nonlinear motion of an electron ionized from an atom in a strong laser field through the quantum tunneling process. The atom essentially acts as a nanoscale radiating quantum dipole antenna, where the highly spatially and temporally modulated accelerating charge distribution of the electron radiates very short wavelength light.

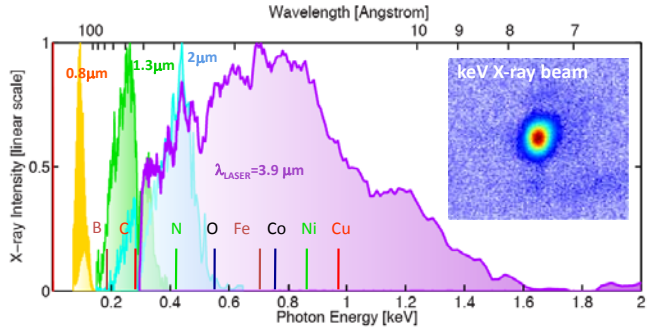

Fig. 2. HHG from tabletop ultrafast lasers is a unique light source, generating coherent beams (insets) that span multiple X-ray absorption edges in atoms. Using this source, nanoscale dynamics can be captured with elemental and chemical specificity, since the positions of these edges are sensitive to the local environment. The different colored spectra correspond to different driving laser wavelengths.

For a nonlinear optical frequency conversion process to be efficient, ideally the phase velocities of the fundamental driving laser field and the harmonic light are matched so that the emissions from many atoms in the medium add coherently. This process is called phase matching. However, until recently there was no method to phase match the HHG process at photon energies > 150 eV. In 2008 we made a surprising theoretical discovery - that by using longer wavelength, mid-infrared driving lasers, bright HHG beams (i.e. full phase matching) could be extended in theory to the kiloelectron volt region of the spectrum, corresponding to wavelength < 10 Å.

This idea was very counterintuitive at the time - in a *traditional* nonlinear optical process, it is always best to combine the smallest number of photons together to maintain efficiency i.e. use the lowest order nonlinear process possible. However, in *extreme* nonlinear optics, the opposite is true: to generate bright soft X-ray beams at high photon energies, the HHG process optimizes when a larger number of lower-energy photons from a longer-wavelength, mid-IR, laser are coherently combined together. In a series of experiments enabled by NSSEFF and using facilities provided by the NSF Engineering Center in EUV Science and Technology, [1-3] we experimentally validated these predictions, as shown in Figs. 1 - 3. This work demonstrated efficient, phase matched, generation of a spatially coherent beam with photon energy as high as 1.6 keV (<8Å wavelength) through a *>5000th order* nonlinear optical upconversion process, shattering many records and opening up new science. Furthermore, this source represents—by a large margin—the broadest bandwidth coherent supercontinuum ever produced, with a bandwidth approaching 1 keV, presenting a realistic prospect that sub-attosecond timescale physics may become accessible.

Finally, since X-rays can penetrate thick samples, and image with elemental and chemical specificity, these ultrafast bursts of light can be used to capture function in molecules, or visualize nanoscale systems relevant to magnetic storage, lithography, spintronics, nanoscience, nanofabrication, energy harvesting, thermal management, cellular imaging and a host of other

applications across a broad range of science and technology. In the future, this technology may even lead to sharper medical x-ray imaging.

In other recent work,[4] we achieved a record spatial resolution for any light-based tabletop microscope - demonstrating a spatial resolution of 22 nm. Future work will extend this tabletop microscope to spatial resolutions less than 10 nm, with the ability to image thick, opaque, nanostructures for nanoelectronics, data storage and energy harvesting. Finally, in collaboration with Technical University Vienna, we also demonstrated the first ultrafast, 10 mJ, mid-infrared laser with sufficient power for coherent X-ray generation.[5]

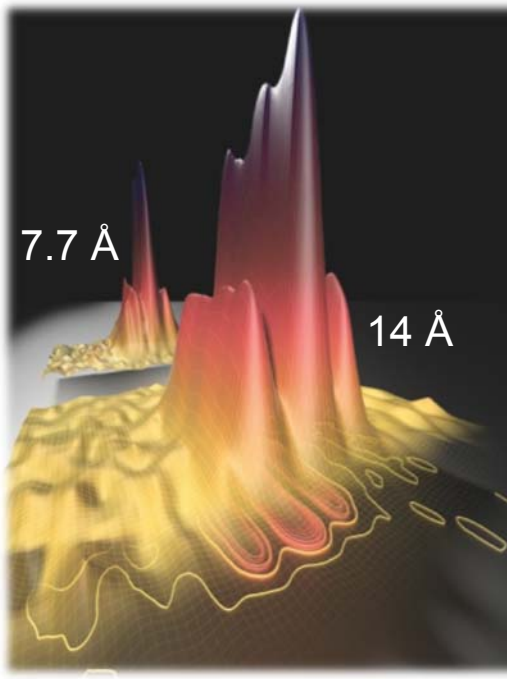

Fig. 3. Young's double slit interference patterns of HHG beams showing full spatial coherence.

These advances are significant because imaging methodologies in support of nano science and nanotechnology are reaching a limit. Approaches using electrons or visible light often work only under specialized conditions after extensive sample preparation. Electron and scanning probe techniques provide image resolutions far better than optical wavelengths, but cannot be applied to thick samples. Large-scale X□ray free electron lasers can probe at nm-fs level, but their repetition rate is low (10-120 Hz) and access is severely limited. From a technological point of view, our capabilities for nanofabrication have far outstripped our ability to capture and understand function at the nanoscale. Design rules for future nanosystems that operate at fundamental limits of density, efficiency and speed, cannot be formulated until nanoscale structure and dynamics in heterogeneous systems can be captured and understood. Coherent soft X-ray imaging could provide revolutionary new capabilities for imaging thick samples using penetrating radiation.

Representative Publications:

1. Popmintchev, T.; Chen, M. C.; Bahabad, A.; Gerrity, M.; Sidorenko, P.; Cohen, O.; Christov, I. P.; Murnane, M. M.; and Kapteyn, H. C. *Proceedings Of The National Academy Of Sciences Of The United States Of America* **2009,** 106, 10516-10521
2. Popmintchev, T.; Chen, M. C.; Arpin, P.; Murnane, M. M.; and Kapteyn, H. C. *Nature Photonics* **2010,** 4, 822-832
3. Popmintchev, T.; Chen, M.-C.; Popmintchev, D.; Arpin, P.; Brown, S.; Ališauskas, S.; Andriukaitis, G.; Balčiunas, T.; MüCke, O. D.; Pugzlys, A.; Baltuška, A.; Shim, B.; Schrauth, S. E.; Gaeta, A.; Hernández-García, C.; Plaja, L.; Becker, A.; Jaron-Becker, A.; Murnane, M. M.; and Kapteyn, H. C. *Science* **2012,** 336, 1287-1291
4. Seaberg, M. D.; Adams, D. E.; Townsend, E. L.; Raymondson, D. A.; Schlotter, W. F.; Liu, Y. W.; Menoni, C. S.; Rong, L.; Chen, C. C.; Miao, J. W.; Kapteyn, H. C.; and Murnane, M. M. *Optics Express* **2011,** 19, 22470-22479
5. Andriukaitis, G.; Balciunas, T.; Alisauskas, S.; Pugzlys, A.; Baltuska, A.; Popmintchev, T.; Chen, M. C.; Murnane, M. M.; and Kapteyn, H. C. *Optics Letters* **2011,** 36, 2755-2757

Fusion and Inference from Multiple and Massive Disparate Data Sources

Carey E. Priebe
Johns Hopkins University, *cep@jhu.edu*
NSSEFF Award Year: 2008

Project Description:

Since beginning our NSSEFF project "Fusion and Inference from Multiple and Massive Disparate Data Sources", we have witnessed the rise of the "big data" obsession. NSSEFF has played an essential role in positioning us as leaders of "big data inference". First, we have answered the question "what is big data?" Our answer: "data derived from multiple and massive disparate sources!" That is, few applications involve simply millions of unstructured high-dimensional observations; rather, big data consists of video, text, speech, social networks, etc., from different sources, in different spaces, stored in different places. If we treat the data merely as a large matrix, then extending inference to this setting, while not without its challenges, is often relatively straightforward. However, if, as is often the case, successful inference demands that we maintain the structure of the data, then we have a fundamental gap in our theories and methodologies re fusion & inference. Our characterization: "big data" = "data derived from multiple and massive disparate sources". This characterization – the raison d'etre for our NSSEFF project – allows us to give a specific and useful answer to the question "what is big data?". Second, we have developed a decomposition of "what to do with big data" into "big data processing" and "big data inference". Our NSSEFF project is specifically addressing Fusion and Inference [on big data]. This has allowed us to concretely identify two separate themes – the computer science aspects of how to process big data, and the statistical aspects of how to perform useful fusion & inference on big data. These two areas must, of course, interact. We think of the computer science big data processing researchers as enablers for our big data inference; of course, they think of our inference as an application of their big data processing! Each of the two separate areas is engendering much activity – and NSSEFF has positioned us as leaders in the "big data fusion & inference" realm. (NB: the interaction between the processing and the inference is fundamentally important and, we believe, whence the next big data wins will come.)

Accomplishments:

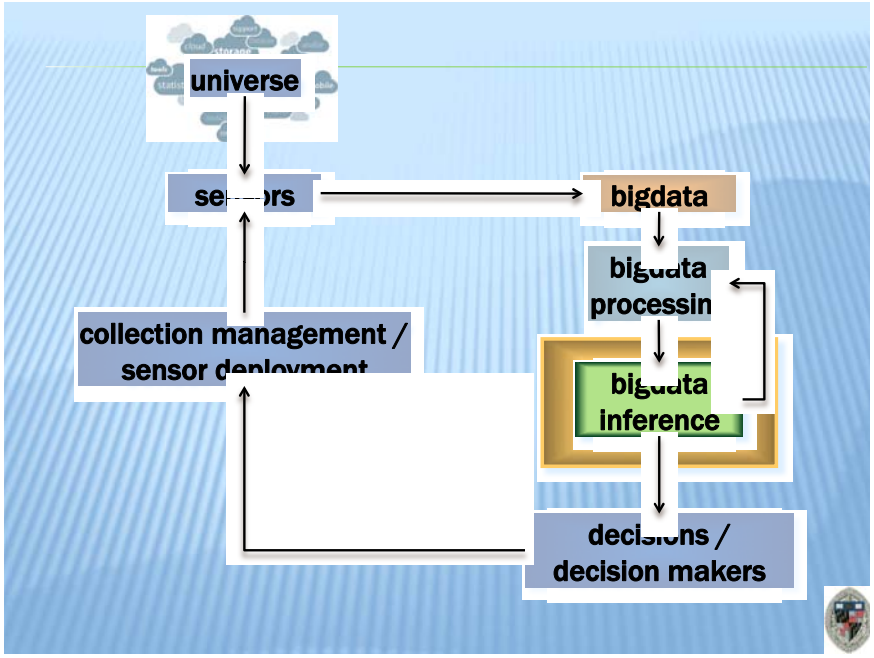

Figure 1. Big Data Inference Our NSSEFF project addresses fusion and inference on big data. We think of the computer science big data processing researchers as enablers for our big data inference; of course, they think of our inference as an application of their big data processing. The interaction between the processing and the inference is fundamentally important and, we believe, whence the next big data wins will come.

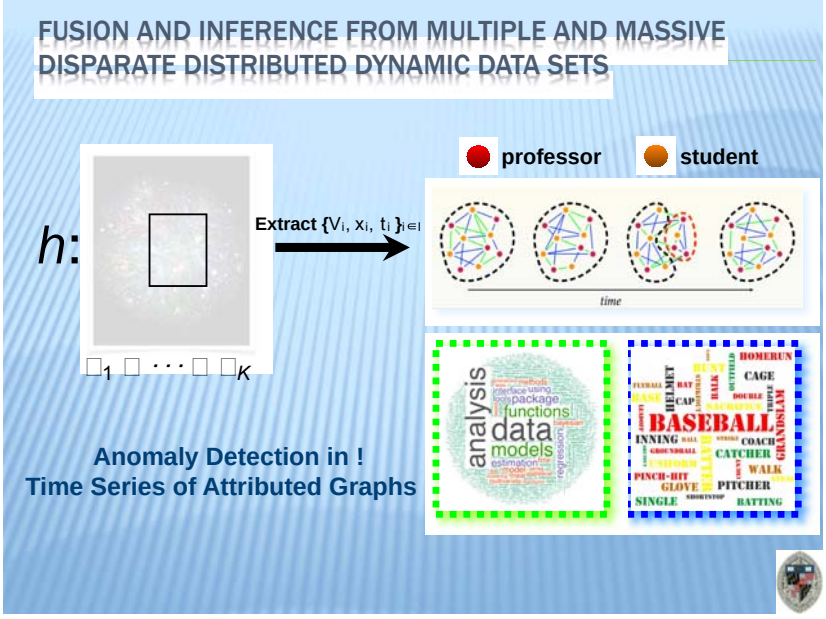

Figure 2. Time Series of Attributed Graphs. Time series of attributed graphs derived from multiple and massive disparate data sets (MMDDS) – e.g., communications networks whose nodes are attributed with information about the actors and whose edges are attributed with information based on the content of the communication – are a fundamental representation for "big data". Statistical inference on MMDDS then reduces to, say, anomaly

Representative Publications:

Z. Ma, A. Cardinal-Stakenas, Y. Park, M.W. Trosset, and C.E. Priebe, "Dimensionality Reduction on the Cartesian Product of Embeddings of Multiple Dissimilarity Matrices," Journal of Classification, Vol. 27, No. 3, pp. 307-321, 2010.

N.H. Lee and C.E. Priebe, "A Latent Process Model for Time Series of Attributed Random Graphs," Statistical Inference for Stochastic Processes, Vol. 14, No. 3, pp. 231-253, 2011.

C.E. Priebe, J.L. Solka, D.J. Marchette, A.C. Bryant, "Quantitative Horizon Scanning for Mitigating Technological Surprise: Detecting the potential for collaboration at the interface," Statistical Analysis and Data Mining, Vol. 5, No. 3, pp. 178-186, 2012.

M. Tang, Y. Park, N.H. Lee, and C.E. Priebe, "Attribute fusion in a latent process model for time series of graphs ," IEEE Transactions on Signal Processing, Vol. 61, No. 7, pp. 1721-1732, April, 2013.

Minh Tang, Daniel L. Sussman, and C.E. Priebe, "Universally consistent vertex classification for latent positions graphs," Annals of Statistics, accepted for publication, 2013.

Managing Acoustic Communications in High-Stress Environments

Barbara Shinn-Cunningham
Boston University, *shinn@bu.edu*
NSSEFF Award Year: 2008

Project Description:

In command and control settings, and in ordinary life, we are bombarded with more information than our brains can process. To manage information flow, we direct attention to and focus our processing resources on behaviorally relevant events. While attentional processing works well in many settings, it can break down when too much critical information arrives in too short a time span. Unfortunately, it is at exactly at moments of crisis when information flow is mostly likely to exceed capacity and information loss likely to lead to horrific outcomes. Indeed, missed information that was easily perceptible but ignored by a human operator processing other information is an all-too-common cause of human error, leading to injury and death (e.g., during airline emergencies, ground battles, and other high-stress settings).

This project seeks to develop methods to determine an observer's mental state from noninvasive brain imaging techniques and to use that information to build feedback into information displays. New techniques for extracting neural signals from noisy sensor data are being developed. Electro-encephalography (EEG; measurements of the voltages on the scalp generated from synchronous brain activity) is used to determine what information in a complex scene was perceived and processed and what information was ignored. Single-trial analysis of neural responses demonstrates the feasibility of a real-time system that analyzes observer state from neural signals. The long-term goal is the development of smart displays that monitor observer perception, and then use the resulting knowledge to control information flow and ensure that key information is not lost (altering how and when information is presented to ensure key points are processed, e.g., by re-presenting critical information that the observer ignored because he or she was already occupied). Such devices can be of use in command and control situations. However, they also could revolutionize the hearing aid industry and provide the basis for transformative assistive communication devices for listeners with impaired executive function and attentional control, including returning war veterans with traumatic brain injury.

Accomplishments:

We have demonstrated the ability to "read the mind" of a human listener using a single trial of EEG data. Attention dramatically changes the strength of the neural response to different sources. Specifically, attention enhances the representation of an attended source and suppresses the representation of a competing source compared to when listeners are engaged in a visual task and ignoring all sound (see Figure 1A). This modulation is sufficiently robust that from voltages on the scalp, we can determine which of two important simultaneous acoustic messages a listener attended and processed, and which was "missed" and not perceived. Using generic pattern classification algorithms that are not "fine tuned" to a particular listener, we can determine what source a listener is attending with under three seconds of EEG data (see Figure 1B). This work was recently published in *Frontiers of Neuroscience* (Choi et al., 2013). Using similar techniques, we have demonstrated the ability to determine what digit a listener is *imagining*. In this study, listeners were given a simple arithmetic problem and asked to imagine the correct

answer, which could be one of three different values. For all tested subjects, classification performance was better than chance. This result demonstrates the potential to decode, in real time, general aspects of listener state.

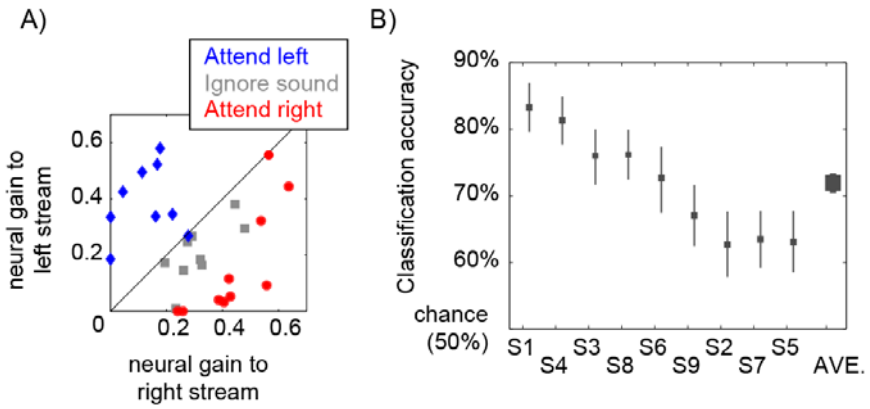

Figure 1. Reading a listener's mind. A) The neural representation of an attended source is enhanced and of a competing source is suppressed, compared to when listeners are engaged in a non-auditory task. In the figure, blue symbols (one per subject) fall above the diagonal, showing that the representation of the left stream is stronger than that of the right stream when listeners attend left; red symbols are below the diagonal, showing the opposite neural gain patterns when subjects attend right; when listeners perform a visual task, the gains are intermediate (grey symbols). B) Using even a simple "generic" pattern classifier not even trained on individual subject data, we can determine which source a listener was attending in under three seconds at levels better than chance for every tested subject, with average performance over 70% correct (adapted from Choi et al., 2013).

We employed magneto-encephalography, which measures the magnetic fields generated by neural activity, to explore the brain networks engaged during attention to different acoustic features. We found that when selective attention is directed to a source with a particular pitch, attentional control signals modulate areas of the cortex that process only auditory inputs. However, for the same mixture of sounds, the control network engaged when listeners direct attention to a source at a particular location overlaps with the control network engaged during visuo-spatial attention. These results, published in *Frontiers of Neuroscience* (Lee et al., 2013), demonstrate that attentional resources work across sensory modality. Our findings help explain why attention to information in one sensory modality interferes with processing of information from a different modality, even though each modality has cortical regions dedicated to processing modality-specific inputs.

We demonstrated that even listeners who have "normal hearing," defined as the ability to detect sounds at the same threshold intensity as an average, healthy young adult, vary enormously in how well they can direct selective auditory attention, work published in the *Journal of the Association for Research in Otolaryngology* (Ruggles, et al., 2011). In a pair of subsequent studies, we showed that these differences are explained by differences in how well clearly audible sounds (supra-threshold sounds) are represented in the auditory periphery (Ruggles, et al, 2011; Ruggles, et al., 2012). These results have important implications for how hearing disorders are diagnosed and treated, as they help to explain why hearing outcomes can differ drastically amongst "normal hearing listeners." In particular, just because different listeners can detect sound at the same low intensity does not mean that their auditory systems are equally good at encoding the fine spectral and temporal detail in sound. These results have special significance for returning war veterans, many of whom suffer from blast exposure and other noise exposure that can damage hearing (indeed, the top-two most common complaints of veterans seeking treatment at VA facilities are for hearing damage and tinnitus, or ringing in the ears, both of which are hearing disorders associated with noise exposure). Our results suggest that hearing

may be damaged in ways that current clinical tests do not specifically identify, and open the way for tests that quantify the fidelity of the auditory system in representing clearly audible sounds like those experienced during ordinary conversations.

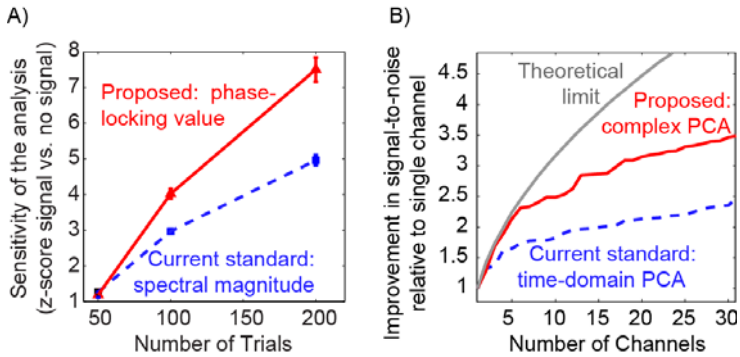

Figure 2. Improving signal-processing methods to extract neural signals from EEG. A) For the same neural data, analysis of the phase-locking value (solid red) is more sensitive than the current standard analysis, which looks at spectral magnitude (dashed blue; adapted from Li et al., in press) B) When combining data across sensors, the theoretical limit (assuming noise is independent in each sensor) cannot be reached (grey); however, analysis that allows different delays of the signal at each sensor gives performance gains much closer to the limit than does the current standard approach for sensor combination (red solid is over dashed blue).

We have developed new signal processing techniques for processing EEG data. In one study, we showed that analysis that looks at the consistency of timing information is more sensitive than analysis analyzing the spectral magnitude of neural responses (see Fig. 2A), work now in press in the *Journal of the Acoustical Society of America*. In a more recent study, we extended standard algorithmsfor combining information to deal appropriately with situations in which a neural signal is observed at different fixed time delays across different sensors. For the same raw data, our approach significantly reduces the number of trials (acquisition time) needed to achieve a desired signal-to-noise ratio (see Figure 2B). This kind of improvement in signal-to-noise ratio is important for developing real-time systems for analyzing and categorizing neural states from EEG responses.

We demonstrated that when there are sound sources coming from different directions, different subsets of neurons in the auditory cortex are biased towards representing each source. This kind of neural segregation can help explain how auditory attention operates. Cortical feedback to these sensory representations, coming from attentional networks in the executive control areas of the brain, can up-regulate the activity of the neural population representing the source at the attended location and down-regulate the activity of the population representing the to-be-ignored source. This work, published in *PLoS Biology* (Maddox et al., 2012), provides key insights into mechanisms of auditory selective attention.

We continue to develop novel methods for analyzing neuroimaging results, applying our knowledge of auditory perception and our signal processing and engineering skills to transform the field of auditory neuroimaging.

Representative Publications:

Ruggles, D.; Bharadwaj, H.; Shinn-Cunningham, B. G. *Proc. Nat. Acad. Sci.* **2011**, *108,* 15516-15521

Maddox, R.; Perrone, B.; Billimoria, C.; Shinn-Cunningham, B. G.; Sen, K. *PLoS Biol.* **2012**, *10*, e1001319

Ruggles, D.; Bharadwaj, H.; Shinn-Cunningham, B. G. (2012). *Curr. Biol.* **2012**, 22, 1417-1422

Lee, A. K. C.; Rajaram, S.; Xia, J.; Bharadwaj, H.; Larson, E.; Hämäläinen, M. S.; Shinn-Cunningham, B. G. *Front. Neurosci.* **2013**, *6*, DOI=10.3389/fnins.2012.00190

Choi, I.; Rajaram, S.; Varghese, L.; Shinn-Cunningham, B. G. *Front. Neurosci.* **2013**, *7*, DOI=10.3389/fnhum.2013.00115

High Strain Piezoelectrics for Miniaturized Actuators and Self-Powered Sensors

Susan Trolier-McKinstry
Penn State, *STMcKinstry@psu.edu*
NSSEFF Award Year: 2009

Project Description:

This is a three-part program to develop (1) next generation high strain piezoelectric films (2) robust processing methods that simplify patterning of complex oxides (3) integration strategies with a wide variety of substrates – including CMOS and polymers. Piezoelectrics are a family of materials that convert between electrical and mechanical energies, so that input strain signals produce an electrical signal for sensors, and input electric fields produce a mechanical deformation. Increased piezoelectric response in thin films boosts the functionality of a wide variety of systems, by providing larger displacements, improves the charge collection efficiency for energy scavenging for unattended sensors, and enables integration of a new set of functional materials with CMOS electronics. This is a cross-cutting program in which advanced materials and materials processing enable breakthroughs in robotics, health care, and persistent surveillance. Among the systems affected by this program are:

- Low voltage, high energy density actuators for rf switches, e.g. for radar systems and electronically steered antennae.
- Self-powered sensors for persistent surveillance.
- Ultrasonic ranging systems for autonomous robots.
- Miniaturized high frequency (potentially wireless) ultrasound system for casualty care, including under battlefield conditions.
- Miniaturized adaptive optics systems for targeting.

Accomplishments:

Piezoelectric Thin Films Materials Development

On this program, we demonstrated the highest known thin film piezeoelectric coefficients for actuator and energy harvesting applications, as shown in Fig. 1. Epitaxial $0.7PbMg_{1/3}Nb_{2/3}O_3$ – $0.3PbTiO_3$ films on Si were shown to have $-e_{31,f}$ coefficients up to 27 C/m^2, measured under strain drive. This exceeds state – of – the art materials by 50%, and conventional piezoelectrics by 4 ×. Strongly imprinted, domain-engineered sputtered $PbZr_{0.52}Ti_{0.48}O_3$ films have figures of merit for piezoelectric energy harvesting, $e_{31,f}^2/\varepsilon_r$ = 1 C^2/m^4, which is a ten fold increase over AlN (the current standard material).

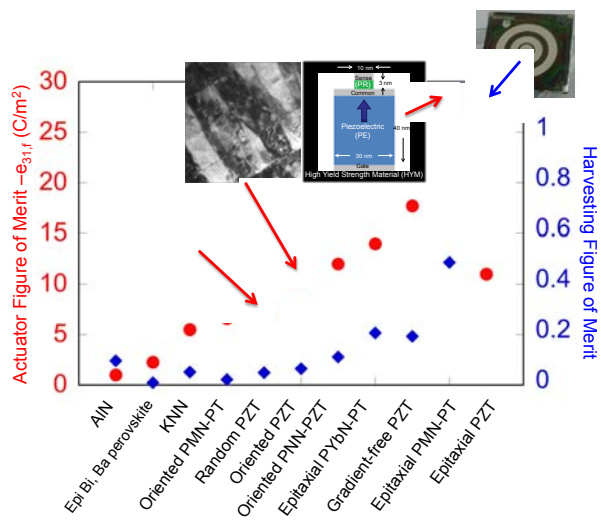

Figure 1. Piezoelectric materials for actuators (red) and energy harvesters (blue), along with examples of uses ranging from next generation X-ray telescopes, to energy harvesters to next generation logic elements

A new measurement method was developed to enable the nonlinear piezoelectric properties to be probed at the nm length scale. It was demonstrated that domain

wall motion occurs in clusters on the 0.5 – 2 μm length scale, significantly larger than the domain size (~tens nm) or grain size (~hundred nm). This demonstrated for the first time that Rayleigh behavior develops due to the cooperative motion of domain walls. Furthermore, it was demonstrated that release of both the local and global stresses in $PbZr_{0.52}Ti_{0.48}O_3$, PZT, thin films, increases both the mobility of domain walls and the length scale over which cooperative motion of walls is observed. For the first time, domain wall mobilities comparable to those of bulk PZT ceramics were demonstrated in thin films.

Finally, it was proven that ZnO thin film transistors can be prepared on PZT films without degradation in the short-term response of either the piezoelectric or the semiconductor. This is an important finding because co-processing of the semiconductor allows local voltage amplification (e.g. from low voltage CMOS electronics) to be performed. Likewise, this will enable local intelligence for control of large arrays of actuators for active and adaptive surfaces, as well as control of active electronics for arrays of energy harvesting devices.

Microcontact Printing of Piezoelectrics

Microcontact printing of chemical precursors to piezoelectric films was demonstrated to provide a high-quality damage-free patterning method for piezoelectric films. Polyurethane stamps (or composite stamps with polyurethane backed by polydimethyl siloxane) were found to enable good wetting of the solutions, and allow printing of features over the size range of a few microns to 1 cm (limited by the original stamp feature size), as shown in Fig. 2. The resulting electrical and electromechanical properties of the films were identical to those of blanket films of the same composition, over a thickness range of 75 – 1000 nm. These data demonstrate that this approach will be extremely useful in preparing inexpensive piezoelectric MEMS devices for switches and energy harvesters, for example.

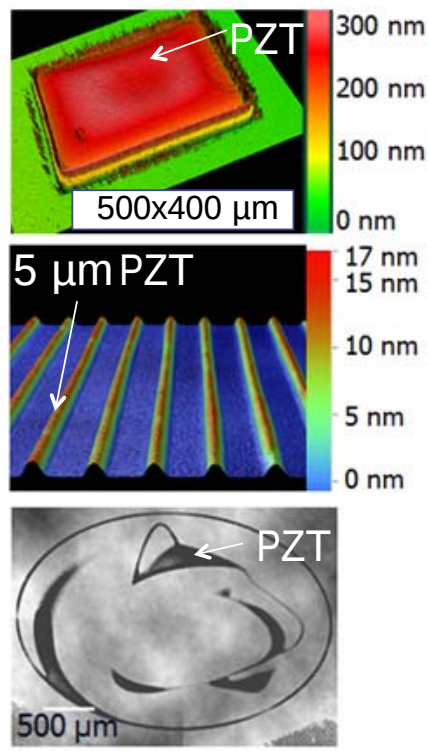

Fig. 2: Examples of microcontact printed PZT features

Integration on Arbitrary Substrates

In order to broaden the range of substrates that could be used for piezoelectric MEMS beyond those which tolerate high temperatures in oxidizing atmospheres, two approaches were adopted: 1) Use of barrier layers that prevent reactions, and 2) *In situ* pulsed laser deposition and annealing. In the first of these approaches, a method was developed for preparing highly oriented, phase pure PZT films on Ni substrates. Ni and PZT are thermodynamically incompatible at processing temperatures. That is, oxygen partial pressures that are adequate to retain oxidized lead zirconate titanate produce NiO at the surface of the metal foils. Conversely, those conditions which produce metallic Ni also reduce the Pb, degrading the piezoelectric properties. Nonetheless, Ni foils are an interesting choice of substrates as they are flexible (which is useful in joints for robotic insects), and they have a high density (which is useful in proof masses for energy harvesting devices). To address this problem, atomic layer deposited HfO_2 was used to protect the Ni foil from high oxygen partial pressures in subsequent annealing. A layer of metallic $LaNiO_3$ was

prepared by chemical solution deposition, and then PZT films were grown by either sputtering or chemical solution deposition. It was found that the resulting films had excellent phase purity, coupled with higher remanent polarizations and lower coercive fields than films on Si substrates. A process for integration of these films into piezoelectric energy harvesting devices is currently being developed.

Secondly, an *in situ* pulsed laser deposition and annealing system was designed and constructed. This system takes the output from an excimer laser and splits it into two beams: one is employed for pulsed laser ablation, while the other is used for laser annealing of the growing film. It was demonstrated that high quality PZT films of 1 μm in thickness can be grown at temperatures as low as 375 °C. For comparison, conventionally prepared films are crystallized at temperature of 650 – 750 °C. This low temperature opens up the possibility of integration of high strain piezoelectric films onto arbitrary substrates (including those with pre-existing CMOS circuitry) or polymers.

Implications of Technologies Developed

The fundamental understandings of piezoelectric response enabled by the NSSEFF funding has opened up the possibilities of scaling high strain piezoelectric thin films over devices with a wide range in length scales. At the longest length scale, we have demonstrated on other funding that piezoelectric MEMS enable an order of magnitude improvement in focusing of X-rays for space telescopes using nested thin flexible glass substrates. Full-scale telescopes made with this approach would require > 10 to ~ 10,000m^2 of actuatable optics, and would produce a revolutionary improvement in scientific data quality. The resulting instruments will be invaluable for studying clusters of galaxies, the first black holes in the universe, X-ray sources in nearby galaxies, and young stars embedded in thick dust clouds. At intermediate length scales (10 μm – 1 cm), a second generation ultrasonic imaging transducer array has recently been fabricated that should ultimately allow ultrasonic pill cameras for assessing gastrointestinal health in every doctors office. The Army Research Laboratory recently demonstrated lift in piezoelectrically actuated insect wings for flying surveillance platforms. At the smallest length scales (~10 to 1000 nm), piezoelectric actuators which induce a change in the electrical resistance of piezresistive thin films have recently been proposed as a post-CMOS technology which could ultimately replace Si for computer and memory platforms. Calculated performance demonstrates an order of magnitude increase in frequency at an order of magnitude lower power than currently available.

Representative Publications:

Bintachitt, P.; Jesse, S.; Damjanovic, D.; Han, Y.; Reaney, I. M.; Trolier-McKinstry, S.; and Kalinin, S. V. *Proc. Nat. Acad. Sci. USA* **2010,** *107,* 7219-7224

Baek, S. H.; Park, J.; Kim, D. M.; Aksyuk, V.; Das, R. R.; Bu, S. D.; Felker, D. A.; Lettieri, J.; Vaithyanathan, V.; Bharadwaja, S. S. N.; Bassiri-Gharb, N.; Chen, Y. B.; Sun, H. P.; Folkman, C. M.; Jang, H. W.; Kreft, D. J.; Streiffer, S. K.; Ramesh, R.; Pan, X. Q.; Trolier-McKinstry, S.; Schlom, D. G.; Rzchowski, M. S.; Blick, R. H. Eom, C. B., *Science* **2011,** *334,* 958-961

Bassiri-Gharb, N.; Trolier-McKinstry, S.; and Damjanovic, D., *J. Appl. Phys.* **2011,** *110* 124104

Griggio, F.; Jesse, S.; Kumar, A.; Ovchinnikov, O.; Kim, H.; Jackson, T. N.; Damjanovic, D.; Kalinin, S. V.; Trolier-McKinstry, S., *Phys. Rev. Lett.* **2012,** *108*, 157604

Eom C.-B.; and Trolier-McKinstry, S., *MRS Bull.* **2012,** *37* 1007-1017

Multi-Physics Simulations of Hypersonic Flows

Graham V. Candler
University of Minnesota, *candler@aem.umn.edu*
NSSEFF Award Year: 2009

Project Description:

The US Department of Defense plans to develop new weapons systems to support prompt global strike, precision strike, and responsive space access. These advanced systems require high-speed flight in the atmosphere, which produces intense aerodynamic heating and an extreme environment. Furthermore, the operation of air-breathing propulsion systems for these vehicles is poorly understood and their design is far from optimal. Ground-based wind-tunnel experiments cannot reproduce the flight environment, and flight experiments are extremely expensive and are often of limited utility. Therefore, future hypersonic weapons systems must be designed with computational methods, and the designs can only be as accurate as the physical models used in the simulations. The NSSEFF research program is systematically addressing critical weaknesses in current hypersonic flow simulations through new physical model development, advanced numerical algorithms, and large-scale first-principles simulations. Major emphasis is placed on validating the simulation results using carefully designed experiments and ongoing Air Force flight experiments. The research has advanced the accuracy of hypersonic flow simulations, and is addressing outstanding puzzles in hypersonic flow physics. Ultimately, it will enable optimized designs of future high-speed weapon systems through large-scale multi-physics simulations.

Accomplishments:

During the NSSEFF program, four topics in hypersonic flow physics have been studied: advanced simulations of air-breathing scramjet engines, analysis of laminar-turbulent transition, high-temperature processes, and shock-dominated flows. In this report, highlights from the first two topics are discussed.

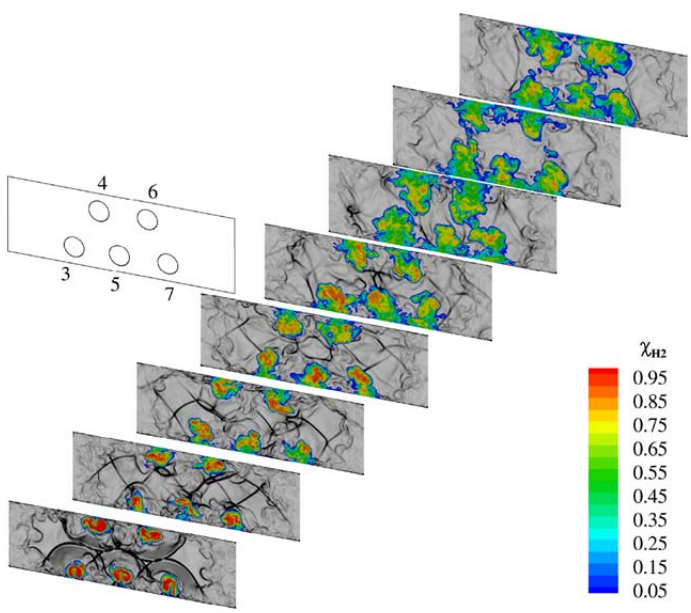

Figure 1. Simulation of H_2 injection into the CUBRC combustion duct through 5 injection ports; gray-scale visualizes shock waves.

Hypersonic air-breathing systems are still in their infancy. For example, there have only been a few flight tests of scramjet-powered aircraft; most notably NASA's X-43 was flown for a short time at Mach 7 and Mach 10. The DoD now has several flight test programs, including the X-51

hydrocarbon-fueled dual-mode scramjet that recently had a second successful flight test. Also, the joint US-Australia HIFiRE program successfully flight tested a novel inlet/engine concept. Even with these successful flight tests, there are still many aspects of air-breathing hypersonic propulsion systems and maneuvering re-entry vehicles that are not understood. Unlike supersonic fighter aircraft, it is not possible to build and fly many prototypes during a development cycle because the time scales and costs would be prohibitive. Thus, the development of future hypersonic weapons systems will rely on modeling and simulation to reduce costs and technical risks.

Under NSSEFF support, we have made great advances in the simulation of turbulent compressible flows at realistic scramjet engine conditions. Figure 1 shows a simulation of the flow in a rectangular duct with five fuel injection ports operating. This flow field is *extremely* dynamic with complex shock interactions and highly unsteady and intermittent plume behavior. This is a wall-modeled large-eddy simulation (WM-LES), in which the near-wall turbulent motion is modeled with a conventional turbulence model, and the large-scale turbulence is resolved. The simulation was performed in three steps: first a simulation of the inlet was used to provide mean turbulent boundary layer data to an unsteady simulation of the isolator. Data were collected and used as inflow to the injector region simulation, which was performed on a grid composed of 138 million hexahedral elements. The near-wall spacing was 0.6 μm, with approximately 14 cells per injector diameter. Second-order accurate implicit time integration was used, allowing much larger time steps (by a factor of 50) to be taken relative to explicit methods. This calculation was run on 1200 2.8 GHz Nehalem cores, and required 14 hours per domain flow-through time. With NSSEFF support, experiments have been performed on this geometry, and simulations are now underway to compare with these data.

Transition to turbulence is a major concern for all hypersonic flight vehicles; when a laminar boundary layer becomes turbulent, the aerodynamic heating increases by about a factor of five. Simple experimental correlations are known to be inadequate and often result in uncertain thermal protection system designs. Furthermore, because the physical mechanisms for transition are not understood, it is impossible to design control schemes to delay or eliminate transition. With NSSEFF support, we have made very significant progress in the prediction of boundary layer stability and transition to turbulence. A new three-dimensional stability code was developed and is now being transitioned to DoD users. We have also developed the ability to perform direct simulations of the transition process. With this approach, the full nonlinear equations are solved on a high-resolution grid using a sixth-order accurate numerical method. Then perturbations are imposed in the free-stream to represent acoustic noise or small surface roughness is added, depending on the problem being studied. In some cases, the flow field is self-excited and no disturbances are required.

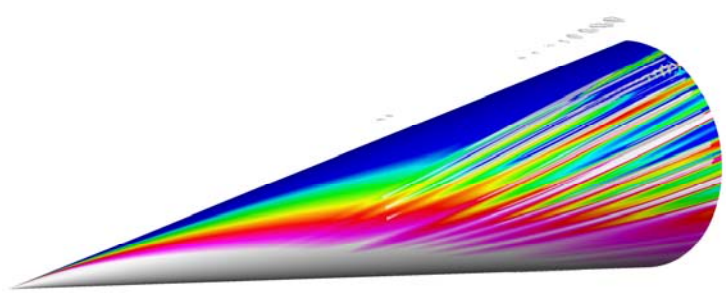

Figure 2. Simulation of crossflow transition on a sharp cone at Mach 6; streaks represent location of crossflow vortices.

A mechanism of transition is crossflow instability that manifests itself as co-rotating streamwise vortices that lead to laminar-turbulent breakdown via a secondary mechanism. Crossflow transition is likely to be important for high-lift extended range re-entry vehicles, as well as for advanced reusable launch systems. Figure 2 shows an example of a direct numerical simulation of crossflow transition on a sharp cone at angle of attack in a Mach 6 flow. Here, small levels of surface roughness are added to the windward side – corresponding to a typical paint finish. The simulation used a sixth-order accurate numerical method on a carefully constructed 140 million element grid. Comparisons with experiments are very good.

Transition to turbulence may also occur when there is a small discrete roughness element protruding into the flow. Large-scale simulations of an experiment conducted at Purdue University were performed with the methods developed under NSSEFF support. Figure 3 is a visualization of the turbulent wake produced by a small cylindrical roughness element. Detailed comparisons with the experiment show excellent agreement for the frequency of the primary instability and its harmonics.

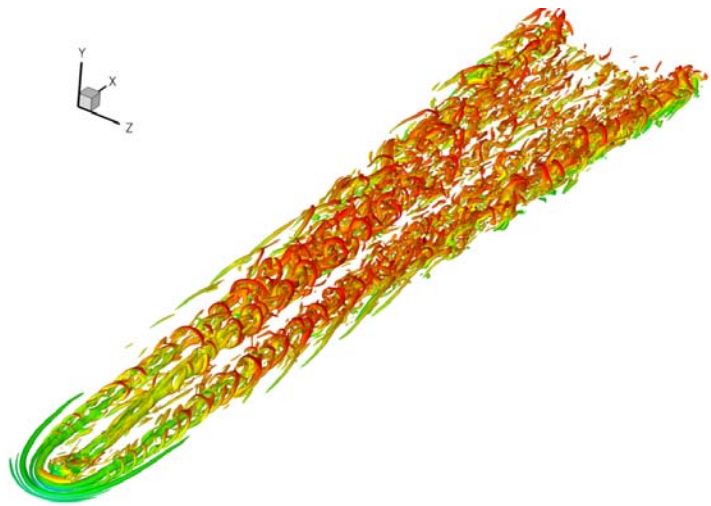

Figure 3. Simulation of boundary layer transition due to a discrete roughness element at Purdue Mach 6 Quiet Tunnel conditions.

The NSSEFF supported the development of advanced methods for the study of transition mechanisms. This work is leading to a better understanding of this long-standing problem, and will ultimately lead to a much more accurate predictive capability.

Representative Publications:

Candler, G.V. *Prog. Aerospace Sci.* **2010**, *46*, 81-86
Peterson, D.M.; Candler, G.V. *AIAA J.* **2011**, *49*, 2792-2804
Gronvall, J.; Johnson, H.B.; Candler, G.V. *AIAA-2012-2822,* **2012**; submitted to *AIAA J.*
Wagnild, R.; Candler, G.V.; Subbareddy, P.K., Johnson, H.B. *AIAA-2012-0922,* **2012**; submitted to *AIAA J.*
Candler, G.V.; Subbareddy, P.K.; Nompelis, I. *AIAA J.* **2013**, *51*, 1245-1254

Manipulating Nearshore Morphology to Determine the Coupling and Feedback Between Waves, Currents, and Bathymetric Change

Steve Elgar
Woods Hole Oceanographic Institution, *elgar@whoi.edu*
NSSEFF Award Year: 2009

Project Description:

Although the path of Hurricane Sandy was predicted accurately, the extreme damage to the shoreline was a surprise. Hurricane Sandy eroded beaches and collapsed homes in Florida, breached a new inlet in Fire Is. that flooded Long Island with every high tide, and eroded almost 100 m of the Martha's Vineyard shoreline, damaging structures. Models have no skill predicting this shoreline change, and thus are of no use to plan for future storms. To be blunt, we still do not have a clue where the sand will go! Although there has been great progress understanding the individual components that combine to produce changes to shorelines, there have been few studies of the coupling and feedbacks between waves, currents, and sediment transport that result in morphological evolution. Owing to logistical difficulties, there are almost no observations of these processes during storms when gradients in fluids and morphology can be huge, causing rapid sediment transport and tremendous shoreline change. After the storm, the morphology becomes smooth, and fluid gradients are small. To investigate the physics that drive shoreline change during storms, my students and I have been creating and monitoring perturbations to the surfzone seafloor. We hypothesize that the perturbations produce storm-like gradients in hydrodynamics and morphology, allowing investigation of these processes without the need to maintain sensors during hurricanes. The perturbations are designed to address hypotheses, with the goal of understanding the physics sufficiently to include it in models. The perturbations include excavating big holes in the surfzone seafloor (Fig 1A, hypothesized to affect waves and currents, and to refill rapidly with sand) and dredging a gap across a surfzone sandbar (Fig 1B, hypothesized to generate a rip current).

Along with determining the physics underlying the coupling and feedbacks between waves, currents, and sediment transport that cause morphological evolution, results from this study will help the development of models that can simulate seafloor change for future scenarios, including more (and stronger) storms, sea level rise, and engineering efforts. In addition to obtaining observations to challenge and improve numerical models, the results from this study will provide information useful to determining the evolution of littoral bathymetry after it has been mapped with remote sensing devices.

Accomplishments:

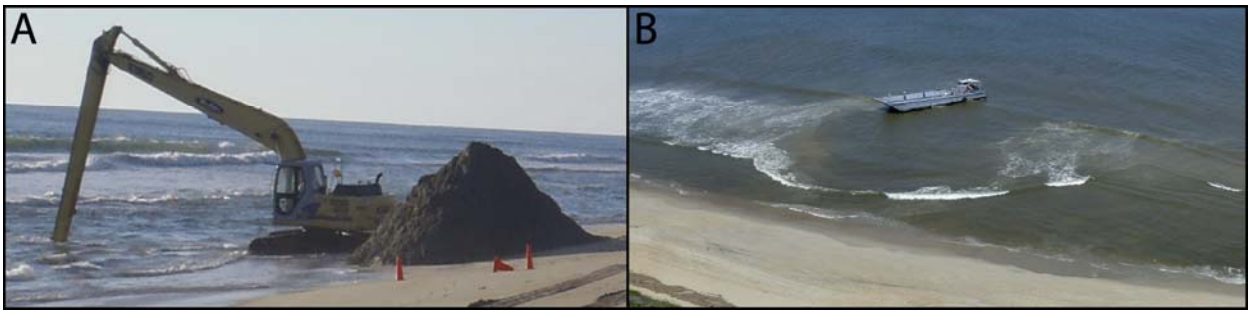

Figure 4. (A) A backhoe adjacent to a pile of sand excavated from the inner surfzone. The hole is beneath the long arm of the backhoe. (B) The propellers of the landing craft were used to dredge a channel across the inner surfzone. Waves refract differently over the deep water in the channel than over the shallower shoals on the sides of the channel, resulting in the curved wave crest onshore of the boat.

PhD Student Melissa Moulton and I excavated several big holes in the surfzone seafloor at the US Army Field Research Facility, Duck NC (Fig 1A). Immediately after the excavation, our team deployed wave and current sensors in and near the hole, and surveyed the bathymetry. The steep-sided holes are similar to steep features formed during storms, and rapidly evolved during large waves from offshore Hurricanes Danielle, Earl, and Igor, Fig 2). In contrast to the common assumption that gravity-driven transport is negligible, Melissa discovered that sediment transported by gravity (grains roll down hill) is the dominant mechanism refilling the steep holes, and thus is important during storms and should be included in models. The observations have allowed Melissa to develop a model for the gravity driven transport (red curves in Fig 2), and to determine the diffusion coefficient as function of waves and currents (Fig 2D).

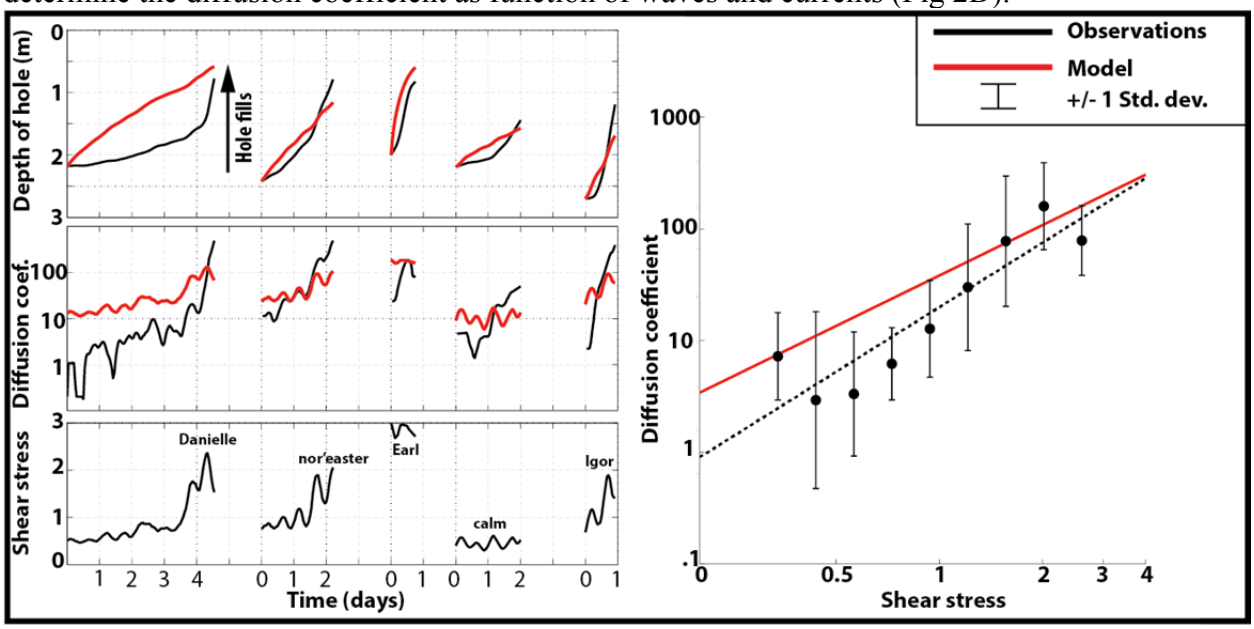

Figure 2. (A) Depth of the hole relative to ambient sand level (m) (arrow indicates the depth of the hole decreasing as the hole fills with sand), (B) diffusion coefficient (arbitrary units), and (C) wave-current shear velocity (arbitrary units, an indication of the strength of wave-orbital velocities and mean currents) *versus* time for each of 5 holes. Black curves are observations and red curves are model predictions. Conditions that generated waves (and bottom shear stress) are labeled with storm names in C. (D) Diffusion coefficient *versus* shear velocity (arbitrary units) for observations (black) and model predictions (red). Vertical bars are +/- 1 std. dev.

Melissa and I also used the propellers from a landing craft (Fig 1B) to dredge trenches across the surfzone seafloor to test hypotheses (Fig 3) for rip currents and sediment transport.

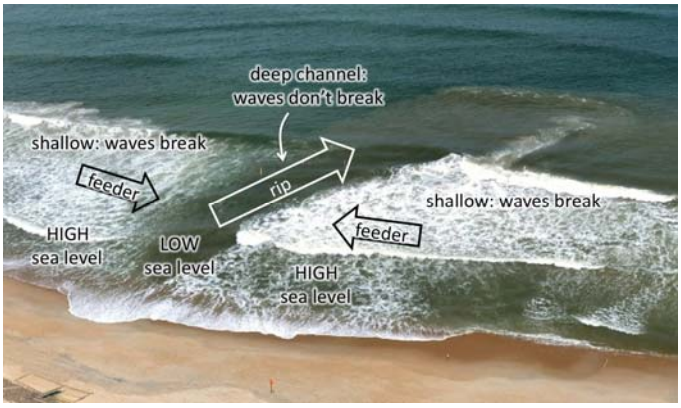

Figure 3. A massive rip current in a dredged channel. Waves break (white foam) on the shoals alongside of the channel, causing a rise in sea level that drives feeder currents that converge at the rip jet. The rip carries sand and bubbles offshore. This may be the longest duration, largest rip observed. Seaward currents varied from 0.3 m/s to more than 1 m/s over several days (Fig 4). The rip carried tremendous amounts of sand (brown water in the rip) that eventually refilled the excavated trench.

If waves were small (Fig 4c) currents flowed alongshore past the trench (Fig 4a, left panel). As waves grew (Fig 4c), a huge rip current was generated (Fig 3, Fig 4a, center panel). The rip carried sediment (Fig 3) that refilled the trench, resulting in decreasing offshore flow until the rip stopped (Fig 4a, right panel). The strong seaward flow was nearly uniform from sea surface to seafloor, with speeds ranging from 0.3 to more than 1 m/s as the tide rose and fell (Fig 4b).

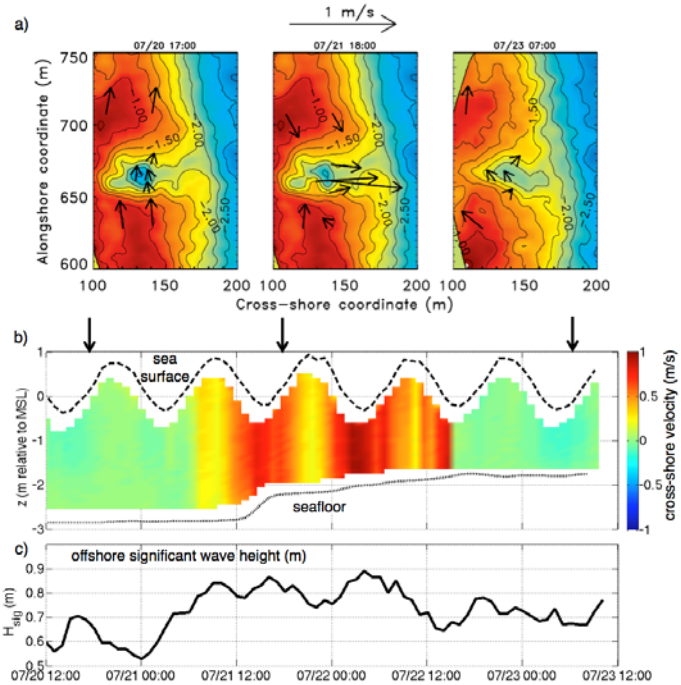

Figure 4. a) Depth of the seafloor (color contours with isobaths every 0.25 m) as a function of alongshore and cross-shore coordinate. Arrows are depth-averaged 1-hr mean flows (scale above center panel). b) 1-hr mean cross-shore flow in the trench center (color bar on right) as a function of elevation z and time (month/day hr:min). The dashed curve above the color contours is the water surface, and the dotted curve below the contours is the evolving seafloor in the center of the trench. The arrows indicate times when horizontal flow structure is plotted in 'a.' c) Offshore significant wave height H_{sig} *versus* time.

Representative Publications [* is student or post-doc]

Gast, R.; *Gorrell, L.; Raubenheimer, B.; Elgar, S. *Cont. Shelf Res.* **2011**, *31*, 1457-1461

Raubenheimer, B.; Ralston, D.; Elgar, S.; *Giffen, D.; Signell, R. *Cont. Shelf Res.*, **2012,** j.csr.2012.02.001

Elgar, S.; Raubenheimer, B.; *Thomson, J.; *Moulton, M. *J. Water., Port, Coast., Ocean Engr.*, **2012**, *138*, 299-302, [Featured as an ASCE "**Reasearch Highlight**."]

*Englestad, A.; Janssen, T.; Herbers, T.; van Vledder, G.; Elgar, S.; Raubenheimer, B.; *Trainer, L.; *Garcia-Garcia, A. *Cont. Shelf Res.* **2012**, *52*, 190-202

***Clark, D.; Elgar, S.; Raubenheimer, B.. (**COVER**) *Geophys. Res. Letts.* **2012**, *39*, L24604

Smart, Autonomous, Adaptive Phenomena in Self-Organizing, Reconfigurable Materials

Sharon C. Glotzer
University of Michigan, *sglotzer@umich.edu*
NSSEFF Award Year: 2009

Project Description:

Next generation materials for defense applications will be distinguished by their ability to adapt in novel ways both on demand and to environmental cues in order to carry out important functions. The ability of materials to perform molecular recognition, autonomously sense and report, or reconfigure to change shape or properties all require that the material's building blocks be able to assemble into target structures that can be "toggled" to other structures.

The fundamental ability of a material's structure to dynamically reconfigure among two or more target structures is predicated on the ability of the structure to self assemble from precursor building blocks whose shapes and interactions conspire to yield the right structure under the right circumstances. The great challenge lies in designing the best building block to optimize assembly, in the absence of a theory of self-assembly connecting building block attributes to assembly structure. Thus, key objectives of this project include: fundamental understanding of the relationship between building block complexity, assembly propensity, and reconfigurability at nanometer-to-micron scales; design rules and experimentally feasible strategies for, and *in silico* demonstration of, the self-assembly of target structures; and the first predictive simulation platform for designing and engineering pathways for assembly of nanoscale building blocks into complex target structures, including those capable of exhibiting reconfigurability for adaptive materials.

Accomplishments:

This NSSEFF award has enabled the discovery of new insights about entropy and its role in how materials self assemble. In particular, we have discovered that entropy can produce "bonds" between nanoparticles as strong as typical chemical bonds, and which are "directional" the way that hydrogen bonds and covalent bonds are between atoms and molecules. Our discovery suggests that entropy is far more important than previously thought in the formation of crystals made of nanoparticles. These "entropic bonds" are so important that entropy alone can be used to make highly ordered crystals with great structural complexity at the one nanometer – 1000 nanometer length scale, allowing new materials with unprecedented properties.

Using a rapid computer-simulation-based screening approach we developed under this program, we are studying in detail over 40,000 different nanoparticle shapes and the crystals and/or the thermodynamic assemblies and packings they form. We discovered many dozens of new crystal structures previously unseen for nanoparticles, many of which have the same structure as (that is, are "isostructural" to) crystals made of atoms and molecules. Examples of crystal structures predicted, by us, for the first time for nanoparticle and colloids include, e.g., diamond, a high-pressure lithium phase with 16 particles in the unit cell, and the Frank-Kasper phases β-Mn, β-U, β-Tungsten and γ-brass. We have predicted the thermodynamic assembly of structures in dozens of space groups, and in systems comprising only one type of shape have found nearly all of the

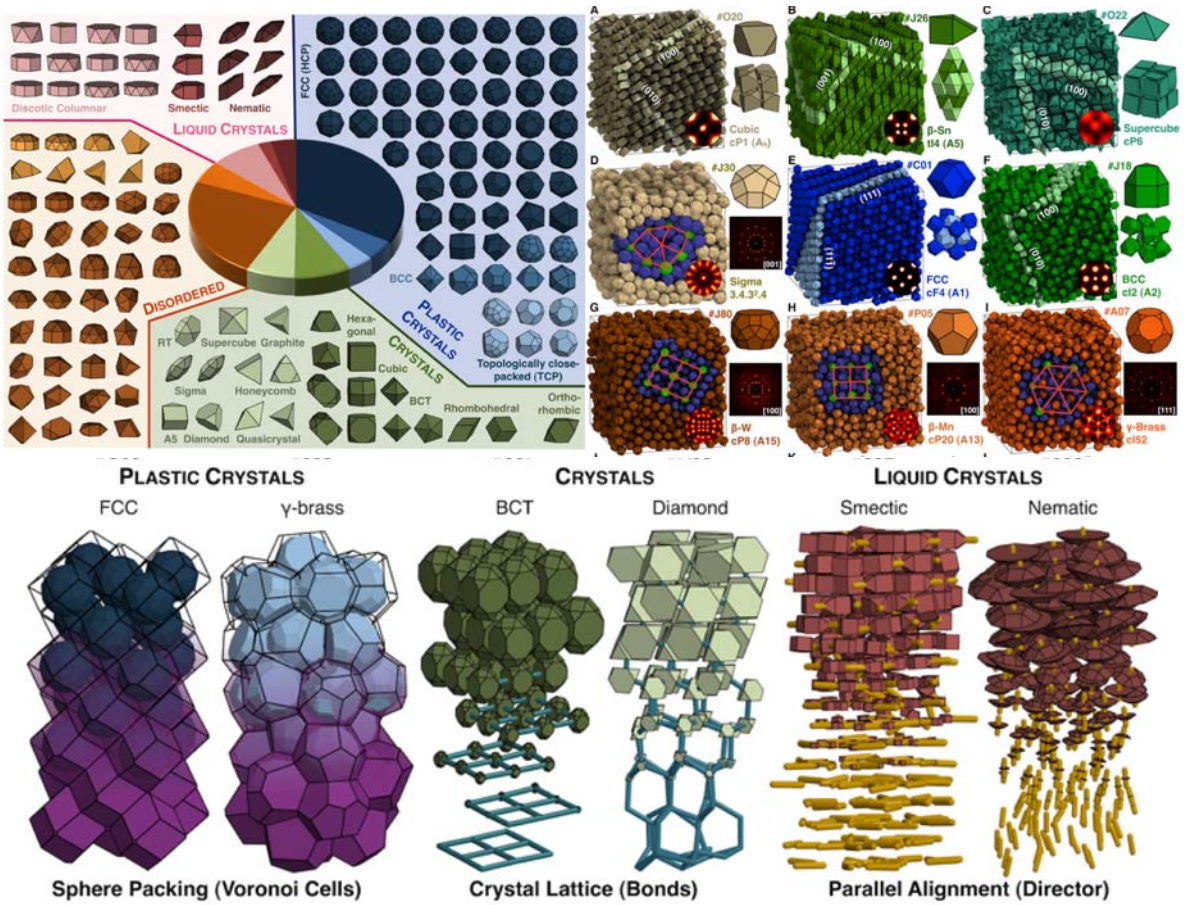

Fig. 1. A major accomplishment of our work under the NSSEFF program. Rapid, high throughput computer simulations predicted assemblies for 145 different nanoparticle shapes (here, polyhedrally shaped.) The four overarching categories of structures predicted include (indicated by different colors): liquid crystals, plastic (rotator) crystals, periodic and aperiodic crystals, and disordered (glassy) phases. Subcategories (classes) are indicated by shades. The assembly category of liquid crystals contains the classes discotic columnar, smectic, and nematic (different shades of pink). Plastic crystal classes are face-centered cubic (dark blue), body-centered cubic (blue), and topologically close packed (light blue). In the case of crystals, we distinguish Bravais lattices (dark green) and non-Bravais lattices (light green). RT stands for random tiling. For the glasses, no assembly is observed, and we distinguish those that strongly order locally with preferential face-to-face alignment (light orange) from those with only weak local order (dark orange). The pie chart (upper left) compares the relative frequency of the ten observed classes. In each of the classes, polyhedra are listed in decreasing order of the isoperimetric quotient, a measure of the particle's shape. A polyhedron is included multiple times if it was found to assemble into more than one ordered structure. Examples of the various crystal and other structures are shown in upper right. Lower half of figure shows the strong influence of directional entropic "bonding" in the case of non-plastic crystals and liquid crystals, and analogies with traditional materials bonding classes. From Damasceno, Engel & Glotzer, *Science* 2012.

14 Bravais lattices. Our studies show, for the first time, the enormous complexity of assembled structures possible solely through entropic "forces". They also isolate the role of shape and entropy from other interactions, allowing the determination of the relative contributions of entropy and enthalpy to self-assembly.

By mining the unprecedented amount of data we generated on assemblies of hard polyhedrally shaped particles, we discovered a strong correlation between particle shape and the local fluid structure prior to assembly. Based on this correlation, we are now able to predict aspects of expected crystal structure from particle shape and information easily and quickly ascertained from relatively quick and easy fluid simulations. Our predictions have since been confirmed on several nanoparticle systems both in experiment and simulation.

We discovered directional entropic bonding in nanoparticle and colloidal crystallization arising solely from particle shape as the underlying mechanism for the shape-structure correlation we observed. Entropy is related to the number of available microstates of a system, which in the presence of solely steric (hard) interactions, is equivalent to the available free volume. Though it has previously not be considered as a "directional" quantity, we have been able to show that particle shape can induce directional entropic "forces" between particles that serves to align and order them. We quantified the magnitude of the entropic forces through an analytical formulation of a potential of mean force and torque, and showed them to be of the order of several kT, on par with other forces in soft matter, such as van der Waals interactions, hydrophobic interactions, and hydrogen bonding. This means that entropy can be a key, determining factor in nanoscale assembly depending upon building block shape and the presence or absence of enthalpic interactions.

To exploit directional entropic forces for assembly engineering of target structures, we recently proposed *entropically patchy particles* as the entropic counterpart to enthalpically patchy particles, an idea we put forward in 2003/2004 as a unifying concept for self-assembly. Entropically patchy particles directly relate shape, entropy, and assembly in colloidal matter, revealing a deep connection between the shapes of nanoparticles and the structures they arrange into and giving materials researchers a new "knob" to tune in materials design and synthesis. The connection is robust enough to allow the first ever predictions of structures that will form from nanoparticles of a given shape. Our predictions are now guiding and influencing experimental research in the US, Europe, and Asia. Ongoing work includes theoretical and computational work elucidating particle "effective" shape and mappings to achievable potentials of mean force and torque, designing optimal assembly pathways, and developing rapid screening and analysis algorithms and tools for assembly engineering.

Representative Publications:

1. P.F. Damasceno, M. Engel and S.C. Glotzer, *Science*, **2012**, *337*, 453-457.
2. P.F. Damasceno, M. Engel and S.C. Glotzer, *ACS Nano*, **2012** *6* (1), 609–614.
3. E. Jankowski and S.C. Glotzer, Soft Matter, **2012,** 8 (10), 2852-2859. Selected as "Hot Article."
4. Xingchen Ye, Jun Chen, Michael Engel, Andres J. Millan, Wenbin Li, Liang Qi, Guozhong Xing, Joshua E. Collins, Cherie R. Kagan, Ju Li, Sharon C. Glotzer and Christopher B. Murray, *Nature Chemistry* (cover article), May 12, **2013**.
5. G. van Anders, K. Ahmed, R.J. Smith, M. Engel and S.C. Glotzer, "*Entropically patchy particles*," Physical Review Letters, under review.

3D Nanophotonics: Bending Light in New Directions

Naomi J. Halas
William Marsh Rice University, *halas@rice.edu*
NSSEFF Award Year: 2009

Project Description:

This program established a major comprehensive research program in the nanoengineering of artificial electromagnetic materials at infrared and optical frequencies to broaden and redefine the capabilities and functionality of nanoengineered structures. The research supported is helping to create a new generation of functional photonic materials that interact with light in new and nonintuitive ways.

The design and fabrication of the photonic nanostructures is closely coupled to theory and multiscale modeling of the nanostructures. Extensive optical and structural studies are used as input to theoretical simulations. The major directions of research are:

1. to develop ***photonic materials with entirely new functional behavior*** based on ***three-dimensional reduced-symmetry metallic nanostructures*** and their unique light-interacting properties;
2. to understand, design and fabricate ***nanoengineered nonlinear optical materials*** based on utilizing the resonant responses of reduced-symmetry nanotructures and their assemblies;
3. to develop ***new responsive photonic materials based on coherent phenomena***, by engineering nanoscale optical elements and their assemblies to exhibit subradiance and superradiance, Fano resonances, and electromagnetically induced transparency (EIT);
4. to design and experimentally realize ***practical metafluids***- liquids or amorphous materials with metamaterial properties independent of polarization or orientation dependence.

Accomplishments:

Photodetection with active optical antennas: We have developed a new mechanism for light detection of specific wavelengths, or "colors", by combining nanoscale antennas directly with semiconductor Schottky diode detectors into a single nanoscale device, a "Nanoantenna-diode".[1] Light detection relies on the plasmons generated in the nanoantennas decaying into hot electrons which directly convert an incident photon into an electrical current. Our initial design for this device

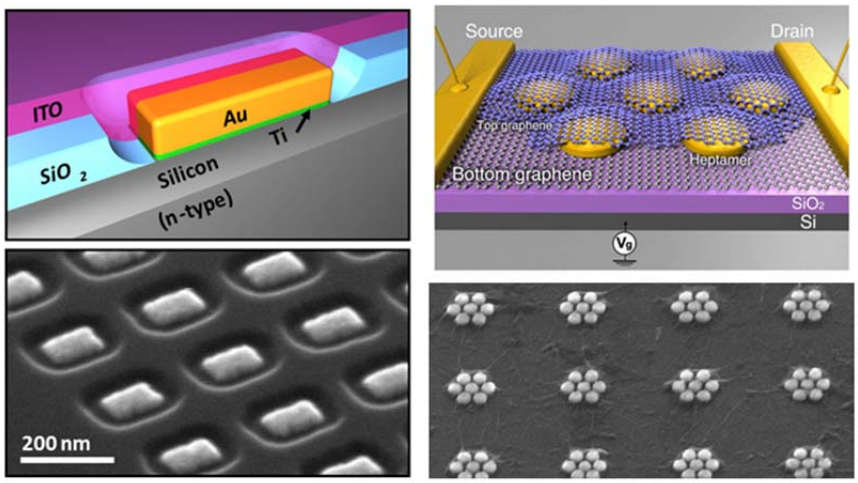

Nanoantenna-diode based devices: a new mechanism for photodetection. Left, top: Representation of a single Au resonant antenna on a silicon substrate. Left, bottom: Scanning electron micrograph of a representative device array imaged at a 65° tilt angle. Right, top: a hybrid plasmonic nanoantenna-graphene based sandwich device. Right, bottom: IR nanoantennas sandwiched between two graphene layers of the device.

consisted of a plasmonic nanorods deposited on silicon. This device detection infrared light below the bandgap of silicon, at wavelengths controlled by the dimensions of the nanoantennas. We have also demonstrated an analogous graphene-based device, where the antennas are sandwiched between two sheets of graphene, injecting hot electrons from the antennas into the graphene device.[2] The latter device demonstrated an internal quantum efficiency of nearly 20%. This light-detecting mechanism can be tuned into the infrared region of the spectrum with these materials, into wavelength regions where costly materials are typically in use.

Three dimensional nanostructures as highly efficient generators of second harmonic light: Plasmonic nanostructures enable the generation of large electromagnetic fields confined to small volumes, potentially providing a route for the development of nanoengineered nonlinear optical media. A metal-capped hemispherical nanoparticle, also known as a nanocup, can be used to generate second harmonic light with increasing intensity as the angle between the incident fundamental beam and the nanocup rotation axis is increased.[3] In this study we generate second harmonic UV light from individual, oriented nanocups whose magnetic dipole plasmon resonance is tuned to the wavelength of incident, fundamental light. We show that by orienting the nanoparticle with respect to incident light, the observed SHG intensity is greatly increased as the 3D symmetry of the nanostructure is reduced, relative to the symmetrically oriented nanoparticle. Nanoparticle orientation also modifies the emission direction of the second harmonic generated light, which is close to, but not precisely directed along, the nanocup axis of symmetry. With conversion efficiencies much larger than those observed for planar structures and similar to nonlinear crystals in widespread use, the structural motif used in this study paves the way for synthetic, "engineered" second-order nonlinear optical materials to replace current nonlinear crystalline materials grown by traditional methods. In addition this capability enables the design of nonlinear optical materials for currently inaccessible wavelength regions of the spectrum where no naturally-occurring materials with these capabilities exist.

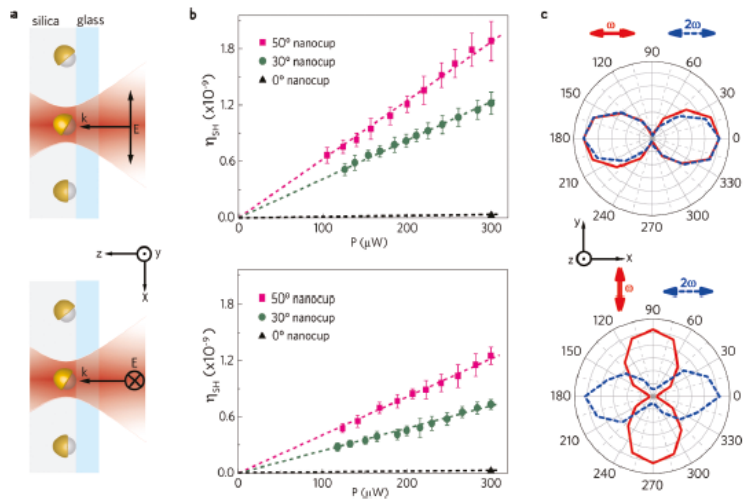

Engineered nonlinear optical materials for second harmonic generation. Nanocups with magnetic plasmon resonances tuned to the wavelength of incident laser light generate second harmonic light at efficiencies as good as inorganic crystalline materials typically in widespread use.

The engineering of optical line shapes using Plasmonic clusters with Fano resonances: Here we examined the plasmonic properties of planar nanoclusters, focusing on arrangements of coupled nanodisks consisting of a central particle surrounded by a ring of peripheral particles.[4,5] We observed that the depth and width of the FR can be controlled by varying the relative size of the inner particle with respect to the surrounding particles. We also observed that the FR is characteristic of optical excitation of this structure. Excitation by a localized electron beam on various components of the structure does not result in a Fano resonance in the cathodoluminescence spectrum, but instead results in the selective excitation of the center disk mode or the peripheral ring mode of the complex. This contrasting behavior can be understood through the coupling between the superradiant and subradiant modes of the cluster, where the contrasting selection rules of optical and e-beam excitation give rise to different superpositions of radiant modes in the corresponding spectra. In this system, cathodoluminescence allows us to "deconstruct" the Fano resonance into distinct superpositions of superrradiant and subradiant modes not observable by optical means. This analysis gives new insight into the interplay between the subradiant and superradiant modes in coherent plasmonic systems. This work paves the way for new classes of both passive and active optical materials for a wide range of commercial as well as defense applications.

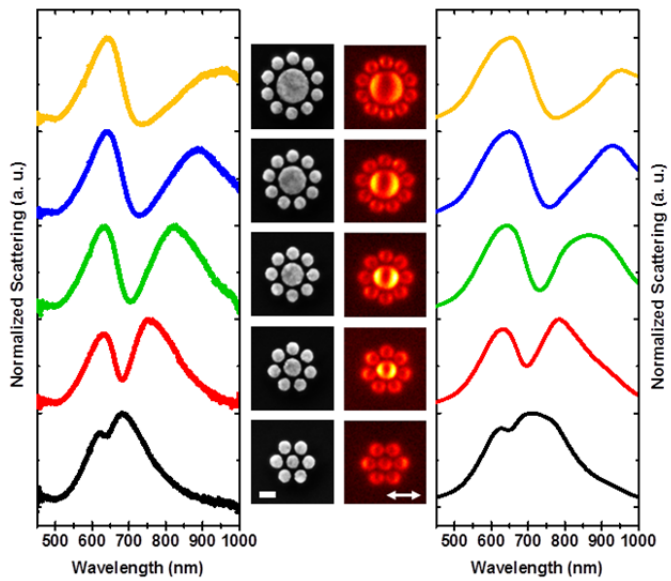

Engineering Electromagnetically Induced Transparency and Fano Resonances in plasmonic clusters: Left: experimental scattering spectra of the clusters shown (Center panels). Right: numerical simulations show predictive capabilities of lineshape engineering at optical frequencies with plasmonic clusters

Representative Publications:

1. Knight, M. W.; Sobhani, H.; Nordlander, P.; and Halas, N. J.; *Science* **2011**, 332, 702-704.
2. Zheyu Fang, Zheng Liu, Yumin Wang, Pulickel M. Ajayan, Peter Nordlander, and Naomi J Halas, *Nano Letters* 12, 3808-3813 (2012).
3. Yu Zhang and N. J. Halas,; *Nano Letters* 11, 5519-5523 (2011).
4. Fan, J. A.; Wu, C. H.; Bao,K.; Bao, J. M.; Bardhan, R.; Halas, N. J.; Manoharan, V. N.; Nordlander, P.; Shvets, G.; and Capasso, F.; *Science* **2010**, 328, 1135-1138.
5. B. Lassiter, Heidar Sobhani, Mark W. Knight, Witold S. Mielczarek, Peter Nordlander, and Naomi J. Halas, *Nano Letters* 12, 1058-62 (2012).

Atomic de Broglie Wave Navigation Sensors

Mark Kasevich
Stanford University, *kasevich@stanford.edu*
NSSEFF Award Year: 2009

Project Description:

We seek to advance the state-of-knowledge for precision de Broglie wave atom interferometry. We are pursuing work which offers the prospect of disruptive performance improvements for precision inertial force sensors, including gravimeters, accelerometers, gyroscopes and gravity gradiometers. Our five year goal is to realize a 1000x advance in the current performance limits for atom-based laboratory instruments, by exploiting innovative atom optics technologies and methodologies. We will validate these advances with fundamental studies of gravitational physics (test of Newton's inverse square law, the Einstein Equivalence Principle, and tests of General Relativity). We will explore new de Broglie wave interferometry approaches involving the production and interference of atomic solitons in Bose-Einstein condensed systems. Soliton-based configurations may enable compact, high performance, sensors.

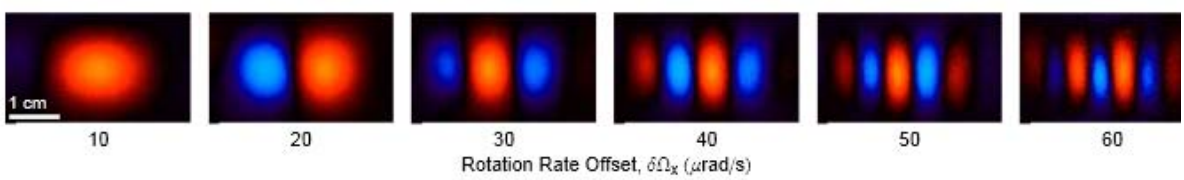

Fig. 1. Images of interference fringes obtained from interfering ensembles of ultra-cold Rb atoms after wavepackets have been separated by a distance of 1.4 cm. Fringe periodicity is determined by the effective rotation rate of the laser beams used to coherently manipulate the atomic wavepackets. For this data, atoms were cooled to temperatures of 50 nK via Bose-Einstein condensation and launched on nearly 10 m high ballistic trajectories lasting 2.3 seconds. False coloring denotes the atomic density (blue is low density, red is high density).

Accomplishments:

We demonstrated new technologies and methods for atom de Broglie wave interferometry that have enabled orders of magnitude improvement over the existing state-of-the-art. For example, we have demonstrated atom interferometric accelerometers which have achieved effective accelerometer noise levels of 7×10^{-12} g in a 2.3 sec measurement time (500x improvement over previously published limits based on atom interferometry) and atom optics methods capable of imparting coherent velocity impulses of nearly 0.5 m/sec on atomic wavepackets (previously limited to ~ 1 cm/sec). We demonstrated new atom optics sensing modalities, including a precision gyrocompass, which achieved 10 millideg precision in determination of true north, and proposed atom interferometry configurations capable of detecting gravitational radiation. Fig. 1 shows characteristic de Broglie wave interference fringes.

We developed a facility which allows design and testing of novel, ultra-precision, atom interferometer inertial sensing protocols (shown in Fig. 2). The facility is based on a 10 m evacuated tower which allows more than 2 sec of inertial free fall time. We exploited this facility to demonstrate rotation, acceleration and gravitational sensing protocols which substantially extend the current state-of-the-art. Our approach is based on sequences of multi-photon Bragg and Raman transitions in combination with optical lattice manipulations. These transitions are driven by a high power laser system which has achieved 43 W quasi-CW power levels. Low phase noise, frequency agile control is achieved using electro-optic frequency tuning and laser stabilization to high finesse optical cavities (our inferred laser linewidth is ~100 Hz). High signal-to-noise levels are obtained using low temperature (as cold as 3 nK), high number (~10^7 atoms) atomic sources. Interferometry is realized in an apparatus capable of supporting nearly 3 sec measurement times, and which can provide an excellent proxy to the conditions expected for space-borne sensors (where the lack of a gravitational bias enables longer measurement times). The apparatus is fully magnetically shielded (~100 microGuass over 10 m) and located in a vibrationally quite (<10^{-8} g/Hz$^{1/2}$ at 1 Hz) environment. We can actuate and control laser pointing stability at the nrad/sec level (using a piezo-electrically controlled mirror), which allows detailed study of the impact of pointing jitter on sensor performance. The performance levels recently obtained in our laboratory exceed levels demonstrated in any other laboratory a factor of more than 500. This gap results from the availability of long free-fall times, our ability to precisely compensate the rotation of the Earth through dynamic control of the sensor input axis at the nrad level, and the use of an ultra-cold (Bose-Einstein condensed), high flux atomic source.

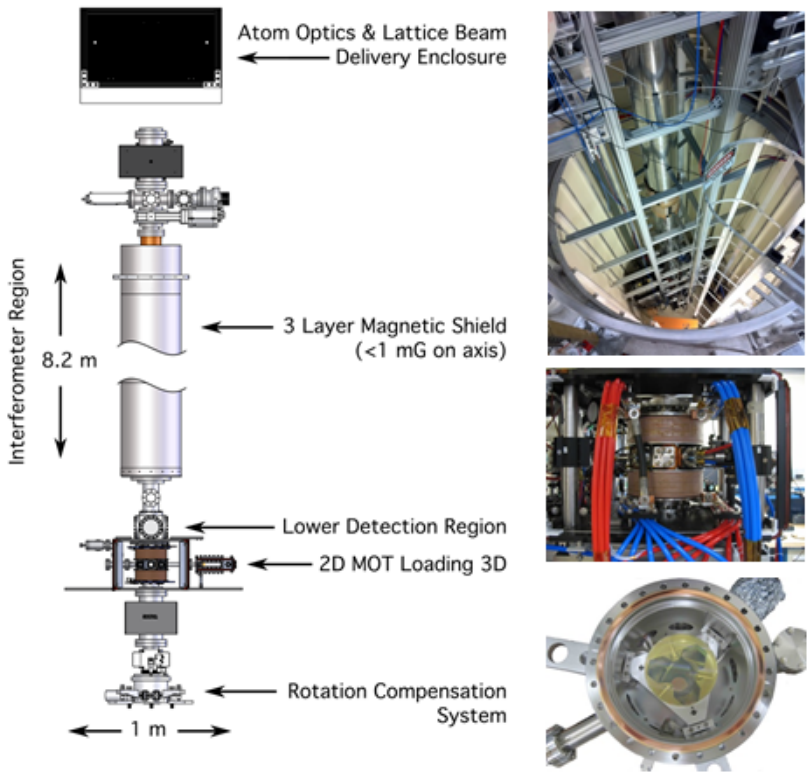

Fig. 2. Illustration of the atom interferometry facility. (Left) Schematic representation of the apparatus, including, from bottom to top, the precision tip-tilt stage (rotation compensation system), atom source, 8.2 m, magnetically shielded interrogation region, and the opto-mechanics enclosure for the delivery of the required laser beams. (Right) Images of representative sub-systems, including the rotation compensation system (lower), atom source (middle) and magnetically shielded vacuum system (upper).

Our work has pushed the interface between quantum physics and the macro-world to new limits. For example, we have observed atom de Broglie wave interference under conditions where atomic wavepackets separate for distances of centimeters over time scales of seconds (in the final year of this program, we hope to push wavepacket separation to meter scales). We have shown that atomic solitons,

comprised of ensembles of hundreds of Li atoms, can behave as a single quantum object – represented by a center-of-mass wavefunction – that time evolves according to the basic laws of quantum mechanics. Most recently, for example, we have observed the center-of-mass diffraction of a single atomic soliton wavepacket (Fig. 3), and demonstrated that our soliton preparation scheme is capable of preparing near uncertainty principle limited wavepackets (e.g. the momentum spread of the soliton wavefunction is related to its inferred size via the Heisenberg uncertainty relations). We are tantalizingly close to realizing a proof-of-concept soliton interferometer. In some sense, observation of wavepacket diffraction at the Heisenberg limit could be considered a first demonstration of such an interferometer.

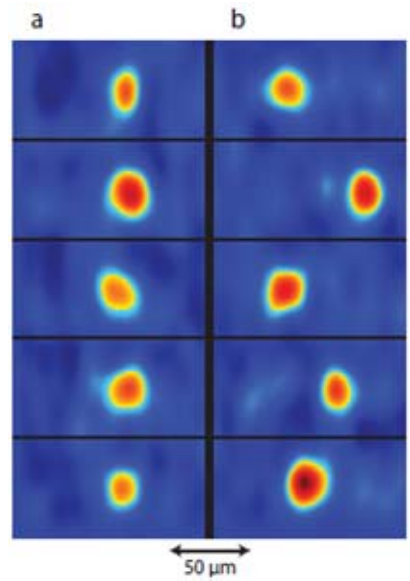

Fig. 3. False color images representing the diffraction of the center-of-mass wavefunctions for Li atomic solitons. (a) Observed soliton positions immediately after release from a confining potential. (b) Observed positions 60 msec after release from the confining potential. Jitter in position is due to the expansion of the soliton wavefunction.

Finally, we have demonstrated supporting photonics technologies that enable advanced atom interferometry methods. These have including demonstration of high power, precision laser systems (43 W, kHz linewidth), serrodyne frequency shifting techniques, and precision angle sensors (1×10^{-12} rad/Hz$^{1/2}$ sensitivity).

Representative Publications:

Sugarbaker, A., Dickerson, S. M., Hogan, J. M., Johnson, D. M. S. & Kasevich, M. A., Enhanced atom interferometer readout through the application of phase shear. *arXiv:1305.3298* (2013), submitted to *Phys. Rev. Lett.*

Dickerson, S. M., Hogan, J. M., Sugarbaker, A., Johnson, D. M. S. & Kasevich, M. A., Multi-axis inertial sensing with long-time point source atom interferometry. *arXiv:1305.1700* (2013), submitted to *Phys. Rev. Lett.*

Graham, P. W., Hogan, J. M., Kasevich, M. A. & Rajendran, S. A, New Method for Gravitational Wave Detection with Atomic Sensors, *Phys. Rev. Lett.,* **110**, 171102 (2013).

Chiow, S., Kovachy, T., Chien, H.-C. & Kasevich, M. A., 102ħk Large Area Atom Interferometers, *Phys. Rev. Lett.* **107,** 130403 (2011).

Vrijsen, G., Hosten, O., Lee, J., Bernon, S. & Kasevich, M. A., Raman Lasing with a Cold Atom Gain Medium in a High-Finesse Optical Cavity, *Phys. Rev. Lett.* **107,** 063904 (2011).

One-Dimensional Nanostructures as Building Blocks for Functional Electronic and Bioelectronic Materials

Charles M. Lieber
Harvard University, *cml@cmliris.harvard.edu*
NSSEFF Award Year: 2009

Project Description

The proposed research focuses on one-dimensional (1D) nanostructures as a broad science and technology platform. These 1D nanostructures – nanowires – are explored as building blocks for functional electronic and bioelectronic materials, with emphasis on developing efficient nanoscale power sources and ultrasensitive, low-power biocompatible nanosensors, together with the heterogeneous two- and three-dimensional assembly of these distinct nanoelectronic elements to yield self-powered functional electronic nanosystems. The scientific and technical approach involves highly interdisciplinary research focused on (i) design, synthesis and structural characterization of nanowire heterostructures with structure/composition variation at the nanometer scale to control specific properties, (ii) nanostructure device fabrication and characterization of fundamental electronic properties, power conversion efficiencies and detection sensitivities, (iii) development of directed assembly strategies capable of multi-step transfer of one or more key nanostructures into controlled size and density arrays on rigid and flexible chips, and (iv) design, assembly, heterogeneous integration and characterization of self-powered nanosystems.

This research will pioneer new classes of functional nanostructures for electrical power generation and ultrasensitive electronic nanosensors on biocompatible chips, and define the fundamental and potentially unique limits achievable through the use of nanostructured materials. In addition, the assembly of self-powered nanosystems will break new ground in the field of nanoscience and point the way toward future applications such as widely dispersed biosensors for monitoring of physiological function and/or trauma treatment in war-fighters, and threats critical to national security. The interdisciplinary approach also will lead to broad and innovative training of next-generation scientists and engineers central to our future technological strength.

Accomplishments

We have made substantial progress in several distinct areas of our NSSEFF program, including (i) Design, synthesis and characterization of novel nanowire heterostructures for photovoltaics, (ii) Design and development of new nanoelectronic bioprobes that can blur the distinction between digital electronics and living matter, and (iii) Cyborg tissues. A summary of advances in these areas follows.

Nanowire-based photovoltaic power elements. We have developed synthetic methods to prepare the first radial or coaxial single-crystal nanowire heterostructures with the general structure p-core/i-shell/n-shell, where p, i, and n refer to p-type, intrinsic and n-type doping, respectively. Following up on our initial electron microscopy work demonstrating that single-crystalline materials with the coaxial structural motif could be synthesized, we prepared a series of coaxial nanowire materials to elucidate fundamental factors controlling efficiency and power output in nanoscale photovoltaics. Specifically, we completed the synthesis and fabrication of p/n, p/i/n, p/p/n and p/p/i/n coaxial devices and characterized their photovoltaic properties at the single nanowire level. These results show clearly that we can synthetically manipulate, in a positive manner, the open-circuit voltage and short-circuit current density via our unique strategy; moreover, analysis of these data demonstrates that the increases in voltage can be attributed to improved interface quality in our coaxial nanostructures. In addition, we have carried out the first single-nanowire wavelength-dependent *absolute* photocurrent measurements. Significantly, these measurements (Fig. 1) reveal size-tunable optical resonances, external quantum efficiencies greater than unity, and current densities double those for silicon films of comparable thickness. In addition, finite-difference-time-domain (FDTD) simulations for the measured nanowire structures agree quantitatively with the

photocurrent measurements, and demonstrate that the optical resonances are due to Fabry-Perot and whispering-gallery cavity modes supported in the high-quality faceted nanostructures [Kempa *et al.*, *Proc. Natl. Acad. Sci. USA* **2012**, *109*, 1407].

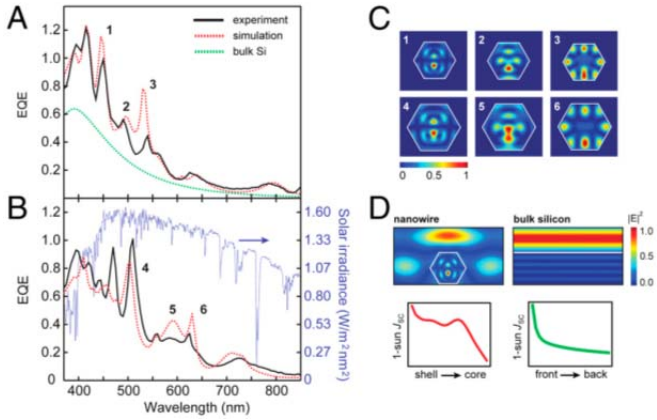

Fig. 1. Enhanced and tunable absorption in nanowires (NWs). (A) External quantum efficiency (EQE) as a function of wavelength for a p⁄in NW (black curve) and simulated EQE spectrum (dashed red curve). Dashed green curve shows the simulated spectrum for same thickness of bulk Si. (B) Measured (black curve) and simulated (red curve) EQE spectrum of a p⁄pin NW compared to the irradiance of the AM1.5G solar spectrum (dashed blue curve). (C) FDTD simulations of resonant mode spatial profiles. (D) Electric field intensity for plane wave interacting with a NW (Left) and bulk Si (Right).

Novel nanoelectronic bioprobes. The past three-plus decades of microelectronic and nanoelectronic work have focused on planar or two-dimensional (2D) device designs. Such structures have necessitated applications in biology focused on 2D sensing and extracellular recording, despite the inherently three-dimensional (3D) structure of biological systems. We have now shown that this limitation can be overcome in a general manner through synthetic integration of nanoscale field effect transistor (nanoFET) devices at the tips of hairpin-like kinked nanowires, where nanoscale connections are made by the arms of the kinked nanostructure and remote multilayer interconnects allow 3D probe presentation. The acute-angle probe geometry represents a breakthrough realized by demonstrating the first controlled synthesis of *cis* versus *trans* crystal conformations in any nanomaterial, and the nanoFET was localized via modulation doping. 3D nanoFET probes exhibited conductance and sensitivity in aqueous solution independent of large mechanical deflections, and demonstrated high pH sensitivity. Additionally, 3D nanoprobes modified with phospholipid bilayers can enter a cell with minimal disruption to allow robust recording of the intracellular potentials of living and electrically excitable cells in a highly detailed manner (Fig. 2). Specifically, these results confirm that electrical recording arises from the highly-localized, point-like nanoFET near the probe tip, which (a) initially records only extracellular potential, (b) simultaneously records both extracellular and intracellular signals as the nanoFET spans the cell membrane, and (c) records only intracellular signals when fully inside the cell. This work was published in *Science* [Tian *et al.*, *Science* **2010**, *329*,830]. Our new nanoprobes exhibit clear advantages over existing techniques, including: recording with kinked nanowire probes is relatively simple, without the need for resistance or capacitance compensation; the nanoprobes are chemically less invasive than pipettes as there is no solution exchange; the small size and biomimetic coating minimizes mechanical invasiveness; and the nanoFETs have high spatial and temporal resolution for recording. Last, these new nanoFET probes allow us to blur the distinction between digital electronic devices and living biological matter and open up many opportunities in both fundamental and applied science.

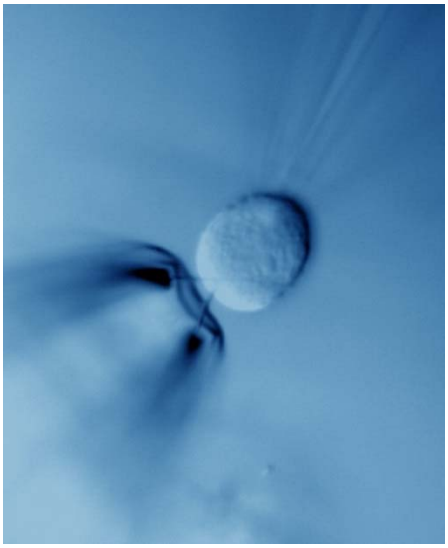

Fig. 2. Optical microscopy image of showing a kinked nanowire nanoelectronic probe inserted into an HL-1 cardiac cell.

Cyborg tissues. The development of three-dimensional (3D) synthetic biomaterials as structural and bioactive scaffolds is central to fields ranging from cellular biophysics to regenerative medicine. As of yet, these scaffolds cannot electrically probe the physicochemical and biological micro-environments throughout their 3D and macroporous interior, although this capability could have a marked impact in both electronics and biomaterials. We have recently made a major advance by addressing this challenge with the introduction of a new form of electronics – macroporous, flexible and free-standing nanowire nanoelectronic scaffolds (nanoES), and the seamless merger of the nanoES with synthetic or natural biomaterials to create innervated synthetic or cyborg tissues. 3D macroporous nanoES mimic the structure of natural tissue scaffolds, and are formed by self-organization of coplanar reticular networks with built-in strain and by manipulation of 2D mesh matrices. NanoES exhibit robust electronic properties and have been used alone or combined with other biomaterials as biocompatible extracellular scaffolds for the 3D culture of neurons, cardiomyocytes and smooth muscle cells. Additionally, we show the integrated sensory capability of nanoES by real-time monitoring of (i) the local electrical activity within 3D nanoES/cardiomyocyte constructs, (ii) the response of 3D nanoES-based neural and cardiac tissue models to drugs, and (iii) distinct pH changes inside and outside tubular vascular smooth muscle constructs. The nanoES concept and implementations described here represent a new direction in merging nanoelectronics with biological systems, since the 3D macroporous material/device platform we have demonstrated is distinct from either engineered tissue or flexible electronics. Looking forward, there are several areas to develop. Cell interactions with nanoES could be tuned by modification of the nanoES with growth determinants. In addition, elements in the nanoES could be expanded to incorporate nanoscale stimulators and stretchable designs to provide electrical and mechanical stimulation to enhance cell culture.

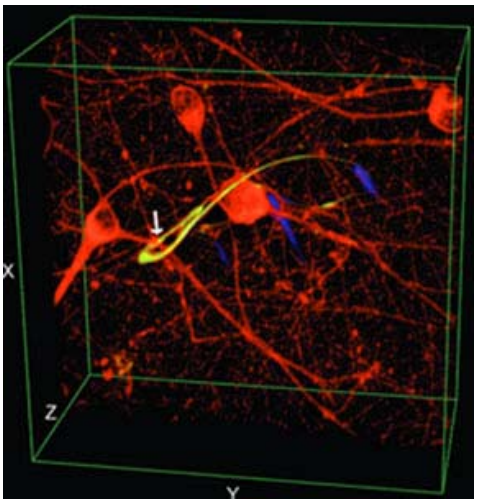

Fig. 3. Reconstructed 3D confocal microscopy image of cyborg neural tissue. The colors are as follows: red, rat hippocampal neurons cultured with the nanoES to yield a neural network; yellow and blue, nanoelectronic network; white arrow, neurite passing through ring supporting nanowire transistor.

Representative Publications

Yao, J.; Yan, H.; Lieber, C. M. A Nanoscale Combing Technique for the Large-Scale Assembly of Highly Aligned Nanowires. *Nature Nanotechnol.* DOI: 10.1038/NNano.2013.55, published online 21 April 2013

Kim, S. K.; Day, R. W.; Cahoon, J. F.; Kempa, T. J.; Song, K.-D.; Park, H.-G.; Lieber, C. M. Tuning Light Absorption in Core/Shell Silicon Nanowire Photovoltaic Devices Through Morphological Design. *Nano Lett.* **2012**, *12*, 4971-4976

Kempa, T. J.; Cahoon, J. F.; Kim, S. K., Day, R. W.; Bell, D. C.; Park, H.-G.; Lieber, C. M. Coaxial Multishell Nanowires with High-Quality Electronic Interfaces and Tunable Optical Cavities for Ultrathin Photovoltaics. *Proc. Natl. Acad. Sci. USA* **2012**, *109*, 1407-1412

Yan, H.; Choe, H. S.; Nam, S. W.; Hu, Y.; Das, S.; Klemic, J. F.; Ellenbogen, J. C.; Lieber, C. M. Programmable Nanowire Circuits for Nanoprocessors. *Nature* **2011**, *470*, 240-244

Tian, B.; Cohen-Karni, T.; Qing, Q.; Duan, X.; Xie, P.; Lieber, C. M. Three-Dimensional, Flexible Nanoscale Field-Effect Transistors as Localized Bioprobes. *Science* **2010**, *329*, 831-834

Natural Armor: An Untapped Encyclopedia of Engineering Designs for Protective Defense Applications

Christine Ortiz
Massachusetts Institute of Technology, *cortiz@mit.edu*
NSSEFF Award Year: 2009

Project Description:

The goal of the Ortiz NSSEFF research program is to create a comprehensive knowledge base of natural armor (exoskeleton) design principles linked to their corresponding threats to be transferred to DOD armor specialists to facilitate gains of implementing the new scientific concepts discovered into current prototype human, vehicle, and structural armor kits (intermediate) and the development of a new, improved biologically-inspired human armor suit and armor structures (long-term). The model systems currently under investigation fall into three categories: (1) articulating/flexible and dynamic, (2) transparent, and (3) functional in extreme environments (i.e. heat, blast, toxins, vacuum, ionizing radiation) (Fig. 1).

Flexible/Articulating Transparent "Extreme"

Figure 1. Selected model systems; *Pseudorinelepis sp.* (armored catfish), *Chiton sp.*, the echinoderm *Colobocentrotus atratus* (helmet urchin), the jamphipod *Phronima*, tardigrade, and Bombardier beetle (*Brachinus*).

Accomplishments:

Articulating/flexible and dynamic exoskeletons

A common feature of the outer layer of biological exoskeletons in structural anisotropy. We have compared nanoindentation data to the predictions of a nanomechanical finite element model to explore the anisotropic behavior of a model exoskeletal system, the outermost ~10 μm ganoine layer of the armored fish *Polypterus senegalus* (Wang et al., 2009). This work was extended by directly quantifying the mechanical anisotropy and fracture of ganoine via uniaxial compression of cylindrical micropillars fabricated via focused ion beam milling (Han et al., 2011). Additionally, we have tooth biting attack simulations, in which parametric studies revealed the effects of tooth geometry, microstructure, and mechanical properties on its ability to penetrate or be defeated by individual scales (Song et al., 2011).

In addition to understanding the role of the inherent material properties of the scales of *P. senegalus* in providing penetration resistance, we have explored geometric design principles at increasingly large length scales including: morphometry of individual scales, scale-to-scale interconnections and anisotropic ranges of motion, and the entire assembled scale squamation and anisotropic ranges of motion of the entire fish body (Fig. 2, Top) (Reichert, S.; Master's Thesis, MIT, 2010). Abstractions of the individual scales, connective material at the peg and socket joint, compliant substrate, and connections between the scales were integrated into a bioinspired 3D armor assembly model (Fig. 2, Bottom). Armor prototypes were fabricated via multi-material 3D printing (Fig. 2, Bottom Right). We continue to explore the geometric design principles of a number of other segmented exoskeletons including the plates of chitons

(Fig. 1, second from left). We recently investigated the passive and defensive conformations of chiton plates, quantifying changes in protection between different states of flexure (Connors et al., 2012)

Transparent natural exoskeletons

In addition to providing protection, natural armor systems are often optimized play a role in non-mechanical functions. Recently, a number of mollusk shells have been found have optical functions including selective light diffusion, photonic coloration, and vision. Through a combination of experimental and theoretical methods, we have investigated the highly mineralized exoskeleton of the limpet *Placuna placenta* (Fig. 3a), which simultaneously achieves high optical transparency (Fig. 3b) and mechanical robustness (Li et al., 2013). Transparency as a camouflage strategy for anti-predation has been found in a number of mollusk groups. To the best of our knowledge, this was the first study the explicitly examines the optical performance and mechanical properties of a natural mineralized transparent structural material system in correlation with its microstructural and crystallographic features.

Exoskeletons in extreme environments

The exoskeletons of some organisms function to protect from less traditional threats than biting and impact, such as heat, toxins, and even blast. The defensive glands of many insects synthesize and store a vast variety of toxic chemicals, ranging from small molecules (e.g. hydrogen cyanide, organic acids, quinones, alkaloids, steroids) to protein toxins. These insects use such chemicals to defend against potential predators, but the adaptations (including exoskeletal) that allow them to not themselves accrue harm from these poisons are not well understood. Bombardier beetles (*Brachinus* species, Fig. 4A) exhibit perhaps the most extreme example of chemical defense in nature, using rapidly repeating internal explosions to synthesize and propel a hot (100 °C) toxic chemical spray at attackers. We have been investigating how brachinine bombardier beetles survive these repetitive internal blasts, starting with microstructural studies of the defensive glands and the diverse hair-like projections which line their interiors and proceeding to high-speed synchrotron X-ray imaging of discharges from live beetles to better understand how the explosions occur.

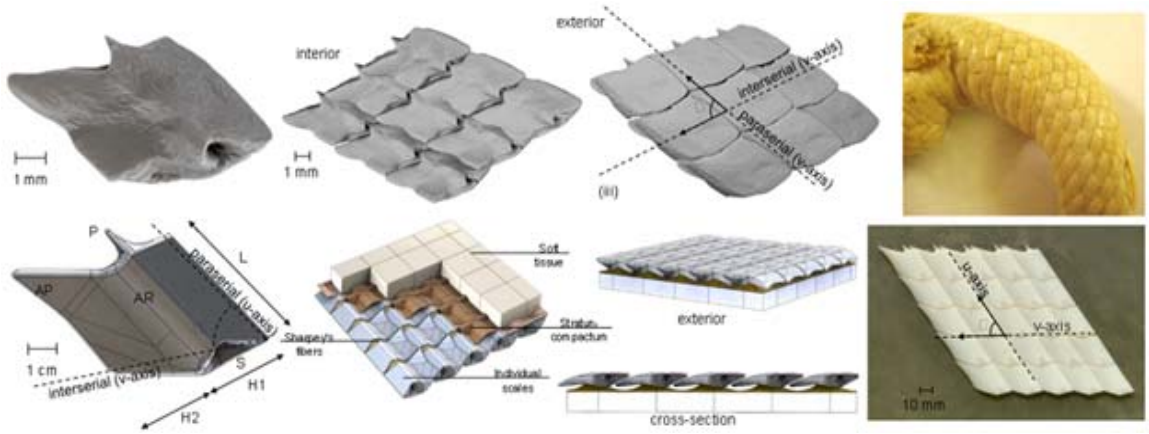

Figure 2. Biological (Top) and Bioinspired (Bottom) Armor Assemblies of *P. senegalus*. Top, left to right) Averaged 3D reconstruction of µCT data of single scale; internal view of homogeneous assembly of the replicated scale geometry on a flat surface; external view of homogeneous assembly of the replicated scales on a flat surface showing the angle between the paraserial (u-axis) along the peg-and-socket joint structure and the interserial axis (v-axis) along the overlapping joint structure; optical photograph of *P. senegalus* exoskeletal armor assembly. Bottom, left to right) Abstracted geometry of a scale unit magnified 10x from the biological scale, showing; internal view of a 3D model of the assembly that incorporates the scale geometry, Sharpey's fibers, and "stratum compactum"; exterior and cross-sectional views; Multi-material 3D-printed prototype of the bioinspired scale assembly.

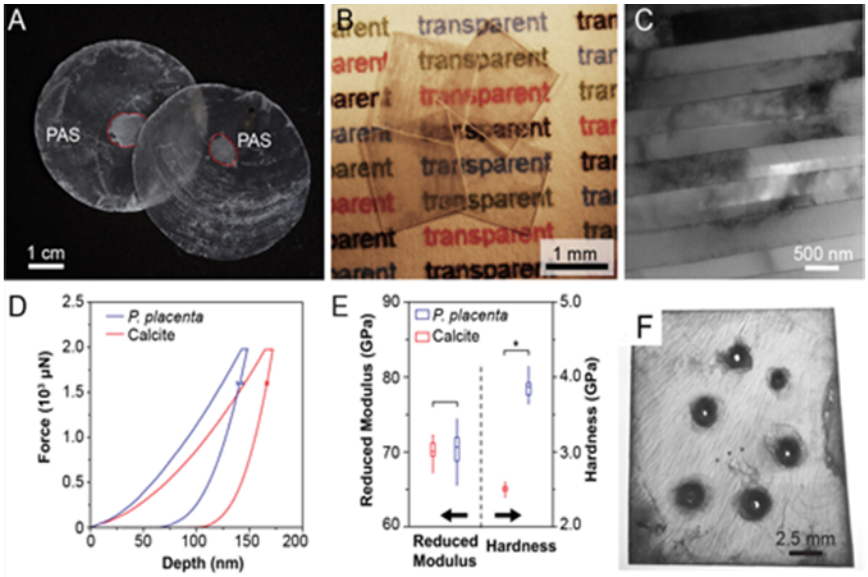

Figure 3. A) *P. placenta* shells with edges trimmed. "PAS" = poster adductor scar. B) Square-shaped tiles cut from shells. C) Cross-sectional TEM image of the foliated microstructure. D) Averaged force-depth data from nanoindentation of *P. placenta* and single-crystal calcite with similar crystallographic orientations. E) Reduced modulus and hardeness of *P. placenta* and single-crystal calcite derived from D). F) *P. placenta* shell after entire shell was penetrated multiple times in a localized area. *Modified from Li et al., 2013*.

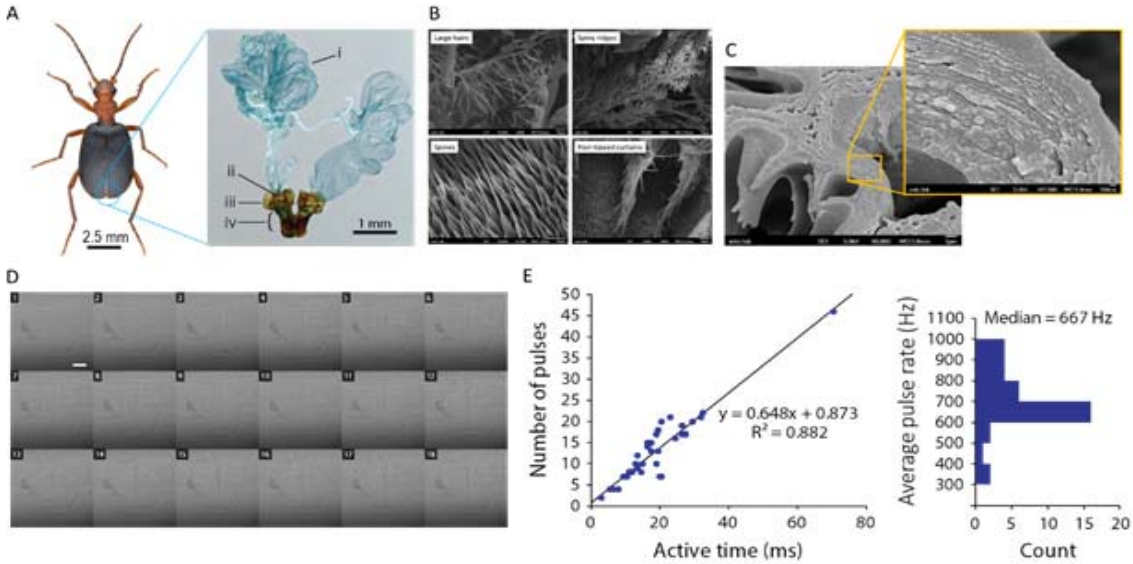

Figure 4. A) Typical *Brachinus elongatulus* (left) and excised defensive glands (right): i. reservoir chamber; ii. valve; iii. reaction chamber; iv. exit pore. Specimen stained with toluidine blue. [Images courtesy W. Moore.] B) Scanning electron micrographs of some types of internal microstructural features of *B. elongatulus* reaction chamber. C) Lamellar structure of reaction chamber wall as revealed by scanning electron microscopy of microtome-sectioned sample. D) Excerpt from 2000-frame/s synchrotron X-ray video showing the beginning and first few explosions of a *B. elongatulus* discharge; scale bar = 250 μm. E). Explosion repetition (pulse) rates measured from 2000-frame/s X-ray video, aggregate of 18 discharges (35 periods of gland activity) from 8 beetles: (left) each point represents a different period of gland activity; the slope of the linear fit predicts a pulse rate of 648 Hz; (right) calculated average pulse rates for each period of gland activity.

Representative Publications:

Li, L.; Ortiz, C. *Adv. Mater*. **2013**, 25, 2344-2350.
Connors, M. et al. *J Struct Bio* **2102** 177, 314-328.
Han, L.; Wang, L.; Song, J.; Boyce, M.C.; Ortiz, C. *Nano Lett*. **2011**, 11, 3868-3874.
Song, J.; Ortiz, C.; Boyce, M.C.; *J Mech Behav Biomed Mater* **2011**, 699-712
Wang, L.; Song, J.; Ortiz, C.; Boyce, M.C. *J Mater Res* **2009**, 24, 3477-3494.

Materials and Mechanics for Stretchable Electronics/Optoelectronics

John A. Rogers
University of Illinois, *jrogers@illinois.edu*
NSSEFF Award Year: 2009

Project Description:

This NSSEFF program developed the basic scientific foundations for a new class of technology -- high performance, mechanically stretchable electronic/optoelectronic systems. The successful strategies that emerged over the course of the research broadly redefine the reach of electronics, from the ultraflat surfaces of rigid semiconductor wafers, to virtually any type of substrate mechanics or shape. Many important applications were demonstrated in areas ranging from intimate integration of electronics with the human body for health monitoring and therapeutic intervention, to bio-inspired device designs for wide field of view digital cameras.

The topics of the research include (1) semiconductor nanomaterials, from single crystalline inorganic (Si, GaAs, GaN and InP) wires, ribbons and membranes, to single walled carbon nanotubes, in the form of electronically homogeneous, organized arrays, (2) deterministic assembly schemes that exploit the physics of soft adhesion for controlled manipulation of these nanomaterials, and (3) Mechanics and structural design in hybrid systems consisting of ultrathin layers of rigid materials intimately coupled to elastomers, to achieve overall architectures that provide high elongation and low effective modulus. The collective scientific outcomes establish a proven route to semiconductor devices and systems with performance comparable to those of state-of-the-art wafer-based technologies, but with the mechanics of a rubber band. These results are now in initial stages of commercialization in health/wellness products and advanced surgical tools.

Accomplishments:

The results of our NSSEFF program establish a base of scientific understanding on essential aspects of materials, mechanics principles and integration techniques for high performance electronic/optoelectronic devices that exhibit linear elastic responses to large strain (~100%) deformations. The resulting technologies create new opportunities for integrating electronics with the soft tissues of the human body, and for exploiting biologically inspired device designs. The following describes the key concepts, and examples of their use in skin-mounted physiological monitors and in electronic eyeball cameras.

The research involves three main areas: (1) semiconductor nanomaterials, in shape-engineered forms, as the active components, (2) strategies to assemble these materials into desired layouts on substrates of interest and (3) circuit/device designs that minimize strains in these and other 'hard' constituent materials when integrated on 'soft', elastomers. Material structures with nanoscale thicknesses yield exceptionally low flexural rigidities (e.g. $>10^{15}$ smaller than the corresponding wafers) and minimize bending strains even at exceptionally small radii of curvature. Specialized growth and etching techniques enable production of high quality, monocrystalline semiconductor nanomaterials, in formats that can be integrated onto substrates of choice, in a controlled, deterministic fashion, by the methods of transfer printing. This process involves retrieval from a growth substrate followed by release onto a surface of interest, using a soft elastomer such as polydimethylsiloxane. Here, passively or actively switching the strength of adhesion between the nanomaterial 'inks' and the PDMS 'stamps' enables operation at high speeds and yields. Material structures with thicknesses spanning the sub-nanometer level

to tens of microns, and with lateral dimensions ranging from the nanometer to centimeter scale can be manipulated in this manner.

Interconnected assemblies of nanomaterials can be exploited to form stretchable electronic/optoelectronic devices. Here, analytical and computational mechanics models define layouts that minimize strains in the semiconductors and other electronic materials, most of which fracture at strains of only ~1%, or less. Two representative geometries appear in Figure 1, as pairs of experimental images (left) and mechanics modeling of the associated strain distributions (right). The first example results from bonding a silicon nanomembrane to a bi-axially pre-strained slab of rubber (Fig. 1a). Compressive stress associated with release of the pre-strain causes non-linear buckling instabilities that create 'wavy' configurations with 'herringbone' layouts in the membrane. When a hard/soft materials construct of this type is stretched by amounts that do not exceed the pre-strain, the wavy structures change in shape to accommodate overall deformations, in ways that involve minimal strains in the membrane. The elastomer support provides the overall restoring force. An improved design involves (1) structuring the membrane into an open mesh geometry, and (2) selectively bonding the resulting mesh to the elastomer only at the nodes. Figure 1b shows the result, for a silicon nanomembrane patterned into an array of rectangular nodes (i.e. islands) connected by pairs of straight bridges that delaminate from the substrate to adopt arch-shaped structures upon release of the pre-strain. Under deformation, these bridges move in response to applied strains (for strains less than the pre-strain), thereby providing a certain level of mechanical isolation for the islands.

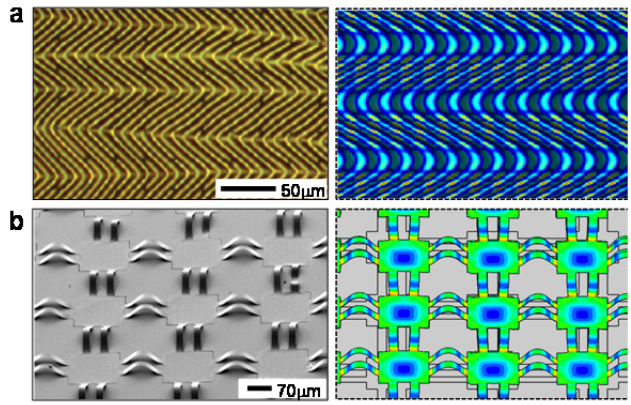

Figure 1. Micrographs (left) and modeling results (right) for silicon nanomembranes configured in stretchable forms and integrated with elastomer substrates.

As testbed applications, we focused on two classes of technology that are not addressable by any existing form of electronics: digital cameras with bio-inspired, hemispherical layouts; and bio-integrated devices for clinical use in cardiology, neurology and other related areas of medicine. Figure 2a shows an electronic 'eyeball' camera that incorporates a hemispherically curved photodetector array with the size and

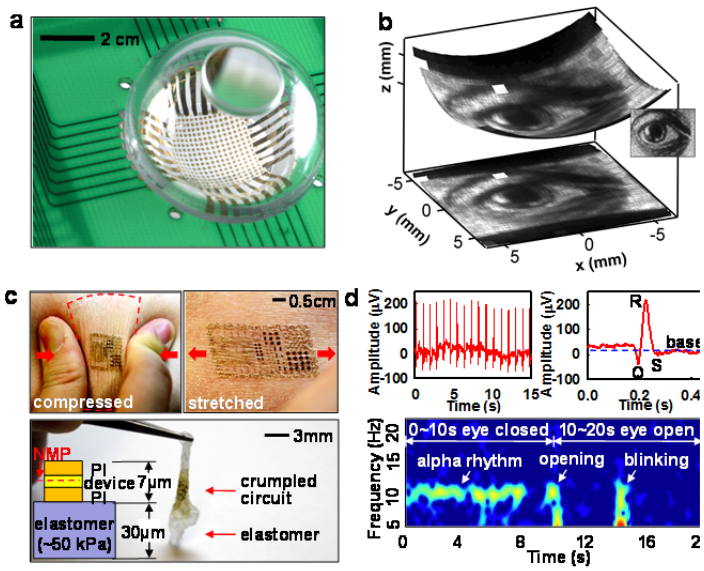

Figure 2. Images of an electronic eyeball camera (a) and skin-mounted electronics (c), with representative data collected from each (b, d).

shape of the human eye. The fabrication begins with the formation of a planar, interconnected array of silicon photodiodes in a mesh geometry to exploit the mechanics of Figure 1b. Controlled compressive deformation using a shaped, thin elastomer stamp accomplishes a planar to hemispherical geometry transformation and transfer to the concave surface of a glass support. Coupling a simple, plano-convex lens fixed in a transparent hemispherical shell completes the camera. The fields of view, levels of aberration and illumination uniformity that are possible with this hemispherical design all exceed those achievable with conventional, flat photodetector arrays when similarly simple optics are used. Figure 2b presents a picture captured with this camera, rendered in the hemispherical geometry of the detector (top), and as a planar projection (bottom); the actual object appears in the right inset.

As an example of bio-integration, electronics can be configured with physical properties, ranging from modulus to degree of stretchability, areal mass density, thickness and flexural rigidity, that precisely match those of the epidermis. Such devices laminate directly onto the surface of the skin, much like a child's temporary transfer tattoo, to provide various types of healthcare and non-healthcare related functions. An image of a demonstration platform appears in Fig. 2c; the structure includes antennas, wireless power coils, silicon nanomembrane transistors and diodes, strain and temperature gauges, along with radio frequency inductors, capacitors and oscillators. Figure 2d presents measurement results for ECG (top) and electroencephalography (EEG; bottom) recorded with EES mounted on the chest and forehead, respectively. The ECG measurements show clear QRS signatures; the EEG traces exhibit characteristic alpha rhythms when the subject's eyes are closed. Many other possible devices, ranging from acute implants to surgical tools, can also be realized.

Representative Publications:

1) Kim, T.-I.; McCall, J.G.; Jung, Y.H.; Huang, X.; Siuda, E.R.; Li, Y.; Song, J.; Song, Y.M.; An Pao, H.; Kim, R-H; Lu, C.; Lee, S.D.; Song, I.-S.; Shin, G; Al-Hasani, R.; Kim, S.; Tan, M.P.; Huang, Y.; Omenetto, F.G.; Rogers, J.A.; Bruchas, M.R. *Science* **2013**, *240*, 211-216.
2) Viventi, J.; Kim, D.-H.; Vigeland, L.; Frechette, E.S.; Blanco, J.A.; Kim, Y.-S.; Avrin, A.E.; Tiruvadi, V.R.; Hwang, S.-W.; Vanleer, A.C.; Wulsin, D.F.; Davis, K.; Gelber, C.E.; Palmer, L.; Van der Spiegel, J.; Wu, J.; Xiao, J.; Huang, Y.; Contreras, D.; Rogers, J.A.; Litt, B. *Nature Neuroscience* **2011**, *14*, 1599-1605.
3) Kim, D.-H.; Lu, N.; Ma, R.; Kim, Y.-S.; Kim, R.-H.; Wang, S.; Wu, J.; Won, S.M.; Tao, H.; Islam, A.; Yu, K.J.; Kim, T.-I.; Chowdhury, R.; Ying, M.; Xu, L.; Li, M.; Chung, H.-J.; Keum, H.; McCormick, M.; Liu, P.; Zhang, Y.-W.; Omenetto, F.G.; Huang, Y.; Coleman, T.; Rogers, J.A. *Science* **2011**, *333*, 838-843.
4) Kim, D.-H.; Lu, N.; Ghaffari, R.; Kim, Y.-S.; Lee, S.P.; Xu, L.; Wu, J.; Kim, R.-H.; Song, J.; Liu, Z.; Viventi, J.; de Graff, B.; Elolampi, B.; Mansour, M.; Slepian, M.J.; Hwang, S.; Moss, J.D.; Won, S.-M.; Huang, Y.; Litt, B.; Rogers, J.A. *Nature Materials* **2011**, *10*, 316-323.
5) Viventi, J.; Kim, D.-H.; Moss, J.D.; Kim, Y.-S.; Blanco, J.A.; Annetta, N.; Hicks, A.; Xiao, J.; Huang, Y.; Callans, D.J., Rogers, J.A.; Litt, B.; *Science Translational Medicine* 2:24ra22. DOI:10.1126/scitranslmed.3000738 (2010).

Investigation of Diesel Producing Fungi as a Renewable Source of Fuel

Scott A. Strobel
Yale University, *scott.strobel@yale.edu*
NSSEFF Award Year: 2009

The Department of Defense (DoD) is the largest single consumer of oil in the United States. Consequently, the DoD has been urged to explore the development of efficient and alternative energy technologies. Our program has used biochemical and genetic approaches to investigate medium chain hydrocarbon production by endophytic fungi with the goal of developing and improving biofuels from cellulosic and other waste stream feedstocks.

Accomplishments. Our focus has been on fungal endophytes, organisms that reside within the inner tissues of plants, which produce a diverse array of secondary metabolites and have developed mechanisms to metabolize the complex polymers they encounter within their hosts. Our search for biodiversity relevant to biofuel applications has been conducted around the world with the involvement of dozens of students, both at the undergraduate and graduate levels. We have collected more than 2700 plants from locations that include Malaysia, Ecuador, Chile, Brazil and several locations within the United States. A total of 4100 fungal endophytes were isolated from the plant samples, of which approximately 20% are new species and roughly 5% are new genera. These isolates represent an incredible reservoir of novel biological and chemical diversity that we screened for the production of potential biofuels, identifying surrogates for gasoline, jet fuel and marine diesel. The organisms of greatest interest that we have pursued are the following:

•*Ascocoryne sarcoides* NRRL50072 produces a mixture of C6-C9 alkanes, alcohols and aldehydes, including hydrocarbons closely related to molecules found in gasoline.
•*Pleosporales spp*. E5202H and E8604B produce a polyene that is a potential gasoline surrogate.
•*Nodulisporium sp.* E7406B produces the terpene cineole, a potential jet fuel surrogate.
•*Phomopsis sp.* BR109A produces a series of monoterpenes and sesquiterpenes that are potential jet fuel surrogates, as well as a novel diterpene that is a potential marine diesel surrogate.
•*Pestalotiopsis microspora* E2712A degrades the complex synthetic polymer polyurethane under anaerobic conditions to produce medium chain alcohols. This organism provides a mechanism to explore the production of biofuels from alternative feedstocks, including human waste streams.
•*Musocodor albus* CZ-620 produces and excretes medium chain alcohols and esters that are toxic to a wide variety of organisms. This organism provides a mechanism to explore product toxicity associated with industrial-scale biofuel production.

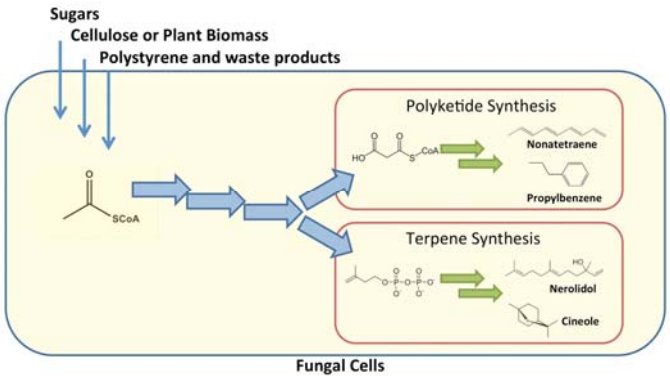

Fig. 1. Scheme for the biosynthesis of biofuels from various feedstocks.

Catabolic production of medium chain hydrocarbons by *Ascocoryne sarcoides*. The initial focus of our research was *A. sarcoides*, an endophytic fungus isolated from Chile that in 2008 was reported to produce a series of hydrocarbons of the same length and type as many of the molecules found in gasoline (previously classified as *Gliocladium roseum*). The hydrocarbons were a mixture of C6-C9 alkanes, alcohols and aldehydes, and they were produced when *A. sarcoides* was grown on a medium where the sole carbon source was cellulose. This represented two significant advancements over existing biofuel technologies. First, the fuel was an improvement to standard biofuels, notably ethanol, as the compounds produced would not require blending or adjustments to engine and transportation infrastructure before being adopted by the market. Second, the feedstock was cellulose, the

world's most abundant carbon source, which could divorce biofuel production from the global food market.

With funding from the DOD we began to study *A. sarcoides* in earnest using a combination of genomic and transcriptomic analyses in order to identify *A. sarcoides's* cellulose degradation and biofuel production pathways. The genome was sequenced, assembled and the genes annotated. The genome assembly remains one of the highest quality fungal genomes to date. We also collected genome-wide transcription data for *A. sarcoides* grown in seven distinct conditions. Several of the growth conditions were targeted to decipher *A. sarcoides's* cellulose degradation pathway and each showed a diverse hydrocarbon production profile. Almost 150 genes were expressed in conditions where only cellulose or cellobiose, its dimeric form, was present. These data inform efforts to increase the efficiency and scale of lignocellulosic degradation.

Efforts to understand the hydrocarbon production pathway of *A. sarcoides* required the development of new methods to integrate the volatile production and transcription data. These methods correlated a small number of genes to the production of each molecule and self-associated into a potential pathway. These results informed metabolic labeling experiments that demonstrated the hydrocarbons of interest derived from the catabolism of longer chain fatty acids, such as linoleic acid. Catabolism of fatty acids is not a pathway of sufficient efficiency for large-scale energy production. As a result we used the pipeline of biodiversity discovery to identify other organisms with properties useful for biofuel production.

Metabolic biofuel production by other novel organisms and the identification of biosynthetic genes. Our workflow has focused on optimizing techniques that are broadly applicable to all isolates, regardless of their species, in order to quickly move from a target phenotype to biochemical validation and scaling. These efforts have relied on high-throughput sequencing and heterologous expression in model organisms. Once a Volatile Organic Compound (VOC) has been detected within a culture, we use metabolic labeling to confirm its production and query the potential substrate molecules. We have identified the VOCs by mass spectroscopy and nuclear magnetic resonance spectroscopy. If it has properties that make it a good surrogate for gasoline, jet fuel or marine diesel, genetic characterization of the host organism has been pursued. Candidate genes have then been tested by expression in heterologous hosts.

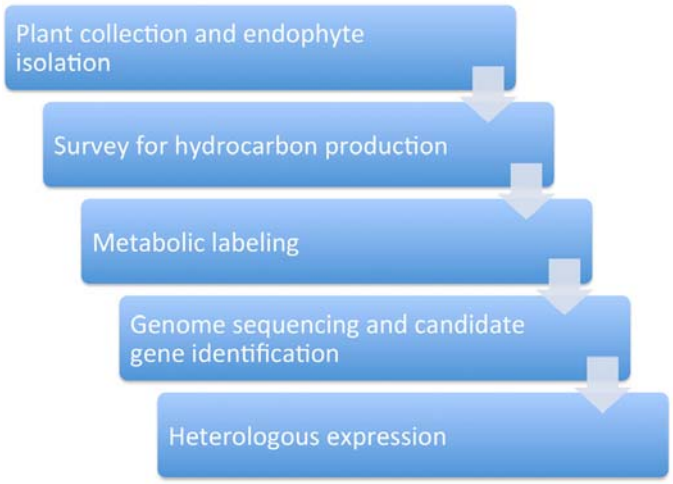

Figure 2. Workflow for the discovery of fungal biodiversity and its application to biofuel production.

Isolate E5202H produces the hydrocarbon (3E,5E,7E)-nona-1,3,5,7-tetraene (NTE), which is predicted to have more desirable energy density and hygroscopicity than ethanol and a higher octane rating than its fully-saturated form. Metabolic labeling studies showed the efficient incorporation of 13-C acetate, suggesting that NTE is produced by a polyketide synthase (PKS) mechanism. There are 32 PKS genes in the E5202H genome. Transcriptomic analyses and comparative genomics were used to narrow the potential genes down to a few candidates. The first of these is currently being tested by heterologous expression in *Saccharomyces cerevisiae*.

We have identified a number of genes responsible for the production of mono-, sesqui- and di-terpene molecules that could serve as fuel surrogates. This class of molecules has been studied as potential biofuels, though the source of these compounds has almost always been from plants. We have identified 87 new terpene synthase genes and transferred a subset of these into the model bacterium *Escherichia coli* for heterologous expression and scale-up. Our initial target for terpene production was isolate E7406B. This organism produces several sesquiterpenes and monoterpenes, including cineole,

which is the main component of eucalyptus oil and an industrially relevant compound with biofuel potential. From this genome we identified the gene responsible for cineole production, representing the first monoterpene synthase identified in fungi. We also identified a nerolidol synthase, a gene that produces a 15 carbon-chain alcohol, and several genes that produce a mixture of sesquiterpenes and monoterpenes. We are currently heterologously expressing these genes in *E. coli* and working to increase production of these molecules. We have also expanded this analysis with candidate genes from other genomes including an isolate from Brazil, BR109A. This fungus produces a mixture of monoterpenes including limonene, sabinene, terpinene, phellandrene and terpinolene, all of which have been proposed as potential biofuels. We are now working to identify the genes producing these useful molecules as well.

Mechanisms of resistance to biofuel toxicity. The endophytic fungus, *Muscodor albus*, produces VOCs with strong antimicrobial activity. This lethality is due to the mixture of VOCs produced, which include a variety of alcohols, esters, acids, and some large polycyclic aromatic hydrocarbons. Many of these compounds are similar or equivalent to butanol, which is used as an alternative biofuels but has limited production due to product toxicity.

We investigated the mechanism of toxicity by screening the sensitivity of single gene knockouts in the background of a resistant strain of *E. coli*. Several genes in the DNA repair and metabolism pathways showed the strongest phenotypes, which establishes a link between VOCs exposure and DNA damage. The morphological phenotypes of sensitive strains are consistent with this conclusion; the organism forms long filamentous cells that never divide. This is the first mechanistic approach to understanding the natural mechanisms of resistance to these VOCs. We have discovered that by fortifying their DNA repair pathways, bacteria can tolerate higher concentrations of VOCs. Understanding the basis of toxicity and the mechanisms of resistance will be useful for increasing biofuel production.

Decomposition of other feedstocks for biofuel production. Fungi play an important role in global carbon and nitrogen recycling. Many of our fungal isolates have displayed cellulolytic activity; however, we are also investigating the use of alternative feedstocks, such as synthetic plastics, to expand the polymers that can be used for biofuel production. Americans throw away over 27 million tons of plastics every year that either accumulate in landfills or pollute the environment. By utilizing plastic waste for biofuel production, we aim to produce biofuels from novel, non-food feedstocks while simultaneously reducing the amount of plastic waste accumulation.

We screened endophytes for the ability to degrade the synthetic plastic polyester polyurethane (PUR) in both solid and liquid media. From the initial screening assays, the fungus *Pestalotiopsis microspora* E2712A was identified as the most promising organism for PUR degradation. *P. microspora* is uniquely able to utilize PUR as its sole carbon source, maintains PUR-degrading activity equally well in aerobic and anaerobic conditions, and produces medium chain alcohol by-products. PUR degradation is attributed to an induced, extracellular serine hydrolase-like enzyme. The enzyme has high stability in thermal denaturation experiments, suggesting that it will be amenable to large-scale industrial use. This enzyme has been heterologously expressed in *E. coli* and the PUR degradation products include the medium chain alcohol 1,6 hexandiol. By investigating and understanding the ability of *P. microspora* to degrade plastic substrates, we have taken important steps towards the use of plastic feedstocks for future production of biofuels.

Representative Publications

Bascom-Slack, C. A.; Arnold, A. E.; Strobel, S. A. *Science* **2012**, *338*, 485-486.
Gianoulis, T. A.; et al. *PLoS Genet.* **2012**, *8*, e1002558.
Russell, J. R.; et al. *App. & Environ. Microbio.* **2011**, *77*, 6076-6084.
Strobel, G. A.; et al. *Mycology* **2010**, *1*, 187–194.
Griffin, M. A.; Spakowicz, D. J.; Strobel, S.A. *Microbiology* **2010**, *156*, 3814-3829.

Novel Ultrabroadband Photonic and Radio-Frequency Systems for Communications, Sensing, and Countermeasures

Andrew M. Weiner
Purdue University, *amw@purdue.edu*
NSSEFF Award Year: 2009

Project Description:

Radio-frequency (RF) technology is ubiquitous in systems such as radar, sensing, wireless communications, and electronic warfare (EW) that are vital to national security. Conventional RF systems are usually designed to operate at low instantaneous bandwidth with signals possessing a well defined (though perhaps slowly tunable) center frequency. Coherent, phase-based signaling schemes are employed, but only within a narrow instantaneous frequency band. On the other hand, optical systems can be extremely broadband, generating pulses with durations down to femtoseconds and with terahertz instantaneous bandwidths. Such ultrashort pulse optical systems are fundamentally time-domain in nature, and control of phase over the full bandwidth is crucial. In our NSSEFF program we have aimed to adapt approaches proven in the field of broadband optics approaches to pursue new opportunities in generation, processing, and application of ultrabroadband RF electrical signals.

Accomplishments:

Our research encompasses thrusts on photonically-enabled RF waveform generation, photonically-enabled RF filtering, and applications of such technologies including ultra-broadband RF propagation in multipath environments. In the following, examples of accomplishments in each of these three thrusts are described.

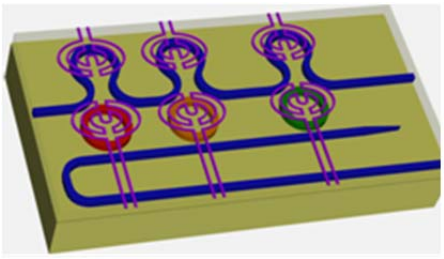

Figure 1. Silicon photonic spectral shaper chip for photonic RF arbitrary waveform generation. The spectrum of a broadband input pulse from a mode-locked laser (not shown) is shaped via interaction with eight cascaded microring resonators. Via thermo-optic tuning and interferometric couplers, both the amplitude and frequency of the various resonances can be programmed independently, leading to substantial flexibility for arbitrary waveform generation.

Photonics-enabled radio-frequency arbitrary waveform generation. Photonic means of arbitrary radio-frequency waveform generation (RF-AWG) can overcome bandwidth limits in electronic signal generation, provide reduced timing jitter, offer immunity to electromagnetic interference, and support remoting applications, with photonic drive signals generated remotely and delivered via fiber optics to a small optical-to-electronic conversion module at the required location. Under NSSEFF support we have:

- Demonstrated the possibility of chip-level spectral shapers that may replace bulk optic pulse shapers used in in photonic RF-AWG, substantially reducing the physical footprint (Fig. 1).

- Devised an approach that improves the information content (technically the time-bandwidth product) in photonic RF-AWG by more than an order of magnitude. This advance has enabled new experiments in which RF waveforms are predistorted in order to achieve self-compression upon propagation in highly scattering indoor wireless environments

(see item 3 below).

- Performed experiments demonstrating agile RF-AWG. Most work on photonic-enabled RF-AWG is constrained by slow reprogrammability (milliseconds) and limited time aperture (nanoseconds). We have demonstrated novel waveform switching schemes – operating at rates from hundreds of MHz to ca. 10 GHz – that provide agility many orders of magnitude faster than previously. Such waveform switching also opens new directions in waveform design. For example, pseudorandom switching between a pair of complementary waveforms leads the way to arbitrarily large time apertures while preserving enhanced signal bandwidth. For the first time this overcomes a seemingly fundamental incompatibility between the time apertures in photonic RF-AWG and typical radar practice.

Photonics-enabled radio-frequency photonic filtering Radio-frequency (RF) photonic filters have received sustained research attention due to their potential for broadband tuning and flexible reconfigurability, among other potential advantages. Previous research has mostly followed a tapped delay line configuration, in which photonics is used to generate multiple samples of the RF input in the optical domain, which are combined with relative delays on a photodetector to realize filtering action. However, previous work has generally been limited to very small number of taps, which precludes high filter quality, and the potential for rapid tuning has not been demonstrated. We have advanced a new approach in which dozens or even hundreds of optical frequencies from an optical frequency comb serve as the taps in the tapped delay line configuration and as a result have demonstrated substantial advances in filter quality, reconfigurability, and agility. Our accomplishments include:

- In a fixed filter configuration, demonstrated RF bandpass filters with ca. 70 dB out-of-band suppression. We have shown that such high filter contrast depends critically on the apodization (smoothing) of the optical comb spectrum. The high filter contrast, which is nearly unprecedented in RF photonics, is key for applications such as radar signal processing.

- In a tunable filter configuration, demonstrated switching of the filter bandpass frequency within ca. 40 ns, orders of magnitude faster than ever reported in RF photonics (Fig. 2). In principle, it should be possible to achieve such agility simultaneously with high filter contrast, to our knowledge a prospect not yet available with any known filter technology.

- Going beyond bandpass filters, we have also conceived and realized novel functionalities, such as programmable pulse compression filters that operate on spectral phase (almost untouched in the conventional RF domain for multi-GHz bandwidths) and comb-based RF photonic filters that simultaneously perform frequency down-conversion.

Control of ultrabroadband indoor RF propagation Exploiting advances report above, we have investigated control of ultrabroadband indoor RF propagation based on waveform design. Short RF pulse propagation in strong scattering environments is subject to severe multipath distortion, where hundreds of partial reflections may arrive at the receiver with different delays. This poses a strong impediment, e.g., to high data rate wireless communications. We have used both electronic and photonic RF waveform generators to achieve pulse compression under such strong scattering conditions, at the same time demonstrating spatially selective propagation control that brings to mind intriguing possibilities for covert wireless communications. The example shown in Fig. 3, performed using photonics waveform generation, achieves operation over a frequency

band up to 18 GHz, nearly an order of magnitude larger than results reported in the previous literature.

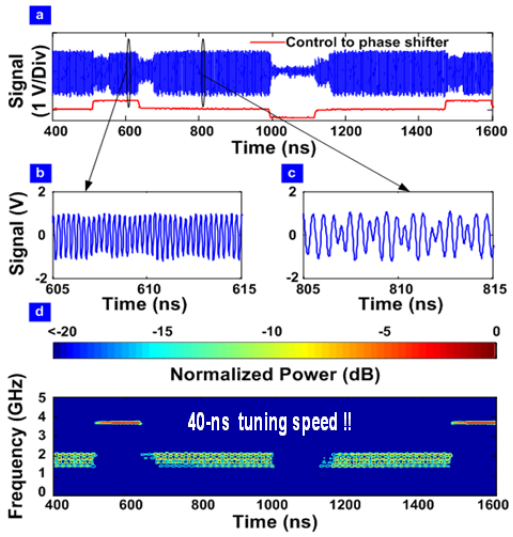

Figure 2. Agile RF photonic filtering. (a) Output of the RF photonic filter (blue) as it is tuned via an electronic control signal (red). The filter is able to select either (b) a 3.7 GHz tone or (c) 600 Mb/s data on a 1.8 GHz carrier, which are superimposed at the input. (d) The time-frequency representation of the data demonstrate frequency tuning in ca. 40 ns, orders of magnitude faster than most previous practice.

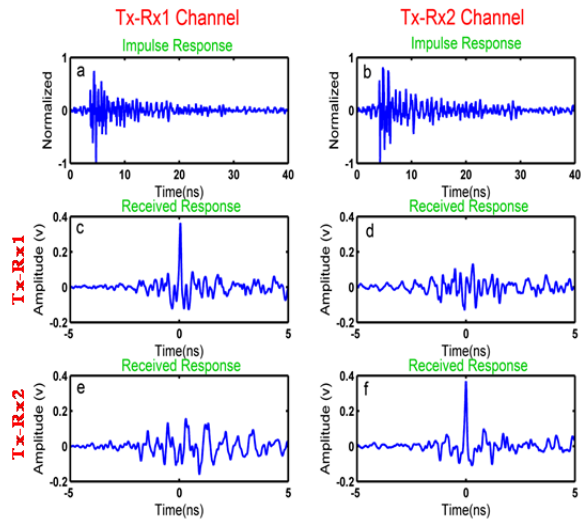

Figure 3. Compensation of ultrabroadband multipath distortion via photonics-enabled RF waveform generation. A 2-18 GHz transmit antenna (Tx) sends RF signals to a pair of closely spaced receive antennas (Rx1, Rx2) in an adjacent room. (a,b) Impulse responses measured between Tx and Rx1/Rx2 antennas. (c,d) Tx waveform set to compensate Tx-Rx1 path, achieving compression to a strong peak. Rx2 signal remains noise-like. (e,f) Tx waveform set to compensate Tx-Rx2 path, achieving compression at Rx2; Rx1 signal remains noise-like. Such spatially selective peaking offers potential for covert communications and increased data rate.

Representative Publications:

1. M.H. Khan, H. Shen, Y. Xuan, L. Zhao, S. Xiao, D.E. Leaird, A.M. Weiner, and M. Qi. "Ultrabroad-bandwidth arbitrary radiofrequency waveform generation with a silicon photonic chip-based spectral shaper." *Nature Photonics* 4 (2010): 117-122.
2. V.R. Supradeepa, C.M. Long, R. Wu, F, Ferdous, E. Hamidi, D.E. Leaird, and A.M. Weiner. "Comb-based radiofrequency photonic filters with rapid tunability and high selectivity." *Nature Photonics* 6 (2012): 186-194.
3. R. Wu, V.R. Supradeepa, C.M. Long, D.E. Leaird, and A.M. Weiner. "Generation of very flat optical frequency combs from continuous-wave lasers using cascaded intensity and phase modulators driven by tailored radio frequency waveforms." *Optics Letters* 35(2010): 3234-3236.
4. M. Song, V. Torres-Company, A.J. Metcalf, and A.M. Weiner. "Multitap microwave photonic filters with programmable phase response via optical frequency comb shaping." *Optics Letters* 37 (2012): 845-847.
5. A. Dezfooliyan and A.M. Weiner. "Experimental investigation of UWB impulse response and time reversal technique up to 12 GHz: omnidirectional and directional antennas." *Antennas and Propagation, IEEE Transactions on* 60 (2012): 3407-3415.

Designing New Higher Temperature Superconductors

Meigan Aronson
Stony Brook University Meigan .Aronson@stonybrook.edu
NSSEFF Award Year: 2010

Project Description:

We propose here a new methodology where electronic structure calculations are integrated with the synthesis of new superconducting materials, with the aim of providing a rigorous test of the apparent association of high temperature superconductivity with electron delocalization transitions occurring at quantum critical points. We will use realistic electronic structure calculations to assess which transition metal monopnictides are closest to electron delocalization, and hence optimal for superconductivity. The functional layer will be matched with a layered host taken from an extensive library of known framework structures, and then single crystals of the desired compound will be synthesized. Rapid turnaround characterization will determine the basic properties of these new materials, identifying the most promising candidates. Optical conductivity and angle resolved photoemission measurements will be used to compare the actual electronic structure with theoretical results, providing feedback to the initial choices of functional and charge reservoir layers.

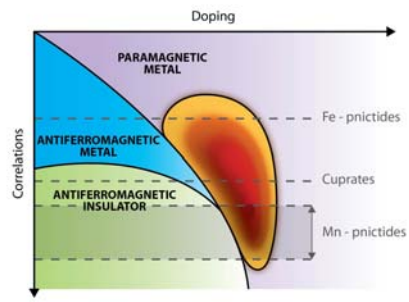

Figure 5 A schematic phase diagram for compounds with different strengths of correlations and differing degrees of charge doping. Compounds with strong correlations like the cuprates are insulating until doping drives them metallic. Weakly correlated compounds like the Fe-pnictides are always metallic, although doping destroys magnetic order. Superconductivity is nestled in the confluence of the metal-insulator transition and the destabilization of magnetic order. Mn-pnictides such as LaMnPO may be more strongly correlated than the cuprates, potentially leading to larger values of T_c.

The senior members of this collaboration are Meigan Aronson (Stony Brook University), Dimitri Basov (University of California, San Diego), Gabriel Kotliar, Martha Greenblatt, and Girsh Blumberg (Rutgers University), James Allen (University of Michigan), Liu Hao Tjeng (Max Planck Institut for Chemical Physics, Dresden), Stephen Julian (U. Toronto), Liling Sun and Zhongxian Zhou (Chinese Academy of Sciences, Institute of Physics, Beijing).

Accomplishments:

The objective of this project is to implement and test a new methodology `Theory – Assisted Synthesis' as a means to design and then synthesize new materials with specific functionalities. The goal of the current project is to develop a new family of compounds with high superconducting transition temperatures, but we expect that this approach should be applicable to different functionalities like thermoelectricity, insulating gap instabilities, and perhaps magnetic order. A collaborative approach is required to carry out this project, where the group of PI Meigan Aronson is responsible for synthesizing new materials and assessing their basic properties. An enabling step is that electronic structure calculations are only now becoming accurate enough to be predictive. Prof. Gabriel Kotliar's group carries out dynamical mean field theory (DMFT) calculations of the electronic structure, providing not only accurate determinations of the electronic structure in these inherently highly correlated materials, but also explicit results for the photoemission and optical conductivity that can be directly compared to experimental results. The group of Prof. Dimitri Basov (University of California San Diego) performs optical spectroscopy experiments, ideal for distinguishing between metals and

insulators, and in combination with DMFT can determine the overall strength of the electronic correlations. Prof. Hao Tjeng's group (Max Planck Institute for Chemical Physics, Dresden) provides information about the transition metal valence state via x-ray absorption, and as well photoemission measurements that can be directly compared to theoretical results from Kotliar's group. Finally, the group of Dr. Liling Sun and Zhongxian Zhou (Chinese Academy of Sciences, Institute of Physics, National Laboratory on Superconductivity) carry out x-ray diffraction measurements and x-ray absorption measurements under high pressures, as well as high pressure resistivity and magnetic susceptibility measurements, needed input for the DMFT to calculate idealized lattice constants for transforming insulators to metals.

Electronic structure calculations are not yet able to predict equilibrium crystal structures, particularly of the types of materials where strong correlations can lead to collective behaviors like superconductivity. It is still necessary to have an overall scheme for understanding the general circumstances under which superconductivity can be found. Our hypothesis is that superconductivity is a potential attribute of metals with strong electronic correlations, provided other sorts of order do not intervene first. In particular, we believe that the combination of ground state entropy and reduced kinetic energy from strong correlations enable superconductivity when the system is close to an electronic delocalization transition (EDT), for instance a Mott-like transition. Unlike the cuprates, where the metallic compositions that support superconductivity are derived by doping strongly correlated Mott insulators, the iron pnictide superconductors are all derived from metals. Isostructural compounds based on Mn are largely insulating, and so we adopted the initial goal of determining whether it could be driven metallic – and thus potentially superconducting – by the addition of charge or by pressure. This goal was intended as a stringent test of how well the theory was able to reproduce key experimental results in this very strongly correlated system.

Optical measurements found that the 1 eV insulating gap in LaMnPO is in excellent agreement with the DMFT predictions, as is the ordered Mn moment determined from neutron diffraction experiments. Indications of incipient charge delocalization were found in the computed electronic states, also evident in x-ray absorption measurements. Encouraged by this agreement, we explored different doping vectors but were never able to transform LaMnPO into a bona fide metal. We turned next to high pressure, and here we met success. Fig. 2 shows the electrical resistivity of LaMnPO, which evolves from strongly insulating to an excellent metal above ~12 GPa of hydrostatic pressure. Using atomic positions derived from high pressure x-ray diffraction measurements, it was possible to determine the pressure dependence of the insulating gap, which was found to vanish at ~10 GPa. Intriguingly, the calculations suggest

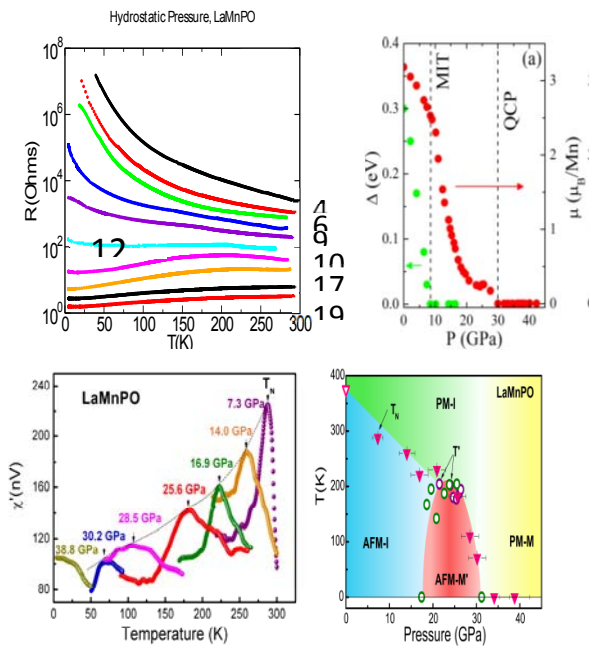

Figure 6 (top left) High pressure resistivity of LaMnPO showing metallization. (top right)Theoretical calculations of the pressure dependencies of the insulating gap and Mn moment. (bottom left) Mn moment collapse at 30 GPa, just as predicted. (bottom right) A proposed phase diagram for Mn compounds.

that the Mn moment does not collapse at the insulator-metal transition, and that an intermediate metallic phase with magnetic order is produced. Only at pressures higher than 30 GPa is the magnetism fully suppressed. This prediction was subsequently tested with high pressure magnetic susceptibility measurements, which found that the antiferromagnetic order vanishes in LaMnPO at 30 GPa (Fig. 2). We understand from these experiments that the conditions under which superconductivity may occur are more diverse than was generally believed.

The excellent quantitative agreement between theory and experiment that was found in LaMnPO proved that Theory-Assisted synthesis is potentially feasible. Unfortunately, no superconductivity was found in pressurized LaMnPO, at least not above ~10 K. We adopted a second goal for our collaboration, which was to use our approach to find a Mn-based superconductor. To date, no Mn-based superconductors are known, and the general consensus is that the Mn magnetism is `too strong'. Our LaMnPO measurements indicate that Mn-based compounds can have the same range of behaviors as are found in successful superconductors like the cuprates and the Fe-based superconductors. Here the challenge is to produce a simultaneous collapse of the insulating gap and the magnetic moments, either as functions of pressure or doping. This work is ongoing. However, we have used the calculated electronic structure of LaMnPO as the template for a larger family of compounds with different Mn-Mn spacings and different Mn coordinations. These calculations were used to form a phase diagram with magnetic insulator, magnetic metal, and nonmagnetic metal (most likely to be superconducting) phases, represented as functions of Mn spacings and angles. This first application of the predictive mode of Theory Assisted Synthesis has narrowed down the range of desired materials attributes from hundreds of possible compounds in the crystal structure data bases to only a few.

We have just passed the three-year mark in our project. We have demonstrated that the electronic structure calculations have the required degree of accuracy for connecting with experiments. We have discovered that while superconductivity likely requires the collapse of both the insulating gap and magnetic order, these phenomena can occur separately or together, depending on the type of transition metal that is present. Finally, we have extended the electronic structure calculations from the specific case of LaMnPO to a new family of hypothetical compounds with improved properties. The future prospects of Theory-Assisted synthesis seem very bright.

Representative Publications:

Simonson,J. W.; Yin, Z. P.; Pezzoli, M.; Guo,J.; Liu, J.; Post, K.; Efimenko, A.; Hollmann, N.; Hu, Z. W.; Lin, H.-J.; Chen, C. T.; Marques, C.; Leyva, V.; Smith, G.; Lynn, J. W.; Sun, L. L.; Kotliar, G.; Basov, D. N.; Tjeng, L. H.; Aronson, M. C. *Proceedings of the National Academy of Sciences* **2012**, 109**,** E1815-E1819.

Simonson, J. W.; Smith, G.; Post, K.; Pezzoli, M.; McNally, D. E.; Nelson, C. S.; Kotliar, G.; Basov, D. N., Aronson, M. C. *Phys. Rev. B* **2012**, 86, 220401.

Thorsmolle, V. K.; Ignatov, A.; Pezzoli, M. E.; Haule, K.; Kolchmeyer, D.; Simonson, J. W.; Aronson, M. C., Blumberg, G. *Phys. Rev. Lett.* **2013** (to appear).

Retuerto, M.; Emge, T.; Li, M. R.; Yin, Z. P.; Croft, M.; Ignatov, A.; Simonson, J. W.; Aronson, M. C.; Stephens, P.; Hadermann, J.; Pan, A.; Basov, D. N.; Kotliar, G, Greenblatt, M. *J. Am Chem. Soc.* (submitted).

Guo, J.; Simonson, J. W.; Sun, L. L.; Wu, Q.; Gao, P.; Zhang, C.; Gu, D.; Kotliar,G.; Aronson, M. C, and Zhao, Z. *Nature Physics* (submitted).

Optimal Design of Resilient Capacitated Networks

Alper Atamturk
University of California – Berkeley, *atamturk@berkeley.edu*
NSSEFF Award Year: 2010

Project Description:

Defending our national infrastructure networks against random failures and malicious coordinated attacks by adversaries and ensuring their resilience is one of the highest priorities of the government. Whereas many of these networks are physical (e.g. oil and gas storage and pipelines, computer networks, power plants and grids), others such as military logistics and information chains are logical ones composed of components of other physical and/or logical networks, e.g., internet, factories, warehouses, ports, satellites, and various modes of transportation and communication channels.

If capacities of the components of a network are random variables, what is the optimal (least-cost) network configuration that guarantees transshipment of a certain percentage of the traffic between sources and targets with a desired probability? What is the optimal (least-cost) network configuration that guarantees transhipment of a certain percentage of the traffic between sources and targets when a network is under coordinated attack by an adversary with resource constraints?

These are the examples of questions we investigate in the current research project. Answers to such questions are not only useful for identifying critical vulnerabilities of our infrastructure networks, but also for efficient allocation of scarce resources to mitigate those vulnerabilities. Furthermore, they can be used to quantify the trade-off between the cost of investment and resilience of our networks for informed decision making.

On the flip side, efficient allocation of assets and resources is a major concern in the effectiveness of surveillance, reconnaissance, and interdiction of terrorist and drug networks. It turns out that the problem of *optimal persistent interdiction* of an enemy network against an adversary who can shore up the links or when link capacities are probabilistic is the dual of optimal resilient network design problem. An interdiction is *persistent* if it disrupts the enemy traffic to a large extent when the enemy network capacities are uncertain. We develop novel methods for quantitative analysis of the trade-off between the cost and effectiveness of interdiction.

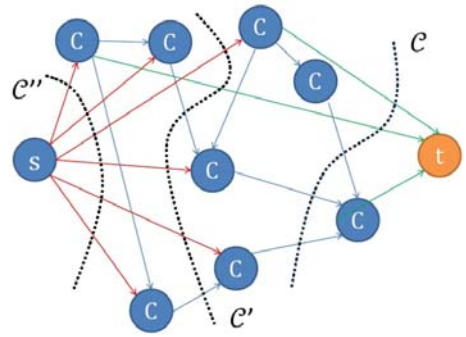

Figure 1. Dual pairs: *resilient network design* and *persistent interdiction*.

Accomplishments:

Probabilistic constraints on cuts

The challenge in optimization over probabilistic constraints on cuts of a network has been to identify the right set of small number of constraints to perform the optimization over as it is practically impossible to include all of the exponentially many constraints. The task required decomposing the overall optimization problem into two subproblems: (a) a relaxed problem with fewer constraints; (b) a separation problem to identify missing constraints for the relaxed problem.

Both of these problems are still nonlinear integer optimization problems, but practically easier to solve than the overall. Using them iteratively could potentially lead to efficient solutions. However, our initial attempts were still not computationally viable as many hours of computing were required even for small instances. Through better understanding of the structure of the problems and tangent hyperplane approximations, we have made major breakthroughs in modeling both problems in a convenient way and solving them in a manner of minutes.

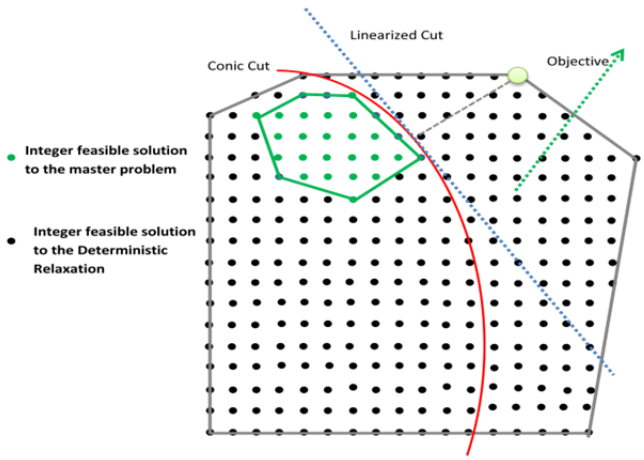

Figure 2. Conic cuts and their gradients.

Probablistic constraints on paths

Unlike probabilistic constraints on cuts of the network, probabilistic constraints on paths of a network cannot be directly modeled using conic quadratic constraints. The nonlinear constraints used for modeling involve power functions. Optimizing over binary variables involving power functions has been a major challenge for addressing probabilistic constraints on paths.

Our earlier research exploited super and submodular functional properties together with superadditive lifting for their effective solution in special cases. Recently, we have considered approximating the power functions using a series of conic quadratic functions. The approach turned out to be not only more general, but also much more effective practically. This appears to be another breakthrough that have led to orders of magnitude computational speed up in our ability to solve the corresponding problems. We expect the results to be of significant use in persistent interdiction operations on networks.

Even if probabilistic constraints are modeled with convex constraints, their separation problem turns out to be a combinatorial problem with a non-convex objective. Finding strong bounds from effective convexifications of the separation problem is thus becomes a very important task for computational solution of combinatorial problems with probabilistic constraints. We have

recently devised new convexifications based on SOS (sum of squares) reformulations and their strengthening. Preliminary computations indicate the effectiveness of these new relaxations.

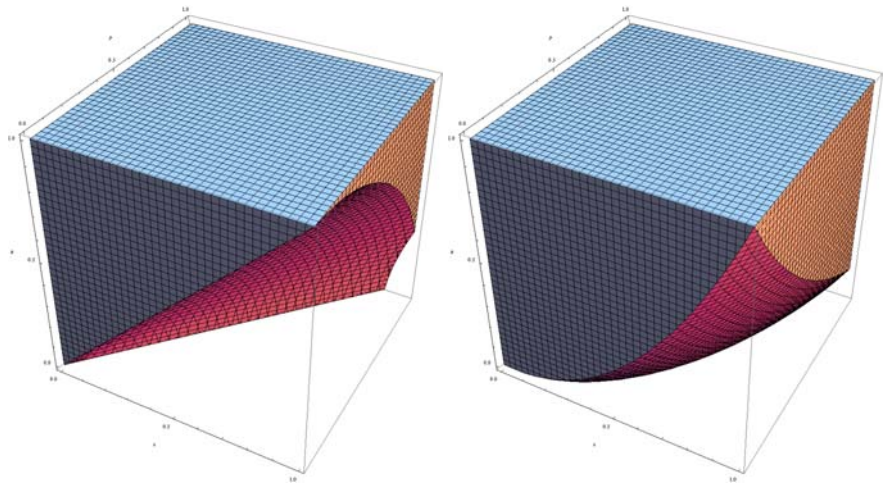

Figure 3. A nonconvex set and its SOS (convex) relaxation.

Cover and pack inequalities for conic quadratic MIPs

Cover inequalities and their extensions have been one of the most effective tools for solving linear MIPs. A natural investigation is consider their use in nonlinear MIPs. However, doing so requires solving nonlinear integer separation and lifting problems, which are quite challenging. We have made significant advances in understanding their structure and put this understanding into algorithmic use. In two separate studies we have shown that a judicious application of special purpose separation and lifting heuristics leads to major computational improvements.

Representative Publications:

Atamturk, A.; Muller, L. F.; Pisinger, P. Separation and Extension of Cover Inequalities for Conic Quadratic Knapsack Constraints with Generalized Upper Bounds. *INFORMS J. on Comp. [Online early access]*. http://joc.journal.informs.org/content/early/2012/06/06/ijoc.1120.0511

Atamturk, A.; Berenguer; G. and Shen, Z.-J. M. A Conic Integer Programming Approach to Stochastic Joint Location-Inventory Problems. *Operations Research* **2012**, *60, 366-381.*

Ahmed, S.; Atamturk, A. Maximizing a Class of Submodular Utility Functions. *Mathematical Programming,* **2011**, *128, 149-169.*

Atamturk, A; Narayanan, V., Lifting for Conic Mixed-Integer Programming. *Mathematical Programming* **2011**, *126, 351-363.*

Atamturk, A; Narayanan, V., Conic Mixed-Integer Rounding Cuts, *Mathematical Programming* **2010**, *122, 1-20.*

Developing Biological Software via Genetically Augmented Proteins

Andrew Ellington
The University of Texas at Austin, *ellingtonlab@gmail.com*
NSSEFF A

Project Description:

The basic technical concept being investigated is how to adapt biology to being rationally programmable, so that organisms can be more readily engineered for a variety of military and commercial applications. The nascent field of synthetic biology has begun to address these issues, by proceeding from the notion that there are component biological 'parts' that can be strung together in 'synthetic circuits' whose function is modular, predictable, and extendable. However, many practitioners in this area assume that extensive descriptions of parts and painstaking characterizations of their ganged function in circuits will on their own provide the basis for an engineering discipline. This limits development and application in the same way that the development of electronic circuits was limited prior to the introduction of standardized digital circuitry and (later) VLSI. In contrast, we have been working towards the standardization of not only the parts but also the underlying logic for their use, by creating highly programmable molecules and systems that are in essence a new type of genetic software.

Extensive genetic programmability will require a new type of biological computer based on chemical reaction networks that execute in space and time; essentially creating amorphous 'matter computers.' Nucleic acid circuitry can serve as the basis for the new genetic software, with progressive Milestones for amplification, pattern formation, and self-assembly. The nucleic acid circuitry can interface with other cellular machinery, such as proteins, by including nucleobase complementarity within the genetic code. To this end, we are expanding the code to include four amino acids, adenyl, thymidyl, cytidyl, and guanyl alanine, and are extensively engineering the translation machinery to better incorporate these new residues into proteins throughout the cell. Ultimately, imbuing biomolecules with programmability through complementary nucleobase interactions should allow for greater control of designed and adapted biological systems for applications that range from bioremediation to the production of commercially relevant small molecules, and cell based sensing systems for diagnostic applications.

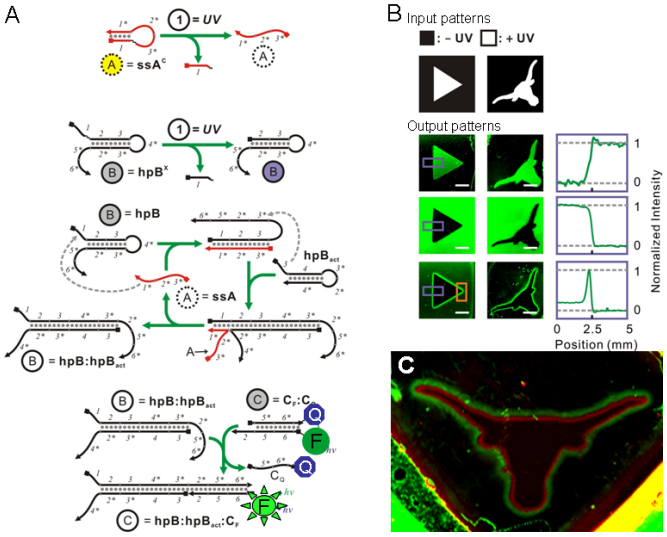

Figure 1. (A) Implementation of the light sensitive edge detector using a CHA circuit. (B) Positive photomask and the green-fluorescent output patterns of the positive image circuit, negative image circuit and edge-detector circuit. (C) Two circuits, red and green, produce an inner and outer edge, respectively.

Accomplishments:

In particular, we have made great progress in achieving amplification, pattern formation, and self-assembly with nucleic acid circuits. A so-called catalytic hairpin assembly (CHA) reaction in which two kinetically

trapped DNA conformers form a duplex via a strand exchange reaction has been optimized and applied to transducing signals from isothermal amplification reactions[1,2,3]. These achievements ultimately resulted in the development of a stacked, non-enzymatic DNA circuit that could amplify input signals by up to 10^6-fold[4].

We have further applied CHA for carrying out amorphous computations leading to pattern formation (**Figure 1)**. In particular, we have developed photosensitive substrates for CHA that, when activated, diffuse to form fluorescent signals in a two-dimensional matrix. By manipulating both the orthogonality of the circuits (easily done via base-pairing) and the downstream fluorescent reporters, we can create patterns of great complexity. Beyond simple photography (patterns that are initiated by exposure to light) the nucleic acid circuits can carry out 'edge detection' computations in which only the border between light and dark becomes fluorescent due to the diffusion of light-activated catalysts into a region of substrates that have not been photo-inactivated. By manipulating the diffusion parameters of different, orthogonal circuits, we can even create double edges in response to a single light image (**Figure 1C**).

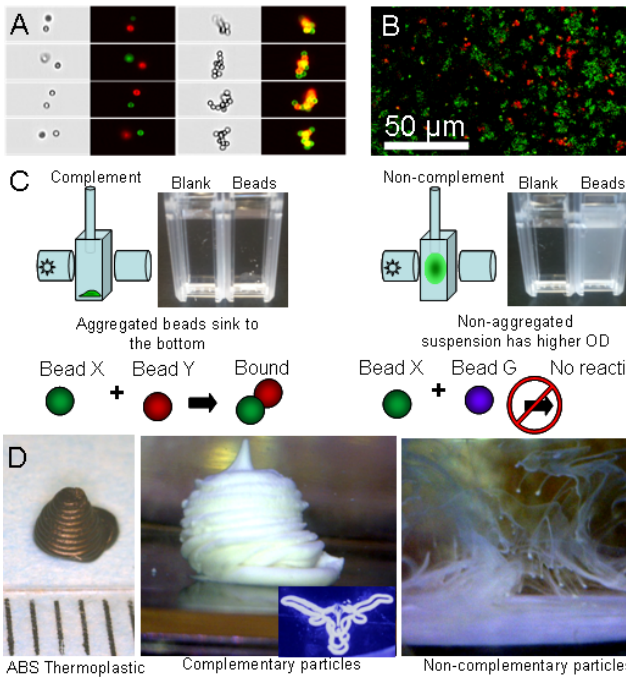

Figure 2. (A) Non-cognate (left, Green-X/Red-Y) and cognate (right, Green-X/Red-X*) 2.3 µm particles show cluster formation. (B) This association is orthogonal; Green-X/Green-X* form clusters simultaneously in parallel with Red-Y/Red-Y*(C) The clusters fall out of suspension due to dense aggregate formation and this can be measured by optical density. (D) The colloidal gel can be printed with a 3D printer into cm scale objects. Non-complementary particles disperse into suspension.

Finally, we have generated novel methods for using DNA for the construction of three-dimensional objects. Polystyrene beads (2.3 µm) coated with DNA can be assembled in a sequence-specific fashion. Using a conventional 3D printer, these beads can then be deposited into objects that hold their shape only in the presence of cognate bonding (**Figure 2**). Once again, the ability to program orthogonal interactions can lead to local structure within a larger material. This advance promises immediate utility for tissue engineering.

Translational Engineering to Enable Programmable Macromolecular Interactions:
To program biomolecular interactions beyond nucleic acids alone, we have generated nucleobase amino acids and have begun to site-specifically incorporate these into proteins. In order to ensure the facile incorporation of these compounds it has been necessary to develop multiple, orthogonal tRNA synthetase:tRNA pairs. We have started with the *Saccharomyces cerevisiae* tryptophanyl tRNA synthetase and its cognate tRNA, recoded to function as an amber suppressor[5]. In addition, we have developed a novel directed evolution system, Compartmentalized Partnered Replication (CPR) that relies on the coordinate improvement of an entire genetic circuit that in turn leads to Taq polymerase production. Those cells that produce

the most Taq can subsequently amplify the circuits that led to their production. Using both rational design and CPR we have greatly improved the performance of the *S. cerevisiae* orthogonal pair, including allowing the site-specific incorporation of the modified amino acid 5-hydroxy tryptophan with efficiency and specificity never before seen, and in multiple positions within a protein (**Figure 3**). For example, previous studies have shown the incorporation of only a single unnatural amino acid into a protein, while we can readily incorporate upwards of three or more unnatural amino acids in the same protein using our optimized system.

We are now applying these methods to the incorporation of nucleobase amino acids. We have both designed and selected tRNA synthetases that can suppress amber codons in the presence of adenyl alanine, and are further characterizing these variants. In order to further augment the code we have also shown that the relatively non-specific pyrrolysyl tRNA synthetase and its cognate suppressor tRNA can incorporate thymidyl alanine into proteins. Thus, we stand ready to introduce the first base-pair interaction into a protein, rather than a nucleic acid.

The ability to incorporate unnatural amino acids is especially useful as it provides new chemistry to proteins, circuits, and entire systems. In this vein, we have begun to evolve entire systems (bacteriophage) that cannot only incorporate unnatural amino acids, but that are actually dependent upon them. For example, we have now generated a variant of bacteriophage T7 that preferentially utilizes 3-iodotyrosine. During the course of evolution, the bacteriophage actually inserted 'stop' codons into its genome in order to acquire the unnatural amino acids (via charged suppressor tRNAs). We are now poised to carry out similar experiments with our novel A:T protein-based base-pair, providing interesting new opportunities for both phage and cells to acquire novel protein:protein interactions and protein:nucleic acid interactions. It can be estimated, based on the current complexity of protein:nucleic acid interactions, that adenyl alanine and thymidyl alanine may accelerate the evolution of regulatory pathways in organisms by up to 10-fold.

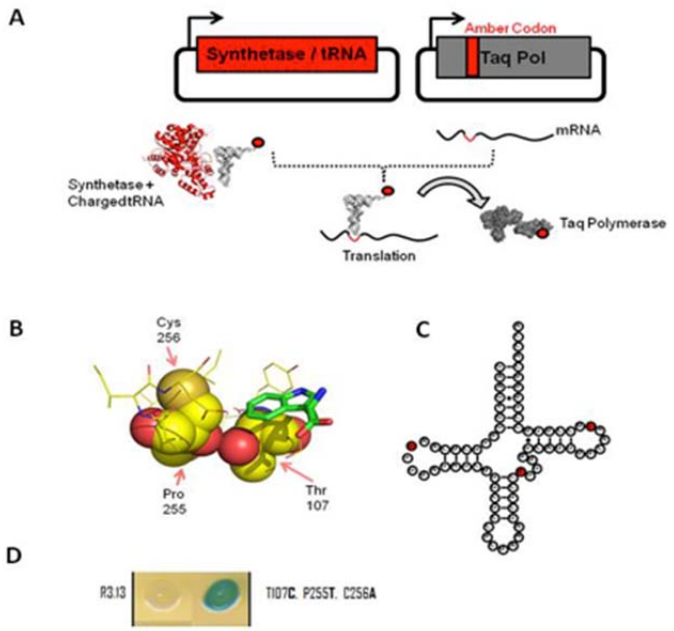

Figure 3. (A) CPR-selection scheme for evolving orthogonal synthetases and tRNAs. (B) Residues in ScWRS modified to accommodate 5OHW. (C) Mutant Orthogonal tRNA from CPR selection (Red spheres show locations of mutations from original). (D) Blue/white Amber suppression assay in the absence (left) and presence (right) of 5OHW to demonstrate evolved substrate specificity.

Representative Publications:

(1) Allen, P. B.; Arshad, S. A.; Li, B.; Chen, X.; Ellington, A. *Lab. Chip* **2012**.
(2) Li, B.; Chen, X.; Ellington, A. D. *Anal. Chem.* **2012**, *84*, 8371–8377.
(3) Jiang, Y.; Li, B.; Chen, X.; Ellington, A. D. *Mol. Basel Switz.* **2012**, *17*, 13211–13220.
(4) Chen, X.; Briggs, N.; McLain, J. R.; Ellington, A. D. *Proc. Natl. Acad. Sci. U. S. A.* **2013**, *110*, 5386–5391.
(5) Hughes, R. A.; Ellington, A. D. *Nucleic Acids Res.* **2010**, *38*, 6813–6830.

Novel methods for electromagnetic simulation and design

Leslie Greengard
Courant Institute, New York University, *greengard@cims.nyu.edu*
NSSEFF Award Year: 2010

Project Description:

Among the many challenges facing designers of advanced communications systems is the interaction between antennas, other electromagnetic sources and the platform itself. Such systems have reached a stage of complexity that design by experimentation is becoming impractical. Thus, in order to deploy functioning systems, to avoid electromagnetic interference, and to add new functionality, accurate computational approaches will be required. These techniques will have to be sufficiently robust to cope with a broad range of frequencies and detailed geometric models, and they will have to be sufficiently fast to allow design by simulation. Our work is aimed at helping to create such tools.

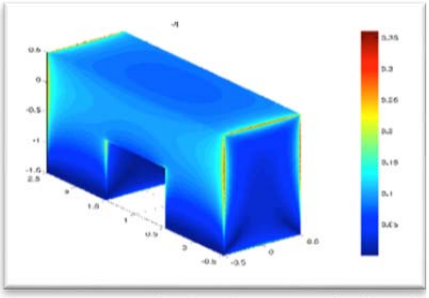

Figure 1. Magnitude of currents induced on perfect conductor with sharp edges

By the end of the project period, we expect to have developed a powerful class of methods for computational electromagnetics, based on new mathematical representations for the Maxwell equations, high order discretization of surfaces and unknowns, and new fast solvers. This will permit high fidelity simulation of geometrically complex and electrically large objects - critical for wideband antenna design, optical component simulation, radar cross section (RCS) prediction and a host of other electromagnetic scattering applications. We intend to produce fully functional simulation environments for micro-structured materials design, planar antenna design, and RCS analysis.

Accomplishments:

The ultimate goal of our research is to create a new generation of highly accurate methods for solving the equations of electromagnetic scattering in realistic environments involving complex geometry. To that end, we are seeking to develop, refine and implement new mathematical representations that overcome many of the obstacles encountered by existing simulation techniques: ill-conditioning, low-frequency breakdown, and the inability to handle multi-connected domains in a robust fashion. We are also developing robust, high-order quadrature schemes for layer potentials defined on surfaces in three dimensions and direct solvers that will permit the efficient pre-computation of the scattering responses of geometric substructures.

After assembling a team in Year 1 with the necessary expertise, we constructed fast solvers for the full Maxwell system (using "Fast Multipole acceleration"), created a user interface compatible with both low and high order discretizations, and implemented the generalized Debye approach of Epstein, Greengard, and O'Neil (*Commun. Pure Appl. Math.* **2010**, 63, 413-463,

Commun. Pure Appl. Math. **2013**, 66, 753-789). Having completed the implementation, we made an important discovery - namely that first order accurate quadrature schemes (which are dominant in existing software) require excessively fine mesh discretizations, so a major effort was initiated to design higher order quadratures that could be implemented efficiently. The lack of fast, high order rules for this purpose has been one of the fundamental obstacles to the development of robust design tools. In the last year, we have developed what appears to be a completely new approach to quadrature. Using only smooth rules, we are now able to evaluate local expansions of the fields induced by weakly singular, principal value and hypersingular integrals at a collection of off-surface points, from which we extract the one-sided limit of the layer potentials with surprising ease. A first paper describing the method (*Quadrature by expansion: a new method for the evaluation of layer potentials*, arXiv:1207.4461) has been submitted for publication. A second paper, entitled *On the convergence of local expansions of layer potentials* is also available on arXiv (arXiv:1212.3868) and has been submitted for publication. This paper provides a rigorous analysis of the convergence theory.

We have developed a new method to overcome low-frequency breakdown in the magnetic field integral equation that permits accurate reconstruction of the electric field in the near and/or far zones. We have shown that one can overcome low-frequency breakdown following the solution of the magnetic field integral equation by solving an auxiliary (scalar) integral equation for the charge. This overcomes the ill-conditioning in computing the electric field. Moreover, both the current and charge can be discretized using simple piecewise polynomial basis functions on triangulated surfaces [Ref 1 below]. Fig. 1, above, was computed using our new scheme.

A classical problem in electromagnetics concerns the representation of the electric and magnetic fields scattered from multiply connected conductors in the low-frequency regime, where topology plays a fundamental role. At zero frequency, the standard boundary conditions on the tangential components of the magnetic field do not uniquely determine the vector potential. We have discovered a (gauge-invariant) consistency condition that overcomes this non-uniqueness and resolves a longstanding difficulty in inverting the magnetic field integral equation [Ref 2 below]. Figure 2 shows the induced surface on a torus at low frequency without and with our new consistency condition. (The solution on the left has lost all digits of accuracy from low-frequency breakdown.)

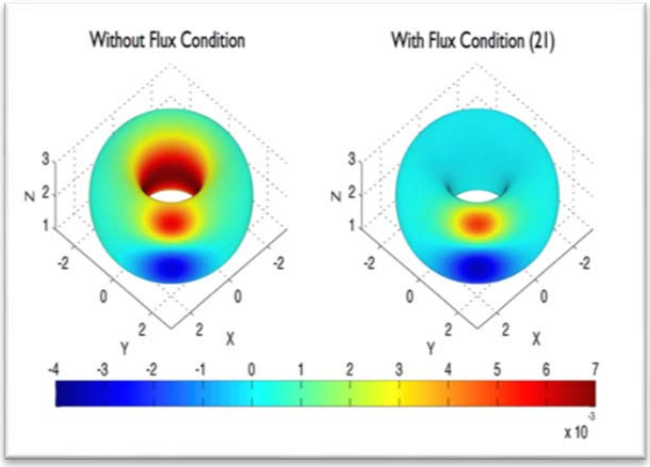

Figure 2: The induced surface current on a torus at very low frequency using the classical and new approach.

We have developed the first robust, well-conditioned integral equation method for the calculation of scattering from periodic and non-periodic structures involving *triple-points* (multiple materials meeting at a single point). The combination of a robust and high-order accurate integral representation and a fast direct solver permits the efficient simulation of scattering from fixed structures at multiple angles of incidence (Figure 3).

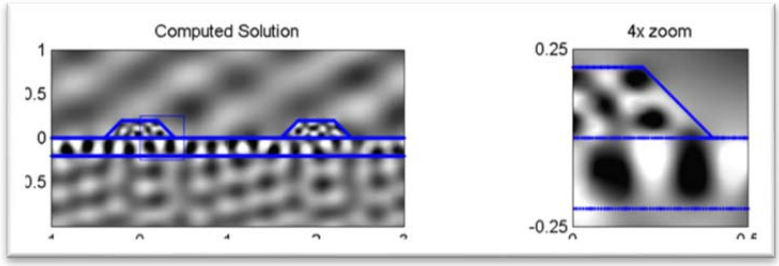

Figure 3: The total field scattered by a periodic array of scatterers on a layered medium. Calculations of this type are common in optics and chip design.

Finally, we have develop a first generation of fast direct solvers for boundary integral equations in both two and three dimensions, based on combining recursive skeletonization with sparse direct methods [Ref 5 below]. Fig. 1 illustrates the use of the solver in rapidly analyzing the interaction of two objects as they approach each other. The solution time for each scattering geometry was approximately one second, using our fast direct solver for each scatterer alone as a preconditioner. This is nearly 100 times faster than a standard iterative approach.

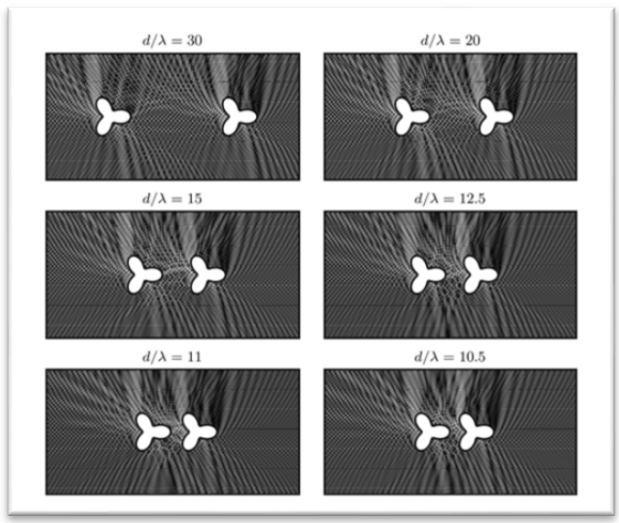

Figure 4: The pressure field in response to an incoming vertical plane wave for various scattering geometries characterized by decreasing the separation distance between the centers of two identical scatterers.

Representative Publications:

1. Vico, F.; Gimbutas, Z.; Greengard, L.; Ferrando-Bataller, M. *IEEE Trans. Antennas Propag.* **2013**, 61, 1285-1290.
2. Epstein, C. L.; Gimbutas, Z.; Greengard, L.; Kloeckner, A.; O'Neil, M., *IEEE Trans. Magn.* **2013**, 49, 1072-1076.
3. Gimbutas, Z; Greengard L. *J. Comput. Phys*. **2013**, 232, 22-32.
4. Greengard, L.; Lee, J.-Y. *J. Comput. Phys*. **2012**, 231, 2389-2395.
5. Ho, K. L.; Greengard, L. *SIAM J. Sci. Comput*. **2012**, 35, A2507-A2532.

Quantum Control of Light and Matter: from the Macroscopic to the Nanoscale

Lene Vestergaard Hau
Harvard University, *hau@physics.harvard.edu*
NSSEFF Award Year: 2010

In our experiments, we stop and extinguish light pulses in a tiny, supercooled atom cloud called a Bose Einstein Condensate (BEC). An extinguished light pulse can subsequently be brought back into existence in another BEC in a separate location. The information carried by the light pulse is transferred from the first to the second atom cloud by converting the light pulse into a travelling matter wave, a small atom pulse that is a perfect matter copy of the extinguished light pulse. After the matter wave enters the second BEC, phase locking induced by the presence of that condensate helps restore the original light pulse. While the matter copy is traveling between the two BECs, it can be trapped for extended time scales and reshaped in whatever form required. The induced changes will then be present in the revived light pulse.

The experiments have given us a much greater control over quantum information than what has ever been achieved before, and the work has important applications in coherent optical and quantum information processing. Very large optical nonlinearities can be induced by injecting several light pulses and converting them to matter. By bringing the matter copies into contact, non-linear effects can be achieved that are many orders of magnitude larger than the non-linearities that can be achieved with photons alone.

We have also built a completely new setup for studies of the interactions between Bose-Einstein condensates and nanoscale structures with the aim of creating novel states of cold atomic matter. The experiments have applications for the development of sensitive atom detectors, including chip-integrated devices for atom interferometry, of importance for precise navigation. As a part of this project, new instrumentation and techniques have been developed for fabrication of novel nanoscale structures.

We are also pursuing completely new research directions focused on light harvesting with hybrid bio-synthetic systems for direct conversion of sunlight to electricity and hydrogen for energy storage. The research combines biological systems with synthetic nanoscale devices and is based on our current studies and experience with light-matter interactions and nanoscale structures**.**

Quantum Networks with Single Atoms, Photons and Phonons

H. Jeff Kimble
California Institute of Technology, *hjkimble@caltech.edu*
NSSEFF Award Year: 2010

Project Description:

A program of basic physics research is being carried out in the area of Quantum Information Science. The goals of the research are to harness fundamental interactions between light and matter to achieve new laboratory capabilities for the processing, storage, and distribution of quantum information. The unifying theme of the proposed research is the realization of quantum interconnects for transferring the quantum states of one physical system to states of another system in a reversible fashion. Such capabilities provide the foundation for the implementation of *Quantum Networks* for quantum computation, communication, and metrology, as well as for the exploration of exotic quantum phases of matter.

This research on *Quantum Networks* presents a unifying set of opportunities and challenges across exciting intellectual and technical frontiers, ranging from the theoretical understanding of entangled states of quantum networks to new experimental tools for the coherent manipulation of quantum dynamical processes. The research program attempts to create new scientific capabilities for the realization of quantum nodes linked by quantum channels that can be assembled into complex quantum networks. The approach is to implement functional quantum networks by way of strong interactions between single atoms, photons, and phonons. Strong interactions can be harnessed for the implementation of quantum logic, for the realization of global quantum-optical interconnects, and for the reliable transport of quantum states across networks. These capabilities provide the basic primitives for the realization of complex *Quantum Networks* and thereby of qualitatively new phenomena in Quantum Information Science.

Accomplishments:

Principal advances in my NSSSEFF research program over the past year are as follows:

1) Enhancement of mechanical quality factors by optical trapping - The quality factor of a mechanical resonator is an important figure of merit for various sensing applications and for observing quantum behavior. In Ref. [1], we demonstrate a technique to push the quality factor of a micro-mechanical resonator beyond conventional material and fabrication limits by using an optical field to stiffen or trap a particular motional mode. Optical forces increase the oscillation frequency by storing most of the mechanical energy in a nearly lossless optical potential, thereby strongly diluting the effect of material dissipation. By placing a 130 nm thick SiO_2 pendulum [Fig. 1] in an optical standing wave, we achieve an increase in the pendulum center-of-mass frequency from 6.2 to 145 kHz. The corresponding mechanical quality factor Q increases 50-fold from its intrinsic value to a final value of $Q = 5.8(1)\times10^5$, representing an improvement of more than an order of magnitude over the conventional limits of SiO_2 for our geometry. Our technique may enable new opportunities for mechanical sensing and facilitate observations of quantum behavior in this class of mechanical systems.

2) A state-insensitive nano-fiber trap - In Ref. [2], my group reports the experimental realization of an optical trap that localizes single Cesium atoms approximately 215 nm from the surface of a dielectric nanofiber. By operating at magic wavelengths for pairs of counter-propagating red- and blue-detuned trapping beams as described in our prior theoretical paper, differential scalar light shifts are eliminated, and vector shifts are suppressed by approximately 250-fold. We thereby measure an absorption linewidth $\Gamma/2\pi = (5.7 \pm 0.1)$ MHz for the Cs $6S_{1/2} \rightarrow 6P_{3/2}$ transition, where $\Gamma_0/2\pi = 5.2$ MHz in free space. Optical depth $d \approx 66$ is observed, corresponding to an optical depth per atom $d_1 \approx 0.08$ (i.e., one atom absorbs 8%

of an incident beam). These advances provide an important capability for the implementation of functional quantum optical networks and precision atomic spectroscopy near dielectric surfaces.

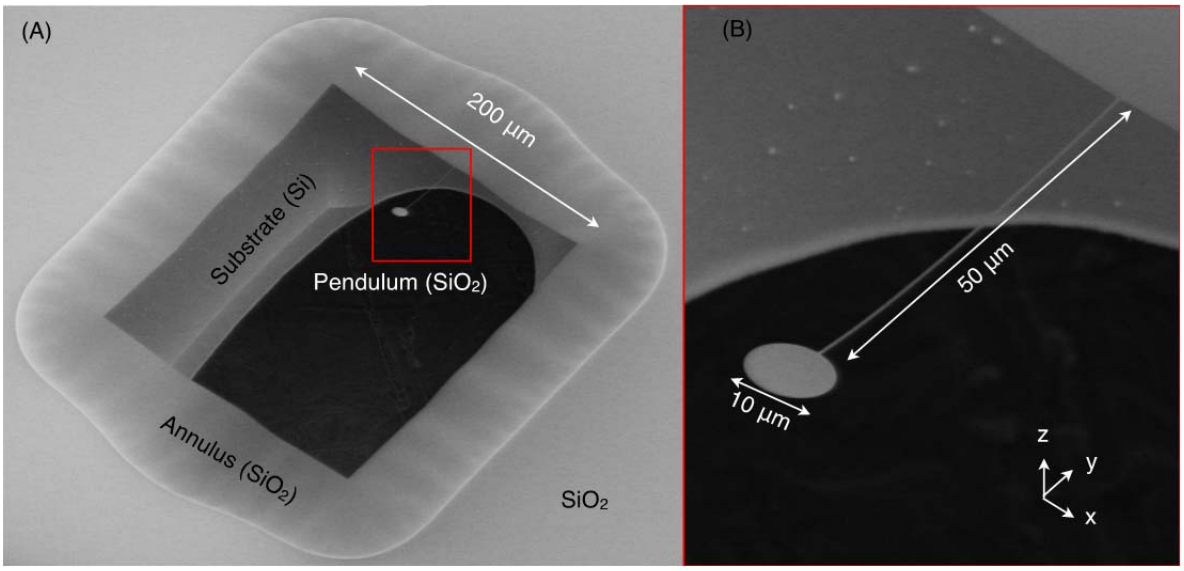

Figure 7 – Scanning electron micrographs of the device from Ref. [1]. A 130 nm thick SiO_2 membrane forms the pendulum, which consists of a 10 micron diameter disk and a 50 micron × 0.43 micron tether. (A) Overview: The pendulum is suspended from a 60 micron wide SiO_2 annulus. The annulus (wrinkled area) and the pendulum are etched into a SiO_2 film for which the Silicon substrate directly underneath has been removed. The dark background in the center is a clear opening of the substrate. (B) Close-up view of the pendulum, which is deflected 10-15 degrees out of the plane of the substrate due to residual stress of the film. The disk is placed in an optical standing wave that provides an "optical spring" to increase the center-of-mass oscillation frequency with an associated quadratic increase in *Q*.

3) A new paradigm for strong interactions of single atoms and photons - A promising approach to merge atomic systems with scalable photonics has emerged recently, which consists of trapping cold atoms near tapered nanofibers, as achieved in our work in Ref. [2]. In Ref. [3], my colleagues and I describe a novel technique to achieve strong, coherent coupling between a single atom and photon in such a system. As illustrated in Fig. 2, our approach makes use of collective enhancement effects, which allow a lattice of atoms to form a high-finesse cavity within the fiber. We show that a specially designated 'target' atom within the cavity formed by the mirror atoms can experience strongly enhanced interactions with single photons in the fiber. Under realistic conditions, a 'strong coupling' regime can be reached, wherein it becomes feasible to observe oscillations of one quantum between the excited impurity atom and a single cavity quantum distributed coherently among the mirror atoms. Our results can provide the basis for a scalable quantum information network by using atom–nanofiber systems.

4) Self-organization of atoms along a nanophotonic waveguide - Atoms coupled to nanophotonic interfaces represent an exciting frontier for the investigation of quantum light-matter interactions. While most work has considered the interaction between statically positioned atoms and light, in Ref. [4] my colleagues and I demonstrate that a wealth of phenomena can arise from the self-consistent interaction between atomic internal states, optical scattering, and atomic forces. As illustrated in Fig. 3, we consider the case of atoms coupled to a one-dimensional nanophotonic waveguide and show that this interplay gives rise to the self-organization of atomic positions along the waveguide, that is, to a one-dimensional 'crystal' formed from atoms and light. We show that the self-organized configurations can be probed through distinct characteristics in the reflection and transmission spectra of the 1-d photonic waveguide.

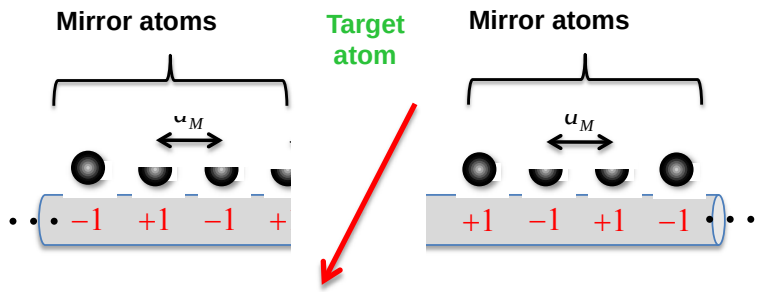

Figure 8 – Illustration an array of atoms (spheres) trapped by optical forces near the surface of a nanoscopic optical fiber (grey cylinder of diameter ≈ 400 nm), as in Ref. [2]. For suitable trapping conditions, two sets of atoms (the black spheres) become highly reflecting mirrors (with reflectivity $R > 0.999$) for light propagating in the nanofiber. A target atom (green sphere) is distinguished from the mirror atoms only by its spatial location along the nanofiber. As analyzed in Ref. [3], such an atomic array can provide a new paradigm for light-matter interactions, here functioning as a novel realization of a cavity QED system, where now the mirrors become quantum objects (e.g., a quantum memory). This system is a promising building block for scalable quantum information processing.

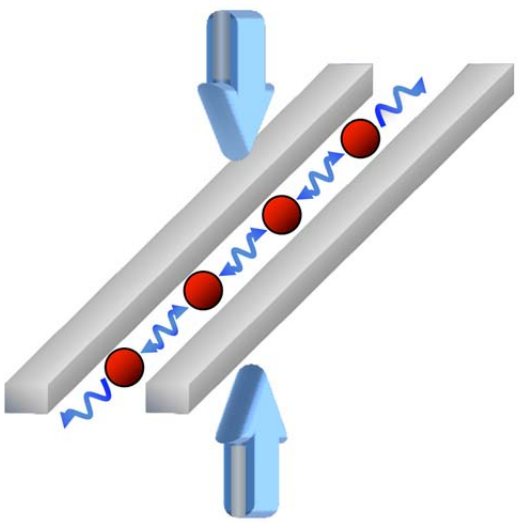

Figure 3 – Illustration of atoms (red balls) coupled to a nanoscopic optical waveguide (parallel grey bars) [4]. The atoms are driven by external pumping lasers (blue vertical arrows). As a result of forces on the atoms due to light emission into the waveguide (wavy blue arrows), the atoms spontaneously organize into a one-dimensional "crystal." Illustration from Physics Focus, *http://physics.aps.org/articles/print/v6/30*.

Representative Publications:

[1] Ni, K.-K.; Norte, R.; Wilson, D. J.; Hood, J. D.; Chang, D. E.; Painter, O.; Kimble, H. J. *Phys. Rev. Lett.* **2012**, 108, 214302(5).
[2] Goban, A.; Choi, K. S.; Alton, D. J.; Ding, D.; Lacroûte, C.; Pototschnig, M.; Thiele, T.; Stern, N. P.; Kimble, H. J. *Phys. Rev. Lett.* **2012**, 109, 033603(5).
[3] Chang, D. E.; Jiang, L.; Gorshkov, A. V.; Kimble, H. J. *New J. Phys.* **2012**, 14, 063003(14).
[4] Chang, D. E.; Cirac, J. I.; Kimble, H. J. *Phys. Rev. Lett.* **2013**, 110, 113606(6).
[5] Hung, C.-L.; Meenehan, S. M.; Chang, D. E.; Painter, O.; Kimble, H. J. arXiv:submit/0637472 [quant-ph] (submitted on 22 January **2013**).

Attosecond Electron Processes in Materials: Excitons, Plasmons, and Charge Dynamics

Stephen R. Leone
University of California, Berkeley, *srl@berkeley.edu*
NSSEFF Award Year 2010

Project Description:

This project investigates condensed phase electron dynamics on the attosecond (10^{-18} seconds) timescale, the native timescale on which electron motion, coherence, and dephasing evolve. Electronic phenomena such as band gap renormalization in semiconductors, multi-exciton generation in quantum dots, and surface plasmon dephasing in metal nanoparticles will be observed in real time as they evolve. This is achieved using state-of-the-art infrared laser pulses lasting only a few optical cycles to generate isolated 100-attosecond bursts of extreme ultraviolet (XUV) light. After initiating an electronic excitation in a solid sample, the attosecond XUV pulses are used to probe the evolution of the excitation after a variable time delay, producing an attosecond-resolved "movie" of the ensuing electron dynamics. Two experimental probe techniques have been implemented for this purpose: measurement of the change in the XUV absorption or reflectivity of the sample as a function of pump-probe delay time, and measurement of the change in velocity distribution of photoelectrons emitted by the attosecond XUV pulse. Both techniques will provide unprecedented insight into processes that govern electron motion in the earliest stages of excitation.

Accomplishments:

Two instruments for attosecond-resolved electron dynamics experiments have been constructed using this award with additional support from the W.M. Keck Foundation. Both apparatuses are equipped with 750 nm chirped pulse amplifiers that produce 25 fs pulses at 1 kHz, with a pulse energy of approximately 1.8 mJ. These pulses are spectrally broadened in a gas-filled hollow core fiber and compressed with a set of chirped mirrors to a duration of ~5 fs and a pulse energy of ~800 μJ. XUV light is generated by tightly focusing these pulses into a gas cell filled with either neon or argon to produce high harmonics. The spectral bandwidth covered by the resulting XUV pulses can support 100 attosecond pulses. Control of the carrier envelope phase of the generating pulses is essential for the production of isolated attosecond pulses, and optical gating is being added to the apparatus to insure high contrast and tunability of the XUV spectrum. For XUV transient absorption experiments, electron dynamics in solid-state samples are probed by monitoring the change in the transmitted or reflected XUV spectrum at a variable delay time after irradiation of the sample by a 5-fs, 750 nm driving pulse. In ßvelocity map imaging (VMI) experiments, photoelectrons are produced from metallic samples using an XUV pulse at a controlled delay time after initiating a plasmon with the driving pulse, and the velocity distributions of the photoelectrons as a result of their interaction with the plasmon's electric field are imaged. Optics for doubling of the 750 nm pulses and temporal compression are being installed to expand the range of accessible pump pulse energies.

These experiments push the frontiers of both attosecond science and solid state physics, incorporating new technologies and theory as part of a comprehensive program in the Leone group. A number of simulations and related experiments have been undertaken to augment the instrumental design and data analysis. Many experiments will involve the interaction of XUV light with matter irradiated by intense infrared pulses. Experiments and computations performed illustrate that extremely intense infrared light can alter the way that gas-phase atoms transmit XUV light, creating a controllable "switch" for the XUV light that is "on" for times on the order of a femtosecond. We have also shown that intense infrared light pulses can be used to shape attosecond XUV pulses when they are transmitted through a material. In addition, the motion of electrons in atoms and ions excited by light can be tracked experimentally using attosecond XUV pulses. The energy levels in atoms irradiated with intense infrared light can be strongly split due to coupling with the field, and we have shown that the observed splitting can only be rationalized using theory beyond the rotating wave approximation. The theoretical and experimental results have provided sophisticated machinery necessary for XUV transient absorption studies. Simulations of photoelectron experiments (Figure 1) show how velocity map imaging and electron time-of-flight spectrometry can be used to map the temporal and spatial properties of plasmon build-up and decay in metallic nanostructures. The interaction of photoelectrons emitted from gold "nanopillar" samples upon irradiation with intense, few-femtosecond infrared pulses has been studied both experimentally and theoretically.

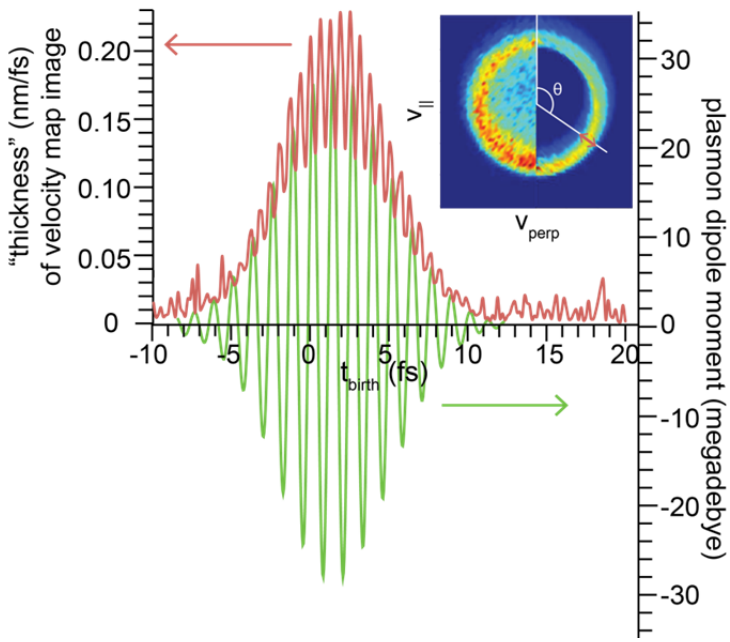

Figure 9. Simulated velocity map imaging-based reconstruction of the dynamical plasmon dipole moment of 80 nm silver nanospheres excited by a resonant 5-fs, 376 nm laser pulse.

These results have led to the construction of the world's first solid-state VMI device, which is currently being tested in preparation for attosecond-resolved experiments. The simulations indicate that Legendre polynomial decomposition of the images, as in conventional gas-phase VMI, will be insufficient to track the dynamics of the plasmon. Instead, other characteristics, such as the width and shape of the photoelectron distribution, will be much more informative. Samples of gold nanodiscs and nanorods resonant at 750 nm have been fabricated in collaboration with the Molecular Foundry at Lawrence Berkeley National Laboratory for initial testing of the VMI device and for dynamics experiments.

Attosecond-resolved transient absorption (TA) experiments are underway. The first transient absorption targets, Fe_2O_3 (hematite) films deposited on Si_3N_4, have been studied in an 80-fs time-resolved XUV TA project. The results indicate a distinct charge transfer signature from oxygen to iron near 56 eV within the 80 fs upon irradiation with 400 nm light. The band gap of Fe_2O_3 occurs near 600 nm, and experiments will investigate the few-fs dynamics of band-gap excitation using broadband, 750 nm pulses and attosecond XUV pulses. Spatial and temporal overlap of the pump and probe beams for the NSSEFF-funded XUV transient absorption apparatus have been confirmed, and the static XUV absorption spectrum of the Fe(III) *M*-edge near 56 eV has been measured (Figure 2). The attosecond-resolved transient absorption spectrum will be measured to reveal the few-femtosecond dynamics of band gap excitation in these materials, such as coherent build-up of excited state population and movement of electrons into surface trap states. A modification to the apparatus to enable production of few-fs 400 nm pump pulses is designed for single-photon excitation of the oxygen-to-metal transition and similar transitions in other semiconductors. Co_3O_4 film samples on Si_3N_4 windows are being fabricated for investigation of the few-fs dynamics of the band gap (690 nm) and a higher electronic excitation at 430 nm, which is thought to be either a ligand-to-metal or metal-to-metal charge transfer.

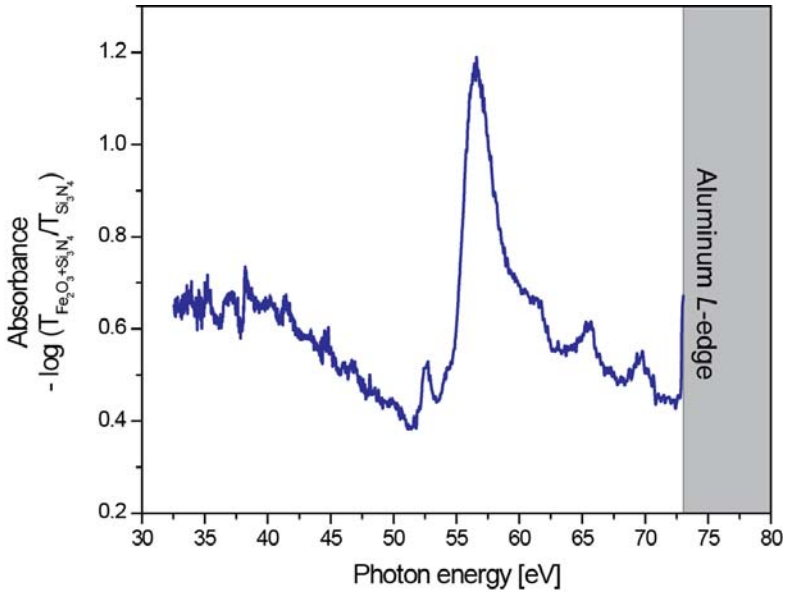

Figure 2. XUV absorption spectrum of Fe_2O_3 on a Si_3N_4 window using XUV pulses prepared using the high harmonic method. The feature near 56 eV is the Fe(III) *M*-edge.

Representative Publications:

Nagel, P.M.; Robinson, J.S.; Harteneck, B.; Pfeifer, T.; Abel, M.J.; Prell, J.S.; Neumark, D.M.; Kaindl, R.A.; Leone, S.R. *Chemical Physics* **2012**, *414*, 106-111.

Pfeiffer, A.N.; Leone S.R. *Physical Review A,* **2012**, *85*, 053422.

Chen, S.H.; Bell, M.J.; Beck, A.R.; Mashiko, H.; Wu, M.X.; Pfeiffer, A.N.; Gaarde, M.B.; Neumark, D.M.; Leone, S.R.; Schafer, K.J. *Physical Review A*, **2012**, *86*, 063408.

Lin, M.F.; Pfeiffer, A.N.; Neumark, D.M.; Leone, S.R.; Gessner, O. *Journal of Chemical Physics* **2012**, *137*, 244305.

Prell, J.S.; Borja, L.J.; Neumark, D.M.; Leone S.R. *Annalen der Physik—Berlin* **2013**, *525*, 151-161.

Computational and Theoretical Design of Photo- and Mechano-Responsive Molecular Devices

Todd J. Martinez
Stanford University, *todd.martinez@stanford.edu*
NSSEFF Award Year: 2010

Project Description:

A holy grail in theoretical chemistry has been the ability to design molecular systems with desired functions from first principles. One of the major obstacles in this quest has been the need for methods that are both accurate and computationally efficient so that a large portion of chemical space can be sampled and explored. This project is aimed at developing new electronic structure and first principles molecular dynamics methods which can overcome this obstacle and applying them to design function in photo- and mechano-activated molecular devices, i.e. large molecular structures such as biological macromolecules, polymers, and supramolecular systems.

The project is developing new tools for chemical simulation exploiting novel computational architectures such as graphical processing units as well as new algorithms to reduce computational scaling inspired by advances in machine learning. These new tools are being used to introduce novel approaches such as interactive *ab initio* molecular dynamics where a human user can guide the simulation to discover new design principles and "discovery-mode" simulations where stable structures can be sampled and automatically cataloged along with chemical reactions connecting these stable structures. Finally, these new tools are being applied to excited states in proteins and biomolecules as well as mechanically induced reactivity in polymeric systems.

Accomplishments:

We have developed our graphical processing unit (GPU) based electronic structure theory code (TERACHEM) in a number of important directions that make calculations both faster and more accurate. The fast single precision calculation capability of the GPU has been exploited with a new "dynamical precision" algorithm that uses single precision for small Coulomb repulsion integrals and double precision for the large integrals. The threshold separating small and large integrals is dynamically adjusted to ensure that the accuracy of the calculation at any given stage is commensurate with the distance from the ultimate solution. Because the solution is determined progressively, i.e. the algorithm focuses on the difference between the improved solution and the previous iteration in the electronic structure calculation, this dynamical precision algorithm can achieve double precision accuracy without *ever* calculating all the Coulomb repulsion integrals in double precision. This algorithm enables calculations to be carried out 2-4 times faster than the conventional double precision algorithm, without loss of accuracy. The insight here is far-reaching and applies not only to numerical precision of the computational unit, but also to approximations such as the neglect of small exchange matrix elements. We are currently using this idea in a broader context – considering sequences of approximate Hamiltonians that approach the desired Hamiltonian at convergence. As in the dynamical precision case, this will lead to acceleration without altering the accuracy of the final result.

We have also incorporated the ability to describe electronic excited states in TERACHEM, using time-dependent density functional theory (TDDFT). We carried out the *first* calculations of excited states

in a protein, with explicit quantum mechanical treatment of all the $O(10^4)$ electrons in the molecule. We have used this to calculate absorption spectra of photoactive yellow protein (requiring thousands of calculations, each of which would have been impossible previously). As shown in Figure 1, these calculations demonstrate that the convergence of hybrid quantum mechanical/molecular mechanical (QM/MM) methods is quite slow and requires QM treatment of 500 or more atoms in the region surrounding the chromophore. Fortunately, such calculations are now routinely possible due to our developments in the algorithms and implementation on GPUs.

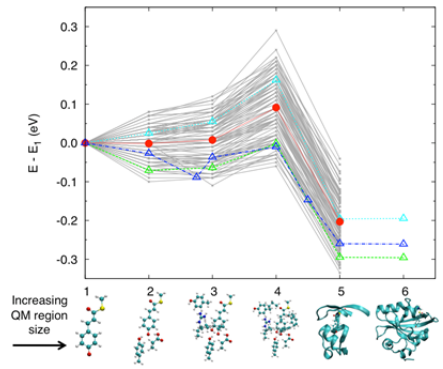

Figure 1. QM/MM electronic excitation energy in photoactive yellow protein (PYP) as a function of the size of the QM region. Excitation energies for several structures (obtained from snapshots of force-field dynamics) are shown (referenced to the value obtained for the smallest QM region containing only the chromophore). Convergence of the excitation energy is not achieved until the second largest QM region containing 500 atoms.

We used TERACHEM to carry out the first *ab initio* molecular dynamics calculation of a solvated protein molecule and further explored possible failures in the empirical force field descriptions that are dominantly used. We found that there are significant charge transfer effects involving protein and solvent that cannot be modeled with an empirical force field. This result implies that charge transfer effects involving the surrounding solvent may be important in a variety of molecular systems ranging from biomolecules to polymers. We also carried out a validation of *ab initio* methods for macromolecular structures, comparing to results from empirical force fields and experimental crystal structures. As shown in Figure 2, empirical force field results are significantly less trustworthy when biological macromolecules are disordered, while the *ab initio* results remain accurate for both ordered and disordered structures. The deficiency of empirical force field derived structures is expected, since these force fields are parameterized to reproduce well-ordered structures (e.g., alpha-helix and beta-sheet structures in proteins). However, the uniform accuracy of *ab initio* methods could not be securely predicted beforehand. Indeed, some of the density functionals commonly considered as the best for molecular structures and chemical reaction energetics (e.g. B3LYP) become questionable for large molecules (with 200+ atoms). Thus, one of the outcomes of this work was the recognition that range-separated functionals (which remove self-interaction errors exactly for distant electrons) may be required for DFT calculations on large molecules.

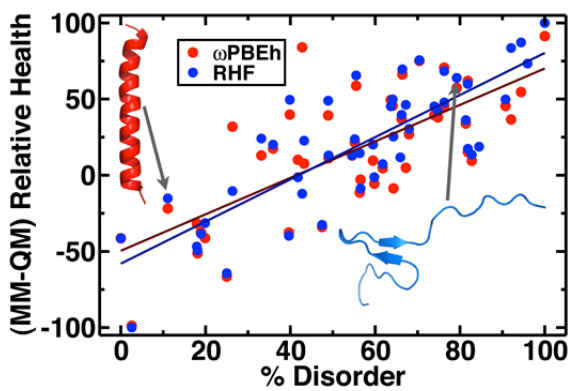

Figure 2. Relative health of force field and *ab initio* determined structures for 51 proteins with up to 590 atoms. When the relative health is negative, the force field provides a better description of the structure. The results are plotted as a function of protein disorder and show that both Hartree-Fock (RHF) and DFT (ωPBEh) *ab initio* methods provide a consistently better description than force fields for disordered structures.

We have exploited the efficiency of TERACHEM to implement an interactive ab initio molecular dynamics method. A haptic input device allowing the user to control the three dimensional position of a pointer with full force feedback is

combined with TERACHEM, three-dimensional visualization, and the VMD molecular graphics program. *Ab initio* molecular dynamics can be visualized interactively (approximately 1 femtosecond of simulation time every second of real time) and the user can select atoms and pull on them. Strong bonds are harder to break (force feedback form the haptic device is stronger) and the user can feel this. We are improving the interface to make it easier to interact with the molecular simulation. We envision that this will be a useful tool to probe mechanical response of chemical units embedded in mechanosensitive polymers, for probing intermolecular interactions, and for providing human input to guide simulations (for example in the context of molecular design). It may also be useful as a pedagogical tool for chemistry students. This further led us to explore new ways to use *ab initio* molecular dynamics – in a "discovery mode" which can augment traditional simulation techniques. The idea is to explore chemical space automatically by following molecular dynamics in a small spherical "beaker" that can be heated and pressurized. Chemical reactions will occur and these are cataloged automatically by the computer, which creates a list of all observed molecular structures. Furthermore, the computer can automatically catalog reactions that transform these molecular structures and refine the reaction paths to determine mechanisms. The temperature and pressure can be varied during the simulation in order to generate more stable structures and/or reactions. We have used machine learning techniques to catalog the structures and identify chemical reactions. We plan to extend this technique to do efficient sampling of conformations in large molecules, for example by selectively heating the region around an enzymatic active site or the chromophore of a photoactive protein. We will also extend this idea to include application of external forces as a means of exploring mechanophores that could be placed in force-sensitive polymers.

Figure 3. Interactive *ab initio* molecular dynamics with force feedback.

Finally, we have used machine learning techniques to develop a new approach to electronic structure theory that reduces the computational scaling with respect to molecular size by *two* powers. This translates to an efficiency gain of 250000 for a molecule with 500 atoms. The idea is based on tensor decomposition of the two-electron repulsion integrals and wavefunction coefficients. Fourth order tensors are represented as a product of five second order tensors. This "tensor hypercontraction" method has been applied to perturbation theory, configuration interaction, and coupled cluster methods. We have shown that the method reproduces energies obtained from conventional methods to better than chemical accuracy (1 kcal/mol). We are currently implementing these methods on GPUs and in parallel, and this will make wavefunction based methods for electronic excited states viable for molecules with $O(10^3)$ atoms.

Representative Publications:

Ufimtsev, I. S.; Luehr, N.; Martínez, T. J. *J. Phys. Chem. Lett.* **2011**, *2*, 1789-1793

Isborn, C. M.; Luehr, N.; Ufimtsev, I. S.; Martínez, T. J. *J. Chem. Theo. Comp.* **2011**, *7*, 1814-1823

Kulik, H. J.; Luehr, N.; Ufimtsev, I. S.; Martínez, T. J. *J. Phys. Chem. B* **2012**, *116*, 12501-12509

Isborn, C. M.; Goetz, A. W.; Clark, M. A.; Walker, R. C.; Martínez, T. J. *J. Chem. Theo. Comp.* **2012**, *8*, 5092-5106

Hohenstein, E. G.; Parrish, R. M.; Martínez, T. J. *J. Chem. Phys.* **2012**, *137*, 044103

Paradigms for Emergence of Shape and Function in Biomolecular Electrolytes for the Design of Biomimetic Materials

Monica Olvera de la Cruz
Northwestern University, *m-olvera@northwestern.edu*
NSSEFF Award Year: 2010

Project Description:

Cells contain charged molecules, organized via reversible interactions into supramolecular structures and materials, which can perform mechanical and chemical functions with precision in fluctuating media. Our work aims to uncover the principles underlying the cellular programming responsible for compartmentalization, communication and replication as well as to subsequently employ these principles to generate assemblies that function as autonomous organisms. Living matter is highly inhomogeneous at the nano-scale both in composition and charge. A big challenge has been to determine how these inhomogeneities generate functions. In this context, the dominant role played by electrostatics during pattern formation is evident, given that nucleic acids and many proteins are charged or possess units with tunable degrees of charge. As a result, the association of biomolecules into functional units has demonstrated strong dependence on local ionic concentrations. Thus, using ionic gradients as one means to control the assembly and disassembly of biological entities is critically important to generate biomimetic functions. We develop models, based on information collected *in vivo* and *in situ*, to better understand the physical properties and functions of biomolecular assemblies in different ionic conditions for designing biomimetic materials with new capabilities.

Accomplishments:

Fluids of charged particles act as the supporting medium for chemical reactions and physical, dynamical, and biological processes. Micro- and nanoscopic polarizable objects deform the local structure in an electrolytic background. Vice versa, the forces between the objects are regulated by the cohesive properties of the background (Figure 1). We studied the range and strength of these forces and the microscopic origin from which they emerge [1], providing an intuitively appealing overview to aid and enhance predictability and control in experiments. We described several distinct ion-induced forces in aqueous solutions of monovalent ions at salt concentrations ranging from 0.01 to 1 M that are expected to compete for dominance with the well-known screened Coulomb forces. The concept of soft structure was introduced to connect the induced

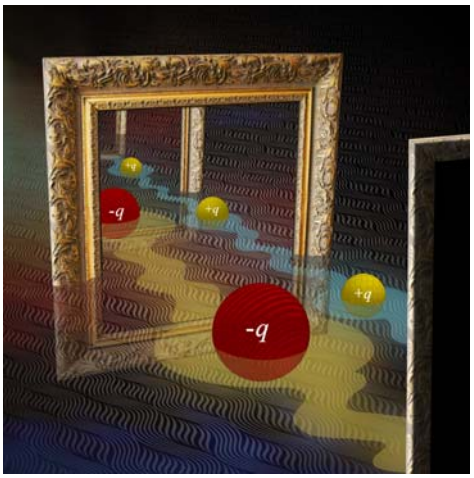

Figure 1: Charged particles in a liquid are enveloped by a cloud of opposite charge that deforms near boundaries, and creates a force away from the boundary. Electrostatically, boundaries act as mirrors, causing additional attractions or repulsions. Theory reveals how ions influence forces between boundaries in an intricate way, and vice versa, with important implications for biological systems (Artistic impression by D. Spjut).

forces to the local microscopic structure in the ionic fluid and visualize the deformation of the local environment around the ions near several types of boundaries that are neutral, adsorbing, charged, polarizable, or a combination of these properties. Until recently, it was computationally costly to simulate the effects of charges on inhomogeneous dielectric media and vice versa, since it required solving the Poisson equation at each simulation step. In a related study, we developed a judiciously designed variational formulation, eliminating the need to solve the Poison equation explicitly. This work will lead to tremendous speed-ups in simulations of charged systems.

Much of the structural stability of the cells's nucleus comes from meshworks of intermediate filament proteins known as lamins forming the inner layer of the nuclear envelope called the nuclear lamina. These lamin meshworks additionally play a role in gene expression. Abnormalities in nuclear shape are associated with a variety of pathologies, including some forms of cancer and Hutchinson–Gilford Progeria Syndrome, and often include protruding structures termed nuclear blebs. These nuclear blebs are related to pathological gene expression. However, little is known about how and why blebs form. We developed a minimal continuum elastic model of a lamin meshwork that we use to investigate which aspects of the meshwork could be responsible for bleb formation (Figure 2).

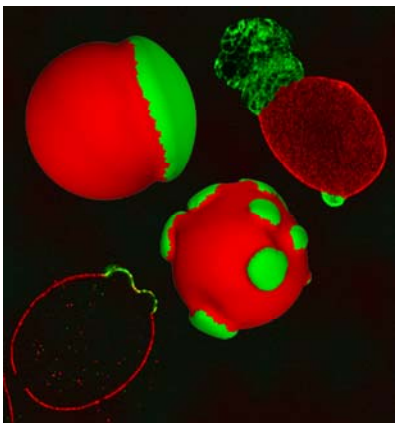

Figure 2: Experimental and computational images of nuclei showing the segregation of two types of lamin proteins in cell nuclei. A-type lamin is shown in green, while B-type is shown in red (Image modified from simulation snapshots and TEMs by M. Seniw).

The model produces structures with comparable morphologies and distributions of lamin types as in real pathological nuclei [2]. Thus, preventing this lamin segregation could be a route to prevent bleb formation, which could be used as a potential therapy for the pathologies associated with nuclear blebs.

A considerable part of our work is aimed at elucidating structure and function relationship in membranes. A large variety of amphiphillic molecules with charged groups self assemble into closed structures such as viral capsids, halophilic organisms and bacterial microcompartments. We formulated a generalized elastic model for inhomogeneous shells, and demonstrated that co-assembled shells with two elastic components buckle into irregular and regular polyhedra besides icosahedra, such as dodecahedra, octahedra, tetrahedra, and hosohedra shells via a mechanism that explains many observations, predicts a new family of polyhedral shells, and provides the principles for designing micro-containers with specific shapes and symmetries for numerous applications in materials and life sciences [3]. For instance, designing polyhedral shells with specific structures can lead to efficient nano-reactors that will perform specific

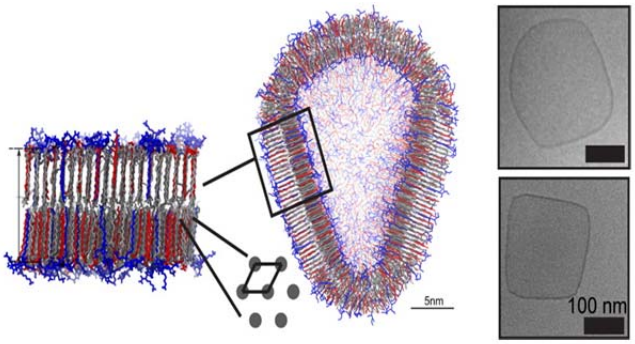

Figure 3: Atomistic simulations, and TEM images of faceted and irregular polyhedral with hexagonal crystalline symmetry, stable in closed shaped and high salt concentration.

catalytic functions. In a collaborative effort with experimental collaborators, we modeled and assembled shells composed of oppositely charged lipids, and were able to regulate the shape of the resulting nanocontainers via pH changes, as evidenced by Transmission Electron Microscopy (TEM, Figure 3) and x-ray scattering [4]. Vesicles or nano-containers with crystalline properties show great promise in nanomaterial fabrication due to their excellent mechanical stability at high salt concentration environments. We also studied by atomistic simulations, the effects of counterion valency on anionic membranes. Our work showed that the inter-tail van der Waals interaction has a dominant role in the electrostatic driven transition from disordered liquid-crystalline phase to the ordered gel phase. Using monovalent counterions, such phase transitions occur at lower temperatures than in scenarios where multivalent counterions are used. We also studied the effects of curvature in multi-component liquid membranes with three components using Molecular Dynamics (MD) simulations to find low-energy structures. The different chemical and physical properties of the components, whose shapes and in-membrane arrangement are coupled through phase-specific bending energies and line tensions, results in a variety of shapes and component patterns. Moreover, we studied shapes of pored membranes, and show that the mean curvature leads to budding-like behavior, while the Gaussian curvature flattens membranes near the pore area. Our work explains shapes of pored membranes that are observed in experiments.

Motivated by the remarkable stability against degradation by nucleases of functionalized spherical nuclei acids-gold (SNA-Au) nanoparticles in blood, we modeled the ion cloud around them by means of classical density functional theory and by computer simulations. For small particles with high density of oligonucleotides, we find that the local salt concentration is enhanced with a pronounced localization of divalent ions near the particle surface. This strong cloud of sodium and calcium ions stabilizes the particle complex in blood, which may prevent enzymes from accessing the DNA and digesting it. We also developed coarse-grained schemes to understand and optimize programmable assembly [5] of grafted nuclei acid-gold nanoparticles. In particular, our MD simulations have identified key elements, such as optimal strength of DNA linkers and percentage of DNA hybridizations, to successfully assemble nanoparticles into a large variety of superlattices. The MD simulations have also elucidated the role that nanostructure coordination plays in the ordering of superlattice assemblies. We constructed detailed phase diagrams that closely match the experimental observations, and showed that highly dynamic hybridization processes between the semi-flexible grafted chains enable crystallization of the functionalized nanoparticles. A model that efficiently captures the competing electrostatic and DNA hybridization interactions in the assembly process was developed to determine the dynamics of the coarsening process that leads to various faceted crystals of functionalized nanoparticles.

Representative Publications:

1. Zwanikken, J. W.; Olvera de la Cruz, M. *Proc. Natl. Acad. Sci.* **2013**, *110*, 5301-5308.
2. Funkhouser, C. M.; Sknepnek, R.; Shimi, T.; Goldman, A. E.; Goldman, R. D.; Olvera de la Cruz, M. *Proc. Natl. Acad. Sci.* **2013**, *110*, 3248-3253.
3. Vernizzi, G.; Sknepnek, R.; Olvera de la Cruz, M. *Proc. Natl. Acad. Sci.* **2011**, *108*, 4292-4296.
4. Leung, C-Y.; Palmer, L.; Qiao, B.; Kewalramani, S.; Sknepnek, R.; Newcomb, C.; Greenfield, M.; Vernizzi, G.; Stupp, S.; Bedzyk, M.; Olvera de la Cruz, M. *ACS Nano* **2012**, *6*, 10901-10909.
5. Li, T. I. N. G; Sknepnek, R.; Macfarlane, R. J.; Mirkin, C. A.; Olvera de la Cruz, M. *Nano Letters* **2012**, *12*, 2509-2514.

Mathematical Modeling in Random media - From homogenization to Stochasticity

Lenya Ryzhik
Stanford University, *ryzhik@math.stanford.edu*
NSSEFF Award Year: 2010

Project Description:

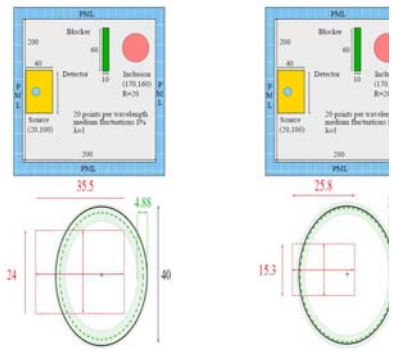

The overarching goal of the grant is to understand the propagation of uncertainty from the (a priori unknown) coefficients in partial differential equations to solutions of such equations. The underlying equations model phenomena as varied as propagation of waves in heterogeneous media (e.g., radars), to heat distribution or electric current in a non-uniform medium. The unifying aspect of these problems is that the physical parameters in the system cannot be perfectly known because of the fluctuations and small-scale heterogeneities. Such phenomena are ubiquitous in nature and the basic problem that is both of the theoretical and practical importance is quantifying the effect of uncertainty at the microscopic scales on the macroscopic phenomena. Such understanding is in particular critical in parameter estimation – one is interested in recovering the macroscopic properties of a complex medium but not the fine scale oscillations, as well as in inverse problems where the goal is to find via remote measurements an object hidden in a medium and obscured by the heterogeneities. Mathematically, the uncertainty in the medium parameters that cannot and should not be reconstructed is modeled as *noise*. Both forward and the inverse problems then hinge on two fundamental questions: (i) find measurements that are as immune to effects of *noise* as possible; and (ii) understand how *noise* propagates up to the macroscopic scales, and affects the large scale phenomena. The work is done by G. Bal group at Columbia University and L. Ryzhik group at Stanford University.

Accomplishments:

Parameter estimation from stable measurements In the setting of wave propagation in heterogeneous media depicted in Figure 1, consider the reconstruction of an inclusion (in red in Fig. 1) buried behind a blocker (in green in Fig.1) and probed by a radiation source (e.g., radar; blue dot in Fig.1). The medium between the source and the inclusion is highly turbid and its precise reconstruction is both practically infeasible, and useless – the fluctuations do not carry useful information. Such turbid media must then be modeled as random. The goal is to understand the effects of randomness on measurements on the detector array (represented in yellow) and recover the inclusion from the noisy measurements. As no direct signal comes from the inclusion to the array due to the blocker, it is only because of the heterogeneities that we can hope to recover the inclusion at all but for the same reason the recorded signal at the array is inherently noisy, making the problem highly challenging.

One of the accomplishments of the grant was the analysis of functionals of the measurements on the array of detectors that would be (i) sensitive to the presence of the inclusion, and (ii) as

immune to the details of the unknown randomness as possible. Examples of such functionals are appropriately defined wave energy densities (WED) as well as field-field correlations (FFC). The above figure shows reconstructions based on WED on the left and FFC on the right. Consistent with theoretical predictions, FFC provide better reconstruction capabilities (with a standard deviation in the reconstruction of the range of the inclusion equal to 38.5 (in units of the probing wavelength) for WED and 25.8 for FFC.

Stability of measurements and propagation of stochasticity The aforementioned wave propagation in heterogeneous media is one example of a problem modeled by a partial differential equation (PDE) involving random and highly oscillatory coefficients. One central component of the grant is to understand and whenever possible rigorously justify how stochasticity propagates from the coefficients in the PDE to its solution. As described above, measurements are functionals of the solutions to the PDE and the errors committed in the reconstructions of parameters of interest are directly related to errors in measurements. All limitations in parameter estimations are therefore to a large extent driven by how stochasticity propagates from noise to measurements.

The analysis of such models has a long history, both in the mathematical and engineering communities. However, most work is done in the so-called homogenization regime, where randomness in coefficients effects solutions of PDEs in a highly non-trivial way but nevertheless solutions are nearly deterministic. This regime is valid when the random fluctuations oscillate on a much smaller scale than the macroscopic size of the domain of interest (in Fig.1, the domain is 200 times larger than the microscopic scale given by the wavelength of the waves). This regime is crucial as it provides us with a model on how measurements depend on the parameters of interest (e.g., the buried inclusion in the preceding example). However, it gives us no information about the size of the inevitable random fluctuations in our measurements that arise as soon as we are slightly away from the homogenization regime, as always happens in practice.

The title of the proposal reflects this core objective of the grant: what are the fluctuations in the available measurements beyond the homogenization limit? How do such fluctuations depend on the randomness in the coefficients of the PDE? Such fundamental questions turn out to be particularly challenging. Only in some PDE models do we have a complete understanding of this problem with major contributions from the grant. Next, we describe some of these results.

Equations with slowly decaying correlations Homogenization regime arises when medium properties have short range correlations, so that the random coefficients rapidly "forget" values at nearby points. In contrast, media with slowly decaying correlations are fractal and have structure on all scales. A major accomplishment of the grant is the discovery of the dichotomy between these regimes – solutions of PDEs exhibit drastically different behavior in these two types of media. One important class of PDEs for which this analysis has been carried out is parabolic equations with random potentials. This class includes the parabolic models of radars in turbid environments. For such models, both when the random potential is strong and weak, we have discovered that the propagation of stochasticity strongly depends on the decorrelation properties of the random potential. For potentials with short-range correlations, we observed that the PDE solution converged to a homogenized solution, as predicted by homogenization theory. Moreover, the random fluctuations in the PDE solution can be asymptotically described by a stochastic partial differential equation with additive noise or random initial data. This completely

characterizes the propagation of stochasticity in this case. In contrast, for a potential with long-range correlations, we have shown that the PDE solution remained stochastic at the macroscopic level, and in the case of weakly random potentials, they affect the solution in a non-trivial way on a time-scale much shorter than that for rapidly decorrelating potentials. We have also discovered a completely new phenomenon that long range correlations introduce a continuum of temporal scales on which various observables become non-trivially affected: for instance, the wave amplitude becomes randomized on a time scale much shorter than the phase. This dramatically effects our understanding of which wave functionals should be measured in turbid media.

Similar results were obtained for other PDE models including those used in wave propagation waves in complex media. The salient feature of such results is a characterization of the effect of the correlation properties of a random medium on the stochasticity of the PDE solutions.

Imaging in weakly heterogeneous media We have developed a new imaging algorithm (GeLMA) that employs the idea that typically the objects that one needs to find in a complex medium are sparse. GeLMA is based on an ODE formulation of an l-1 minimization problem and works extremely well even in the presence of a relatively strong noise. Introduction of the a priori information (sparsity) into the imaging problem dramatically accelerates the rate of convergence in complex media.

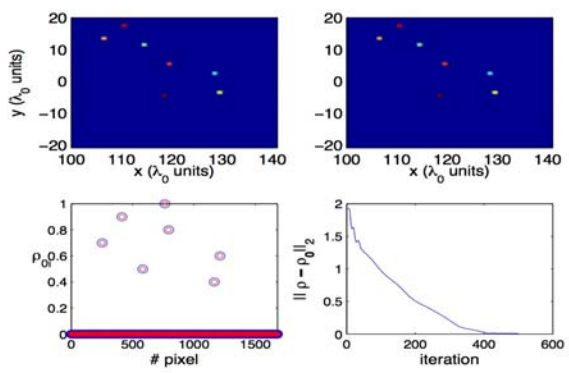

Top row: Original configuration of the scatterers (left) and the recovered image with GELMA (right). Bottom row, left: Comparison between the exact solution (large blue circles) and the GELMA solution (small red circles). Bottom row, right: Convergence rate of the GELMA algorithm.

Representative Publications:

Bal, G. and Pinaud, O., Imaging using transport models for wave-wave correlations. *Math. Models Methods Appl. Sci.*, **2011,** 21(3), 1071-1093.

Zhang, N. and Bal, G.., Homogenization of the Schroedinger equation with large, random potential. To appear in *Stochastics & Dynamics*, **2013**

Komorowski, T. and Ryzhik, L., Long time energy transfer for the random Schroedinger equation, submitted, 2013.

Moscoso, M., Novikov, A., Papanicolaou, G. and Ryzhik, L., A differential equations approach to l_1 minimization with applications to array imaging, Inverse problems, 2012, 28, 1050012012.

Komorowski, T, Olla S. and Ryzhik, L., Asymptotics of the solutions of the stochastic lattice wave equation, to appear in Arch. Rat. Mech. Anal., 2013.

Information Acquisition, Analysis and Integration

Guillermo Sapiro
Duke University, *guillermo.sapiro@duke.edu*
NSSEFF Award Year: 2010

Project Description:

We are at a unique time for science and technology, driven in part by the availability of previously unimaginable quality and amounts of data, including but not limited to, images and videos. The image sharing site flickr.com has over 6,000 images uploaded a minute, and over 2.7 millions images geotagged in one month. Similar amounts of images and medical records are produced daily in hospitals around the world. Millions of surveillance and monitoring cameras produce 24 hours a day of data and information, e.g., the Minneapolis-Saint Paul International Airport has about 2,000 monitoring cameras. The Department of Defense acquires several Tera-bytes of video imaging a day from different locations around the world. The Human Connectome Project as well as http://www.openconnectomeproject.org/ are also producing Tera-bytes of data to be analyzed a day. Basically, all areas in our daily lives are producing these incredible amounts of data, from a large variety of sources. The current fundamental and urging question is how to exploit this data. While still being developed, acquisition technologies have advanced significantly more than analysis theories, and the bottleneck has moved from acquiring information to analyzing and exploiting it. Here is where the proposed project enters into the picture. The goal is to develop novel theoretical, computational, and practical theories and frameworks to exploit the rich information being produced by common data sources as those exemplified above. In particular, the project aims at developing novel representations, for intrinsically high dimensional and multimodality data, that facilitate the critical analysis tasks. Such representations are tuned both to the data and the task, and are integrated from the acquisition all the way to the end application. The proposed project is based on fundamental tools covering numerous areas of science, moving away from more common ad-hoc approaches that have dominated data representation so far.

Accomplishments:

Main accomplishments

- *Real-time and state-of-the-art algorithms for image and video enhancement.* These are based on the theory of sparse modeling and Gaussian Mixture Models, integrated with novel video camera design. Both theoretical results and practical algorithms have been developed, with public domain code released to the community.
- *Optimizing to optimize.* We developed a new paradigm in optimization where we are learning the optimal optimizers for a given task and (on-line learned) data distribution, in contrast with standard optimization techniques that by being generic, are intrinsically one to two order of magnitudes slower.
- *Real-time and state-of-the-art algorithms for audio source separation.* Based on a new model of robust non-negative matrix factorization, and combined with the above-mentioned

optimization technique, we developed audio source separation running in real time in portable devices like the iPad.

- *Pioneered new design of still and video sensing protocols with integrated analysis.* Based on novel and low-power paradigms for coded aperture, we developed fast frame-rate video cameras with low-rate cameras hardware. This integrates the camera design with the above mentioned video reconstruction algorithms.
- *Developed new image models with applications to integrated sensing and reconstruction.* We showed that the developed GMM framework leads to improved design of task-oriented sensing protocols, both for reconstruction and classification.
- *Developed image compression algorithm deployed in the Mars Rovers.* Our JPEG-LS lossless image compression algorithm has been once again deployed in the NASA/JPEL Mars Rovers (it was already in the 1st expedition and has been incorporated now into the second).
- *Developed video segmentation algorithm in Adobe's After Effects, highlight of the product release.* The *RotoBrush* product in Adobe was co-developed with them and resulted from licenses from the UofM to Adobe.
- *Developed algorithms for best-known reconstruction of HIV Env shape.* These, also used for Influenza viruses, are developed once again integrating sensing and processing, with algorithms based on sparse modeling and low-rank decompositions.
- *Developed algorithms for deep brain stimulation neurosurgery.* We are, in close collaboration with neurosurgeons and neurologists, developing unique image processing and analysis tools for helping in DBS surgeries, currently being tested in a weekly basis at a number of leading hospitals.
- *Developed state-of-the-art algorithms for hyperspectral image analysis.* In collaboration with the National Geospatial-Intelligence agency, we developed state-of-the-art reconstruction and classification algorithms that exploit both the class of data and the acquisition protocol, including hyperspectral data acquired at only 2% of the normal rate.
- *Developed state-of-the-art frameworks for image inpainting.* We showed how to unify a number of approaches for image inpainting into unique variational formulations, leading to state-of-the-art results and theoretical foundations.
- *Developed state-of-the-art algorithms for activity detection in video.* In collaboration with the National Geospatial-Intelligence Agency we developed techniques based on sparse modeling and dictionary learning for human activity recognition in video.
- *Network inference.* We developed a new framework based on convex optimization for collaborative network inference with constraints and domain knowledge.
- *Delivery the first free Internet class on image and video processing (via Coursera) with a registration in the order of 30,000.*

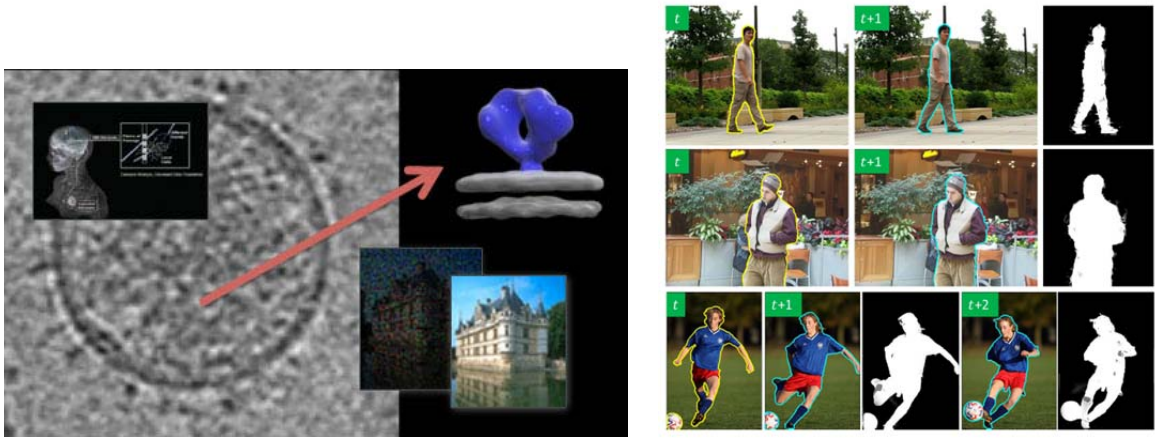

A colleage of images from my research (left) and results on video segmentation, part of Adobe's After Effects, and a component of our activity recognition framework (right).

Technology Transfers

An integral part of our work is the transfer of technology, and the ones performed during this award include:

- Algorithm, technology, and code delivery to Navy and National Geospatial-Intelligence Agency (multiple occasions and multiple codes, including segmentation, image modeling, anomaly detection, hyperspectral image analysis, video analysis for activity detection, etc).
- PhD advisor of a full time DoD employee (NGA, just graduated).
- Delivery of numerous short courses for DoD audiences at DoD facilities.
- Support of companies under DoD and DHS contracts.
- Hosted a number of times a year researchers from DoD, providing full day descriptions of our technology.
- Delivery 3 times the Annual Success Story at the National Geospatial Intelligence Agency program review.
- Delivery of invited talks at DoD organized meetings, both in internal and international conferences

Representative Publications:
(from about 100 supported by the project)

Fiori, M.; Muse, P.; Sapiro, G. *Neural and Information Processing Systems (NIPS)*, December 2012.

Ramirez, I.; Sapiro, G.; *IEEE Trans. Image Processing* **21**, pp. 3850-3864, 2012.

Castrodad, A.; Sapiro, G.; *International Journal of Computer Vision* **100**, pp. 1-15, October 2012.

Yu, G.; Sapiro, G.; Mallat, S.; *IEEE Trans. Image Processing* **21**, pp. 2481-2499, 2012.

Yu , G.; Sapiro, G.; IEEE Trans. Signal Processing **59**, pp. 5842-5858, December 2011.